Identification and characterization of differentially expressed microRNAs in adult tissues of the long-lived *Drosophila dilp2-3,5* mutant

I n a u g u r a l - D i s s e r t a t i o n

zur

Erlangung des Doktorgrades

der Mathematisch-Naturwissenschaftlichen Fakultät

der Universität zu Köln

vorgelegt von

Jennifer Annette Werner

aus Leverkusen

Berichterstatter: Prof. Dr. Linda Partridge

Prof. Dr. Thorsten Hoppe

Tag der mündlichen Prüfung: 07.03.2014

Dedicated to my beloved mother.
18/6/1958 – 08/1/2013

Acknowledgements

I am grateful to Linda Partridge for her supervision, invaluable help and advice during the course of my PhD and foremost for providing me with the opportunity to work as a part of her research group.

Thanks also go to Sebastian Grönke for excellent mentorship throughout the PhD.

I am also indebted to Eric Lai for the genetic tools used in this study and the fruitful discussion when we met on the conference in Washington.

I appreciate the cooperation and assistance from the bioinformatic facility, especially Christoph Dieterich and Corinna Klein.

Big thanks to Bruno Hüttel who did the sequencing no matter how small the input material was.

I would like to thank all people from the Partridge lab, past and present, for their friendship and who made the time so enjoyable. In particular, I will remember all the get-togethers and the coffee breaks in Petit Noir with Marianna Gorsky and Sunita Afschar. Thanks also go to the technicians, not only for technical assistance, but also for the wonderful atmosphere in the lab.

I want to thank Stephan Dietz for his support, encouraging words and foremost for his endless love.

Finally, I want to thank my friends, my father Christian, my mother Elisabeth of blessed memory, my brothers Daniel, Andreas and Arthur for tracking the course of my PhD with interest and supporting me with love, good food and magic.

Table of contents

Abbreviations

Ago	Argonaute protein
bp	base pairs
C. elegans	*Caenorhabditis elegans*
cDNA	complementary deoxyribonucleic acid
cm	centimetre
CO_2	carbon dioxide
Cre	cre recombinase
CT	controlled temperature
Cyp4e2	bytochrome P450-4e2
daGS	daughterless-GeneSwitch
DDT	dichlorodiphenyltrichloroethane
DEPC	biethylpyrocarbonate
DILP	*Drosophila* insulin-like peptide
dNTP	desoxynucleosidtriphosphate
dFOXO	*Drosophila*Forkhead box protein
DNA	deoxyribonucleic acid
EDTA	ethylenediaminetetraacetic acid
EtBR	ethidium bromide
EtOH	ethanol
et al.	*et alii*
E. coli	*Escherichia coli*
e.g.	*exempli gratia*
FC	fold change
FOXO	forkhead box protein
F1	filial 1
g	gram
Gal4	yeast transcription activator protein Gal4
GS	GeneSwitch
HCl	hydrogen chloride
HIF	hypoxia-inducible factor
hsp70	70 kilodalton heat shock protein
h	hour
H_2O	water
H_2O_2	hydrogene peroxide
IGF	insulin-like growth factor
IGF1R	insulin-like growth factor 1 receptor
IIS	insulin/IGF-like signaling
InR	insulin receptor
InR^{DN}	insulin receptor dominant negative mutant
INSR	mammalian insulin receptor
IPCs	insulin producing cells
IRS	insulin receptor substrate
JNK	c-Jun N-terminal kinase
KCl	potassium chloride
KO	knock-out
Lnk	link adaptor protein
LB	lysogeny broth
M	molar

mA	milliampere
$MgCl_2$	magnesium chloride
$MgSO_4$	magnesium sulfate
MHC	myosin heavy chain
min	minute
ml	milliliter
mM	milli molar
mNSCs	median neurosecretory cells
miRISC	micro - ribonucleic acid induced silencing complex
miRNA	microRNAs; micro ribonucleic acid
mRNA	messenger ribonucleic acid
µg	microgram
µl	microliter
µM	micromolar
NaCl	sodium chloride
NaH_2PO_4	monosodium phosphate
Na_2HPO_4	disodium phophate
NaOH	sodium hydroxide
ng	nanogram
nt	nucleotides
PBS	phosphate buffered saline
PCR	polymerase chain reaction
pH-value	hydrogen ion concentration
pM	picomolar
polyA	polyadenylation
pre-miRNA	precursor micro ribonucleic acid
piwiRNA	piwi-interacting
pri-miRNA	primary micro ribonucleic acid
PTEN	phosphatidylinositol-3,4,5-trisphosphate 3-phosphatase
qRT-PCR	quantitative real-time reverse transcription-PCR
RISC	ribonucleic acid induced silencing complex
RNA	ribonucleic acid
RNAi	ribonucleic acid interference
RNase	ribonuclease
rpm	rotations per minute
rRNA	ribosomal ribonucleic acid
RU486	Mifepristone
SDS	sodium dodecyl sulfate
sec	seconds
siRNA	short interfering ribonucleic acid
SIRT1/2	silent information regulator 1/2
SSC	saline-sodium citrate
SV40	simian vacuolating virus 40
SYA	sugar yeast agar
S6K	S6 kinase
TAE	tris-acetate-EDTA-buffer
TEMED	N,N,N´,N´-tetramethylethylendiamine
TBE	tris-borate-EDTA-buffer
Tris	2-amino-2-(hydroxymethyl)1,3-propandiol
Tm	melting temperature
tubulinGS	tubulin GeneSwitch

U	units
UAS	upstream Activation Sequence
UV	ultraviolet
V	Volume
w^{Dah}	white Dahomey
wt	wild type
w/v	weight per volume
2nd	second
3rd	third
°C	degree celsius

Kurzzusammenfassung

MicroRNAs sind kleine regulatorische Moleküle, welche in Eukaryoten diverse Funktionen durch die Steuerung der Expression von Genen auf post-transkriptioneller Ebene in spezifischen Geweben ausüben. In der Fruchtfliege *Drosophila melanogaster* sind 238 miRNA Gene annotiert, die nur vereinzelt funktionell charakterisiert sind. Einige miRNAs spielen eine Rolle in biologischen Prozessen des Alterns und stehen im direkten Zusammenhang mit altersmodulierenden Signaltransduktionswegen, zu denen auch der Insulin/IGF-ähnliche Signalweg (IIS) zählt. Ob miRNAs die phänotypischen Effekte von reduziertem IIS, wie Lebensverlängerung und Resistenz gegenüber Stressfaktoren, vermitteln, ist gänzlich unbekannt. Für eine umfangreiche Charakterisierung von miRNAs ist die Information über gewebespezifische Expression unerlässlich. Bei der adulten Fliege wurden bisher nur Ovarien untersucht und es wurde zwischen der Expression in Köpfen und ganzen Körpern unterschieden. In der vorliegenden Arbeit wurden erstmals spezifische miRNA-Expressionsprofile der vier folgenden adulten Gewebe erstellt; des Gehirns, des Thorax, des Darmes und des Abdomens. Des Weiteren wurden in dieser Arbeit differenziell regulierte miRNAs in Geweben von langlebigen *Drosophila dilp2-3,5*-Mutanten identifiziert und mittels miRNA-Überexpressionsanalysen sowie einer im Rahmen dieser Arbeit generierten miRNA-Knockout-Mutante auf IIS-assoziierte Phänotypen funktionell untersucht. Die vorliegende Arbeit leistet einen wesentlichen Beitrag zur Charakterisierung von miRNAs in *Drosophila melanogaster* im Allgemeinen, liefert insbesondere eine umfangreiche Analyse identifizierter differenziell regulierter miRNAs in langlebigen Insulin-Mutanten und trägt so zur Aufklärung der dem Alterungsprozess zu Grunde liegenden biologischen Mechanismen bei.

Abstract

MicroRNAs are small, regulatory molecules that execute diverse functions in eukaryotes through the post transcriptional control of gene expression in specific tissues. In the fruit fly *Drosophila melanogaster* 238 miRNA genes are annotated and only few have been functionally characterized. Some miRNAs play a role in the biological processes of aging and are directly linked with aging-modulating pathways, including the insulin/IGF-like signaling (IIS) pathway. Whether miRNAs mediate phenotypic effects of reduced IIS remains unknown. For a comprehensive characterization of miRNA function, information about tissue-specific expression is indispensible, and so far in the adult fly is limited to ovaries and the analysis of heads and whole bodies. In the present study for the first time miRNA expression profiles from four adult tissues, namely the brain, thorax, digestive tract and abdomen, were generated. Furthermore, differentially expressed miRNAs in tissues of the long-lived *Drosophila dilp2-3,5* mutant were identified and functionally characterized for IIS-associated phenotypes, by overexpression analysis and by a miRNA knock-out mutant generated within the scope of this study. The present study provides fundamental information for the characterization of miRNA function in *Drosophila* in general, and supplies particularly an analysis of identified, differentially expressed miRNAs in long-lived insulin mutants, and thus contributes to the elucidation of biological mechanisms underlying the process of aging.

1 Introduction

1.1 MicroRNAs

MicroRNAs (miRNAs) are a class of small non-coding regulatory RNAs that act as post-transcriptional regulators of gene expression. Three types of small regulatory RNAs have been described. Short interfering RNAs (siRNAs) operate in *cis* by regulating the expression of the transcripts from which they have evolved (Katayama *et al*., 2005). Piwi-interacting RNAs (piwiRNAs) are usually expressed in germline cells and probably act as a defense mechanism against transposable elements and in gametogenesis (Siomi *et al*., 2011). MiRNAs act in trans by inhibiting the expression or causing the degradation of protein-coding mRNAs.

1.2 MicroRNA-mediated gene silencing and origin of microRNAs

The process of inhibiting mRNA expression by binding of complementary miRNAs or siRNAs is referred to as RNA interference (RNAi). Although prokaryotes have a regulatory system functionally analogous to RNAi (Hale *et al*., 2009), conventional miRNA silencing seems to be restricted to eukaryotes. MiRNAs are found in all multicellular eukaryotic organisms ranging from sponges (Grimson *et al*., 2008) and algae (Cock *et al*., 2010) to higher animals and plants, suggesting miRNA regulation of gene expression to be an evolutionary ancient mechanism. However, miRNA families are not conserved between plants and animals. Consistently, biogenesis (Reinhart *et al*., 2002), cellular localization of miRNA processing (Park *et al*., 2005; Lee *et al*., 2003) as well as mode of regulation (Zhang *et al*., 2007) differs between animal and plant miRNAs, suggesting that miRNAs arose independently in plants and animals.

In plants, miRNAs probably originated by inverted duplication of protein coding genes, as the sequence of plant miRNAs is perfectly complementary to the sequence of their target mRNAs (Allen *et al*., 2004). In contrast, miRNAs in animals do not share high sequence similarity with their target genes (Nozawa *et al*., 2010). However, many miRNA share sequence homology with transposable elements or inverted genomic repeats, suggesting that during evolution miRNAs may have evolved from transposable elements or inverted repeats (Piriyapongsa and Jordan, 2007). Within the genome miRNAs are often arranged in clusters, suggesting that new miRNA genes also evolved by gene duplication of already existing miRNAs.

1.3 Evolutionarily conservation of microRNAs and their mRNA targets

Many miRNAs are highly conserved during evolution (Axtell and Bartel, 2005; Pasquinelli *et al*., 2000). However, although miRNAs can be evolutionarily conserved, their mRNA targets can differ between species (Chen and Rajewsky, 2006) and clade-specific changes in miRNA targets have been proposed to contribute to speciation and diversification of life (Grün *et al*., 2005). Interestingly, the number of miRNAs present in a species is positively correlated with organismal complexity (Grimson *et al*., 2008). This finding has led to the hypothesis that fine-tuning of gene expression via regulation by miRNAs was necessary for the evolution of complex organisms (Heimberg *et al*., 2008).

Although miRNA targets can change during evolution, there are several miRNAs described for which the mRNA targets are conserved between species. One example is the *let-7* miRNA family. Let-7 was first described as an essential regulator of development in the nematode *Caenorhabditis elegans* and is involved in the heterochronic pathway. Heterochronic genes control the relative timing of events during development. Interestingly, as in *C. elegans*, let-7 is both necessary and sufficient for the appropriate timing of developmental processes in the fruit fly *Drosophila*, indicating that its function as a heterochronic miRNA is evolutionarily conserved (Caygill and Johnston, 2008). Furthermore, targets of let-7 are conserved between humans and *C. elegans* (Chen and Rajewsky, 2006) and the expression pattern of let-7 is also similar between worms, flies and humans (Pasquinelli *et al*., 2000), suggesting that let-7 may regulate similar processes in these organisms.

In general, it is suggested that conserved miRNAs are expressed at high levels and more broadly than non-conserved miRNAs, whereas non-conserved miRNAs often show low expression levels and spatial and temporal specific expression patterns (Ruby *et al*., 2007).

1.4 Genomic arrangement of microRNAs and their control of transcription

Consistent with the correlation of miRNA number and organismal complexity, up to now 1872 miRNA genes are annotated in humans, 1186 in mice and 223 in *C. elegans*. In the *Drosophila* genome 238 miRNA genes have been identified and the number is still increasing (Griffiths-Jones, 2006). MiRNAs are distributed throughout the *Drosophila* genome and are located in intergenic sites, intronic sites or gene clusters (Nozawa *et al*., 2010) and, very rarely, also in exons (Berezikov *et al*., 2011). Approximately 50 % of *Drosophila* miRNAs are arranged in clusters with at least two or more miRNAs (Bartel, 2004). In general, transcription of miRNAs is regulated by their own promoter. Transcriptional regulation of intronic miRNAs is dependent on the orientation of the miRNA gene in relation to the protein

coding gene it resides in. If an intronic miRNA is arranged in antisense orientation, its transcription is regulated by its own promoter. In contrast, if the intronic miRNA is arranged in sense orientation within the protein coding gene then its transcription is more likely to be under the control of the promoter of the protein coding gene (Baskerville and Bartel, 2005). However, there are exceptions, e.g. the expression pattern of *Drosophila miR-7* is distinct from its host gene bancal (Aboobaker *et al*., 2005).

MiRNAs in gene clusters are often transcribed as entity in an operon-like manner (Ruby *et al*., 2007), e.g. *Drosophila mir-100, -125, and let-7* are arranged within a single cluster and were shown to be coup-regulated during metamorphosis. Interestingly, transcriptional regulation of this miRNA cluster is mediated *via* ecdysone and juvenile hormone. Chromosomal clustering of these miRNAs is evolutionarily conserved suggesting that their transcriptional regulation *via* hormones may also be conserved (Sempere *et al*., 2003). Transcription factors that regulate miRNAs expression include FOXO3a. In mammalian cells it was shown that FOXO3a binds to the promoter of a cluster consisting of *miR-106b*, *miR-93*, and *miR-25* and activates its expression. Interestingly, predicted targets of miR-25 include members of the insulin/IGF-like signaling (IIS) pathway, suggesting that miR-25 is part of a feedback loop within the IIS pathway in mammals (Brett *et al*., 2011). Indeed, feedback loops formed by miRNAs and transcription factors have already been demonstrated. For example, p53 induces the expression of miR-34a in mammalian cells and *in vivo* in mice. miR-34 targets silent information regulator 1 (SIRT1) and SIRT1 in turn promotes p53 deacetylation and decreases p53 activity (Yamakuchi and Lowenstein, 2009).

Little is known about the nature of miRNA core promoters. For *in vivo* analysis most studies define miRNA promoter regions as the genomic sequence 300-2000 bases upstream of miRNA genes (Martinez *et al*., 2008). MiRNA promoters seem to be highly similar to promoters of protein-coding genes (Corcoran *et al*., 2009).

1.5 MicroRNA biogenesis pathway

Maturation of miRNAs from a pre-miRNA transcript to the mature ~22bp long miRNA is controlled by the miRNA biogenesis pathway. Like protein-coding genes, miRNAs genes are transcribed by RNA polymerase II (Lee *et al*., 2004), with a few exceptions that are transcribed by RNA polymerase III (Borchert *et al*., 2006). The primary miRNA transcript (pri-miRNA) can be several kilobases long and can contain multiple miRNA precursors. Within the nucleus the pri-miRNA is recognized by Drosha, a RNase III enzyme. Together with the RNA binding protein DGCR8 (in *Drosophila*: "Pasha") Drosha cleaves the pri-

miRNA into smaller precursor miRNAs (pre-miRNAs), which typically form stem-loop structures (Denli *et al*, 2004). The pre-miRNA is exported by Exportin-5 (Yi *et al*., 2003) in a GTP-dependent manner into the cytoplasm. There, the pre-miRNA is further cleaved by the RNase III enzyme Dicer (in *Drosophila*: "Dicer-1") (Bernstein *et al*., 2001). The resulting approximately 22 nucleotides long miRNA duplex is incorporated into the RNA induced silencing (RISC) complex (Hammond *et al*., 2000). Only one strand of the miRNA duplex is selected for target gene regulation while the other strand is degraded (Gregory *et al*., 2005). The final complex (miRISC) consists of the single stranded mature miRNA, Dicer, Argonaute (Ago) and RNA-binding proteins (in *Drosophila*: "loquacious"). The miRISC mediates either repression of translation by imperfect binding of the miRNA to the mRNA target or mRNA degradation by perfect complementary binding (Hutvágner and Zamore, 2002). In addition to cleavage by Drosha and Dicer, pri-miRNAs and pre-miRNAs can be modified by editing (Kawahara *et al*., 2007). Editing includes adenosine to inosine transitions (Kawahara *et al*., 2008) or addition of nucleotides (Landgraf *et al*., 2007) and provides a way to regulate biogenesis and target specificity of miRNAs. An alternative to the canonical miRNA pathway is used by "mirtrons". Mirtrons are short intronic hairpins that bypass Drosha-mediated cleavage and enter the canonical miRNA pathway at the stage of export into the cytoplasm (Okamura *et al*., 2007). Mirtrons are a source of miRNAs and were first identified in *Drosophila*. Shortly after, it was shown that mirtrons also exist in other species including nematodes (Ruby *et al*., 2007) and mammals (Berezikov *et al*., 2007).

1.6 MicroRNA functions in *Drosophila*

The first described miRNA in *Drosophila* was bantam. The target of bantam is the pro-apoptotic gene *hid* and it was shown, that bantam controls cell proliferation and apoptosis during development (Brennecke *et al*., 2003). Later it was shown that indeed several *Drosophila* miRNAs play roles in cell proliferation and apoptosis, including miR-2 (Leaman *et al*., 2005), miR-14 (Xu *et al*., 2003) and miR-278 (Nairz *et al*., 2006). But also muscle differentiation (Kwon *et al*., 2005), neurogenesis (Li *et al*., 2006), energy homeostasis (Teleman *et al*., 2006), homeotic transformation (Ronshaugen *et al*., 2005) and meta-morphosis (Sempere *et al*., 2002) are functions that are under the control of miRNAs. However, assigning miRNAs to specific functions is arbitrary since one miRNA can target several mRNAs that play roles in different cellular functions (Lim *et al*., 2005). For example, miR-278 is not only involved in cell proliferation, but also affects energy homeostasis (Teleman *et al*., 2006). Thus, miRNAs control basic organismal functions. In doing so,

miRNAs are not just restricted to fine-tuning of gene expression but mutations of miRNAs can cause severe phenotypes. For example, loss of miR-1 causes lethality due to the dysfunction of muscle gene expression maintenance in flies (Kwon *et al*., 2005). Therefore, miRNAs play pivotal roles in *Drosophila*.

1.7 MicroRNAs and aging

MiRNAs have been implicated in the regulation of age-related diseases as well as the aging process itself. For example, miRNAs are differentially expressed in age-associated diseases like Alzheimer's Disease (Zovoilis *et al*., 2011) or cancer and the expression profile of miRNAs is changed in tumor cells (Munker and Calin, 2011). The tumor suppressor p53 is known to impact aging and lifespan in worms (Derry *et al*., 2001), flies (Lee *et al*., 2003; Bauer *et al*., 2005) and mice (Lavigueur *et al*., 1989; Chin *et al*., 1999). miR-29 is expressed in response to DNA damage in a p53-dependent manner and is up-regulated in a mouse model of progeria as well as during normal aging (Ugalde *et al*., 2011). Indeed, in mice miRNAs have been suggested to be biomarkers for aging. miR-34a level increases with age while the level of its target SIRT1 decreases. As changes in miR-34 levels can be measured in blood, miR-34a expression levels are a potential biomarker for the aging process (Li *et al*., 2011). In the worm *C. elegans* the expression of certain miRNAs is regulated in an age-dependent manner (Pincus *et al*., 2011). Furthermore, the single miRNA lin-4 has been shown to be able to modulate lifespan in worms. Overexpression of lin-4 increases lifespan and its reduction shortens lifespan (Boehm and Slack, 2005). Since then, several other miRNAs have been identified that modulate lifespan in worms, including miR-71 and miR-239 (de Lencastre *et al*., 2010). Recently, also in *Drosophila* it has been shown that a single miRNA can regulate survival, since mild overexpression of miR-34 extends lifespan and mitigates induced neurodegeneration (Liu *et al*., 2012).

1.8 The IIS pathway extends lifespan in diverse organisms

The IIS pathway is an evolutionarily conserved, nutrient-responsive pathway that coordinates metabolic homeostasis, growth, development, stress resistance and reproduction (Broughton and Partridge, 2009; Toivonen and Partridge, 2009). Interestingly, decreased IIS has been shown to extend lifespan in organisms as diverse as worms (Kenyon *et al*., 1993; Lin *et al*., 2001), flies (Tatar *et al*., 2001; Giannakou *et al*., 2004) and mice (Holzenberger *et al*., 2003; Selman *et al*., 2008). Moreover, in humans there is a correlation between longevity and certain alleles of the IIS downstream transcription factor FOXO3A, suggesting a conserved

role of IIS signaling in lifespan extension including humans (Willcox *et al*, 2008; Flachsbart *et al*., 2009).

In the fruit fly *Drosophila melanogaster* several intracellular components of the IIS pathway have been implicated in the control of lifespan. Flies carrying hypomorphic mutations of the insulin receptor (InR) or mutants for the insulin receptor substrate CHICO have greatly extended lifespan (Tatar *et al*., 2001, Clancy *et al*., 2001). The adaptor protein Link (LNK) functions in parallel to CHICO (Werz *et al*., 2009) and *Lnk* mutant flies as well are long-lived (Slack *et al*., 2010). Furthermore, adult-specific overexpression of the downstream transcription factor dFOXO or the Phosphatidylinositol-3,4,5-trisphosphate 3-phosphatase (PTEN) in the fat body is sufficient to increase lifespan (Giannakou *et al*., 2004; Hwangbo *et al*., 2004). dFOXO has been shown to be a key downstream factor mediating the lifespan response to reduced IIS, since loss of dFOXO abolishes the lifespan extension of flies with ablated median neurosecretory cells (mNSCs) and flies expressing a dominant negative version of the InR (InR^{DN}) (Slack *et al*., 2011).

In addition to the intracellular IIS components, the ligands of IIS have also been implicated in lifespan control in flies. The *Drosophila* genome encodes seven insulin-like peptides (DILP1-7). Three of the DILPs, DILP2, DILP3 and DILP5 are expressed in the mNSCs of the fly brain and genetic ablation of mNSCs causes increased lifespan (Broughton *et al*., 2005). Furthermore, the combined knock-out of DILP 2, 3 and 5 (*dilp2-3,5* mutants) also results in lifespan extension. *dilp2-3,5* triple mutants are not only long-lived but also show other characteristic phenotypes linked to reduced IIS including developmental delay, reduced body weight, reduced fecundity, altered metabolic homeostasis and resistance to oxidative stress (Grönke *et al*., 2010). Currently, the mechanisms why these mutants are so long-lived are not well understood, neither is it known whether miRNAs are involved in the regulation of lifespan extension or other phenotypes associated with reduced IIS.

1.9 MicroRNAs regulate the activity of the IIS pathway

There is evidence that miRNAs are involved in the regulation of IIS pathway activity. Insulin synthesis and secretion are both modulated by miRNAs in *Drosophila.* It was shown that miR-278 targets the mRNA of *expanded*, while expanded promotes dILP expression. *miR-278* mutant flies have elevated insulin production due to elevated *expanded* mRNA. Thus miR-278 controls insulin levels in flies (Teleman *et al*., 2006). Insulin levels are also

regulated by miRNAs in mammals (Poy *et al*., 2004, Sun *et al*., 2010; Melkman-Zehavi *et al*., 2011). Additionally, miRNAs directly target components of the IIS pathway. Insulin-like growth factor 1 (IGF-1) is modulated by miRNAs in human cells (Shan *et al*., 2009; Elia *et al*., 2009) and in rats (Wang *et al*., 2009). IGF-2 (Ge *et al*., 2011), IGF-1 receptor, S6 kinase (S6K) (McKinsey *et al*., 2011), insulin receptor substrate 1 (IRS-1) (La Rocca *et al*., 2009; Karolina *et al*., 2011) and IRS-2 (Dávalos *et al*., 2011) are targeted by miRNAs in mammalian cells.

1.10 MicroRNAs and the regulation of IIS dependent lifespan extension

Evidence exist that miRNAs regulate IIS-dependent lifespan extension. Flies mutant for *miR-14* are obese, have reduced insulin levels and are sensitive to starvation. miR-14 acts in the mNSCs by targeting the transcription factor sugarbabe, which in turn controls DILP levels (Varghese *et al*., 2010). Interestingly, *miR-14* mutant flies have a reduced lifespan under thermal stress (Xu *et al*., 2003). If this is true under normal thermal conditions was not shown. Interestingly, in worms several miRNAs have been identified that regulate lifespan by modulating activity of the IIS pathway. Overexpression of lin-4 results in long-lived worms. The target of lin-4 is lin-14, which acts in parallel or upstream of the IIS receptor DAF-2 (Boehm and Slack, 2005). In addition, overexpression of miR-71 increases lifespan in worms while overexpression of miR-239 decreases lifespan. This effect on lifespan could be modified by RNAi against the IIS components DAF-2 and DAF-16, suggesting that miR-71 and miR-239 act in the IIS pathway to modulate lifespan (Pincus *et al*., 2011; de Lencastre *et al*., 2010). Thus, there is evidence for a crucial role of miRNAs in IIS-mediated regulation of lifespan in worms. However, it is currently unknown whether IIS-mediated lifespan extension is controlled by miRNAs in other species nor it is known whether miRNA expression is changed in long-lived IIS *Drosophila* mutants.

1.11 Aims of the project

Aim 1: Generation of a *Drosophila* miRNA expression atlas

For the characterization of miRNAs, information about their spatial expression is indispensible. So far for adult *Drosophila* tissues only data for heads, whole bodies and ovaries exist. In this study, microarrays and next-generation sequencing were used to generate comprehensive miRNA expression profiles of adult *Drosophila* tissues including brain, thorax, digestive tract, and abdomen.

Aim 2: Identification of differentially expressed microRNAs in tissues of a long-lived *Drosophila* IIS mutant

Whether miRNA expression is differentially regulated in IIS mutants is not known. In order to identify differentially expressed miRNAs in long-lived IIS mutants, next generation sequencing and microarrays were used to compare miRNA expression between adult tissues of wild type flies and long-lived *dilp2-3,5* mutants.

Aim 3: Functional *in vivo* analysis of differentially expressed microRNAs

In order to analyze the role of miRNAs in IIS-associated phenotypes, differentially expressed miRNAs were functionally characterized *in vivo* using overexpression and knock-out fly lines. For one selected candidate miRNA a null mutant was generated by homologous recombination. To further dissect the role of miRNAs in different tissues, miRNAs were overexpressed tissue-specifically and analyzed for IIS-associated phenotypes.

Aim 4: Comparison of microarray data with next-generation sequencing data

Microarray and next-generation sequencing are two techniques which are used to study miRNA expression. Both techniques were compared for performance in the detection of absolute and differential expression as well as for the detection of tissue-specificity.

2 Results

The downstream mechanisms of IIS related phenotypes including lifespan extension and stress resistance are still elusive and it is not known whether miRNAs may be involved in the regulation of these phenotypes. In order to investigate whether miRNAs are differentially expressed in tissues of long-lived *Drosophila* IIS mutants I used microarrays and next generation sequencing to compare miRNA expression profiles of wild type control flies with long-lived *dilp2-3,5* mutant flies. Therefore, I collected brain, midgut, abdominal fat and muscle tissue from the thorax of 10 day old wild type control and *dilp2-3,5* mutant flies (Figure 2.1).

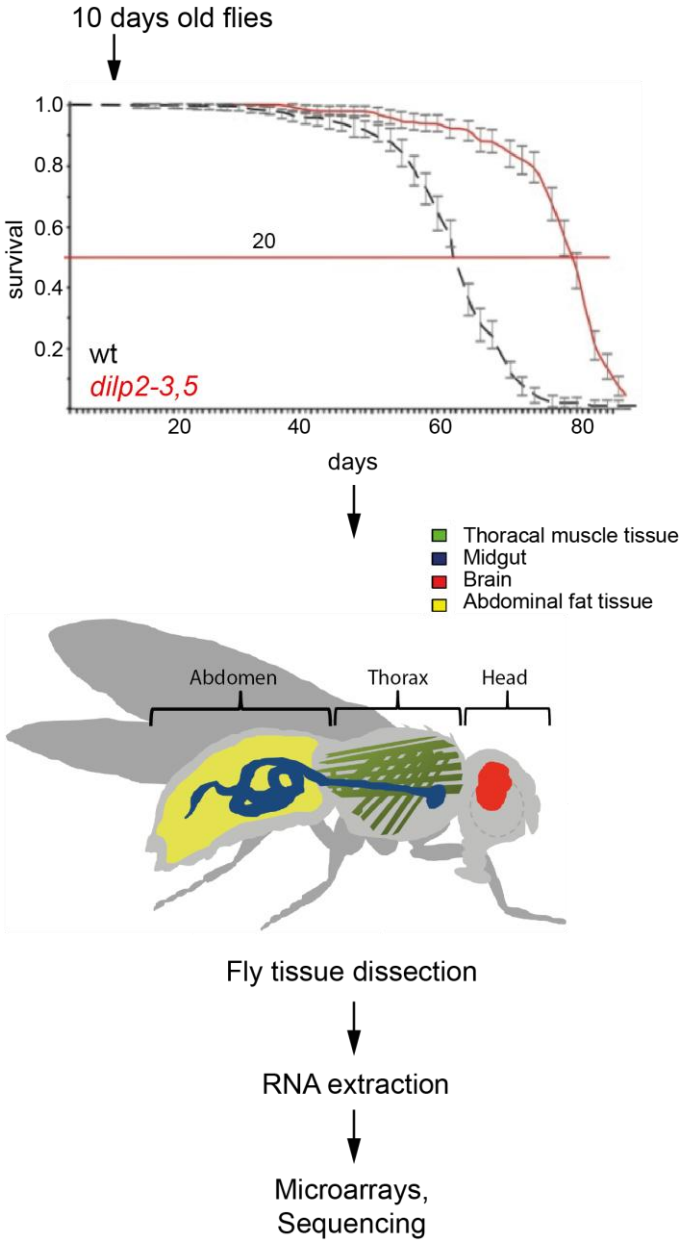

Figure 2.1: Project outline for the identification of differentially expressed miRNAs in tissues of adult *Drosophila* IIS mutants. 10 day old wild type and *dilp2-3,5* flies were dissected, RNA was extracted and used for microarrays and next generation sequencing, respectively.

2.1 Tissue-specific microRNA expression profiling using microarrays

2.1.1 Pre-test - Identification of differentially expressed microRNAs in thoraces of *dilp2-3,5* mutants

In order to establish purification conditions for *Drosophila* miRNAs and to test whether miRNAs are differentially expressed in long-lived IIS mutants, I did a pre-test using thoraces of *dilp2-3,5* mutants. Microarrays were used for the detection of miRNAs, because they are cost effective and allow fast high throughput analysis of miRNAs. For the pre-test we used the Affymetrix GeneChip for miRNAs 1.0, which contained probe sets for 152 mature *Drosophila* miRNAs.

28 miRNAs were significantly changed in expression between *dilp2-3,5* mutants and controls (summarized in Table 1). Interestingly, most differentially regulated miRNAs were up-regulated (>80 %). However, most miRNAs showed only minor expression changes, but 14 miRNAs had a fold change of more than 1.5 or below 0.5, respectively. mir-986-5p was the strongest regulated miRNA with a fold change of more than 14. Since I was able to successfully identify differentially expressed miRNA with this protocol, I extended the analysis to further tissues in order to ask whether the observed expression changes were specific to the thorax or a general miRNA response in all tissues.

Thorax (Pre-test)

miRNA	Mean wt	Mean *dilp2-3,5*	FC	p-value	p-value (adjusted)
miR-980-3p	1506.10	819.86	0.54	0.002	0.04
miR-274-5p	19618.64	14535.94	0.74	0.003	0.04
miR-305-5p	11599.09	9390.98	0.81	0.01	0.07
miR-998-3p	1001.22	816.01	0.82	0.04	0.23
miR-263a-3p	29387.56	26889.01	0.91	0.01	0.06
miR-124-3p	7590.66	8869.21	1.17	0.04	0.23
miR-995-3p	4504.08	5352.13	1.19	0.02	0.12
miR-304-5p	2.86	3.68	1.29	0.001	0.04
miR-133-3p	2395.58	3088.96	1.29	0.02	0.12
miR-932-5p	668.50	897.49	1.34	0.003	0.04
miR-7-5p	129.24	174.14	1.35	0.01	0.08
miR-957-3p	4769.43	6803.66	1.43	6.6×10^{-5}	0.01
miR-10-3p	249.48	358.31	1.44	0.003	0.04
miR-307-3p	117.23	168.39	1.44	0.04	0.23
miR-1017-3p	448.85	662.38	1.48	0.002	0.04
miR-972-3p	2.88	4.36	1.52	0.02	0.15
miR-1000-5p	342.44	534.47	1.56	0.01	0.07
miR-1004-3p	296.16	463.78	1.57	0.003	0.04
miR-999-3p	101.00	162.49	1.61	0.05	0.26
miR-1001-5p	140.07	233.20	1.66	0.0001	0.01
miR-981-3p	212.30	394.25	1.86	0.02	0.15
miR-987-5p	70.54	138.56	1.96	0.001	0.04
miR-989-3p	41.22	85.56	2.08	0.04	0.23

miR-87-3p	11.35	23.83	2.10	0.01	0.10
miR-13a-3p	18.32	46.02	2.51	0.005	0.06
miR-210-3p	1187.92	3110.32	2.62	0.03	0.18
miR-954-5p	194.93	627.01	3.22	0.01	0.07
miR-986-5p	36.64	525.31	14.34	0.001	0.04

Table 1: Differentially expressed miRNAs detected in mechanically separated *dilp2-3,5* thoraces used for the pre-test by microarray. Mean represents miRNA expression in three independent replicates each genotype. p-values are calculated by Student's t-test and adjusted by Benjamini-Hochberg procedure. FC, fold change; wt, wild type

2.1.2 *Drosophila* tissues have characteristic microRNA expression profiles

Based on the results from the pre-test, the miRNA microarray analysis was extended to three more tissues, namely the brain, the digestive tract and the abdomen. Furthermore, the analysis for the thorax was repeated. In contrast to the pre-test, thoraces for this experiment were manually dissected and thus exclude gut tissue (for dissection details see chapter 4.14). Three replicates were used per tissue. In addition, I used a newer generation of miRNA microarrays (Affymetrix GeneChip for miRNAs 2.0), which contained probe sets for 186 mature *Drosophila* miRNAs.

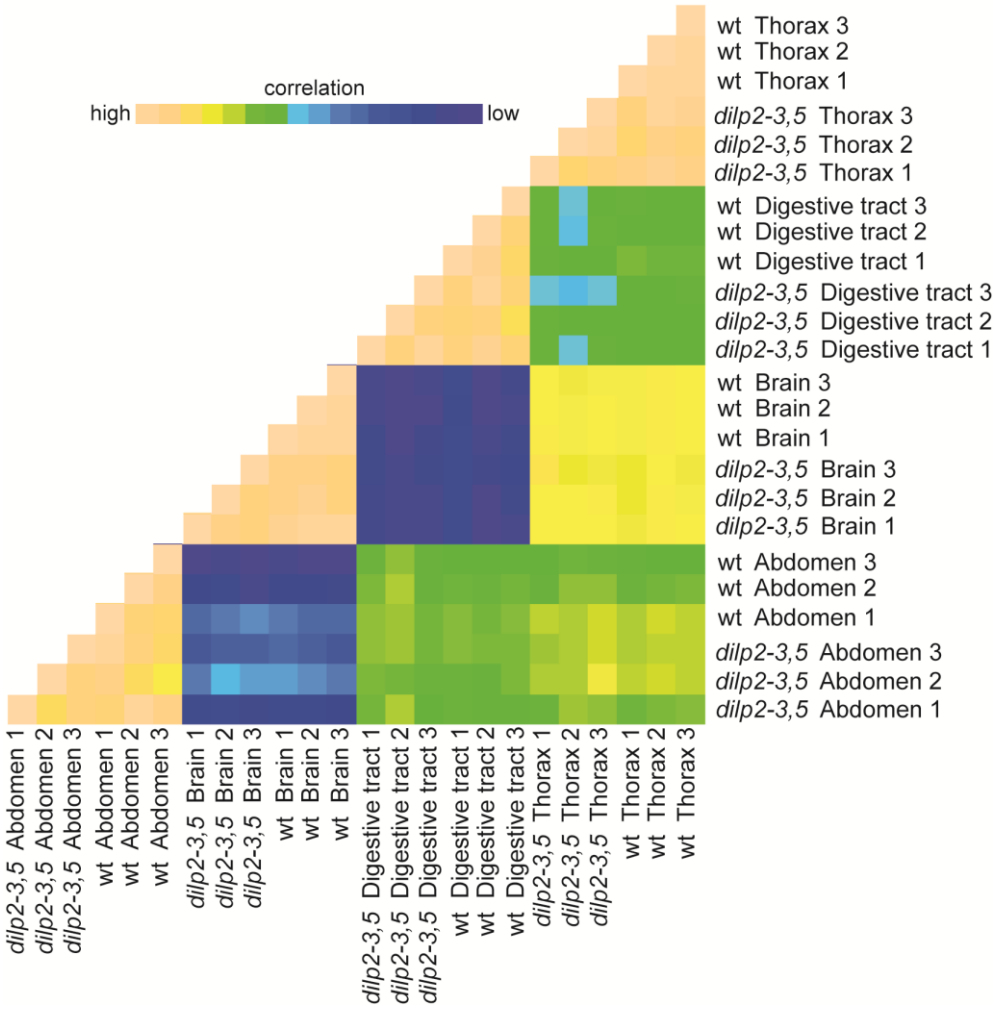

Figure 2.2: Comparisons of microarray tissue profiles. Pearson correlation coefficient for all pairwise comparisons was computed and the values are depicted color-coded. Samples from the same tissue cluster indicating high quality of tissue preparation and tissue-specific miRNA expression.

In order to discover whether miRNAs are expressed in a tissue-specific manner and to verify reproducibility between tissue preparations, I tested the correlation of miRNA expression profiles by Pearson analysis. The Pearson coefficient gives information about the similarity in a pairwise miRNA profile comparison. Indeed, correlation coefficients between microarrays of the same tissue showed clustering indicating that each tissue had a unique miRNA expression profile and that tissue preparation was consistent between replicates (Figure 2.2).

2.1.3 Identification of tissue-specific microRNAs by microarray

Each tissue is characterized by a specific miRNA expression profile as discovered by Pearson correlation. In order to identify tissue-specific and ubiquitously expressed miRNAs, we qualitatively evaluated tissue specificity of single miRNAs by a tissue specificity score (Landgraf *et al*., 2007). The calculation of the score is based on quantification of information, based on the information-theoretic concept of Claude Elwood Shannon (Shannon, 1948). It takes into account the distribution of the cloning frequencies in each tissue. The tissue-specificity score is dependent on the number of tissues and varies between 0, when the expression of a miRNA is evenly distributed across tissues, and 2 when a miRNA is highly specific for a given tissue (Landgraf *et al*., 2007). MiRNAs with expression under the detection threshold were filtered out in the analysis. We identified miRNAs whose expression is evenly distributed across tissues, such as miR-317-3p and miR-276a-3p (Figure 2.3). However, many miRNAs were expressed in a tissue-specific manner. Interestingly, most tissue-specific miRNAs were expressed in the brain, including miR-981-3p and miR-990-5p. We also found miRNAs specific for abdomen, like miR-2494-5p and miR-1015-3p, and miRNAs specific for digestive tract, like miR-314-3p and miR-956-3p. Only few miRNAs were specific for the thorax, like miR-993-3p.

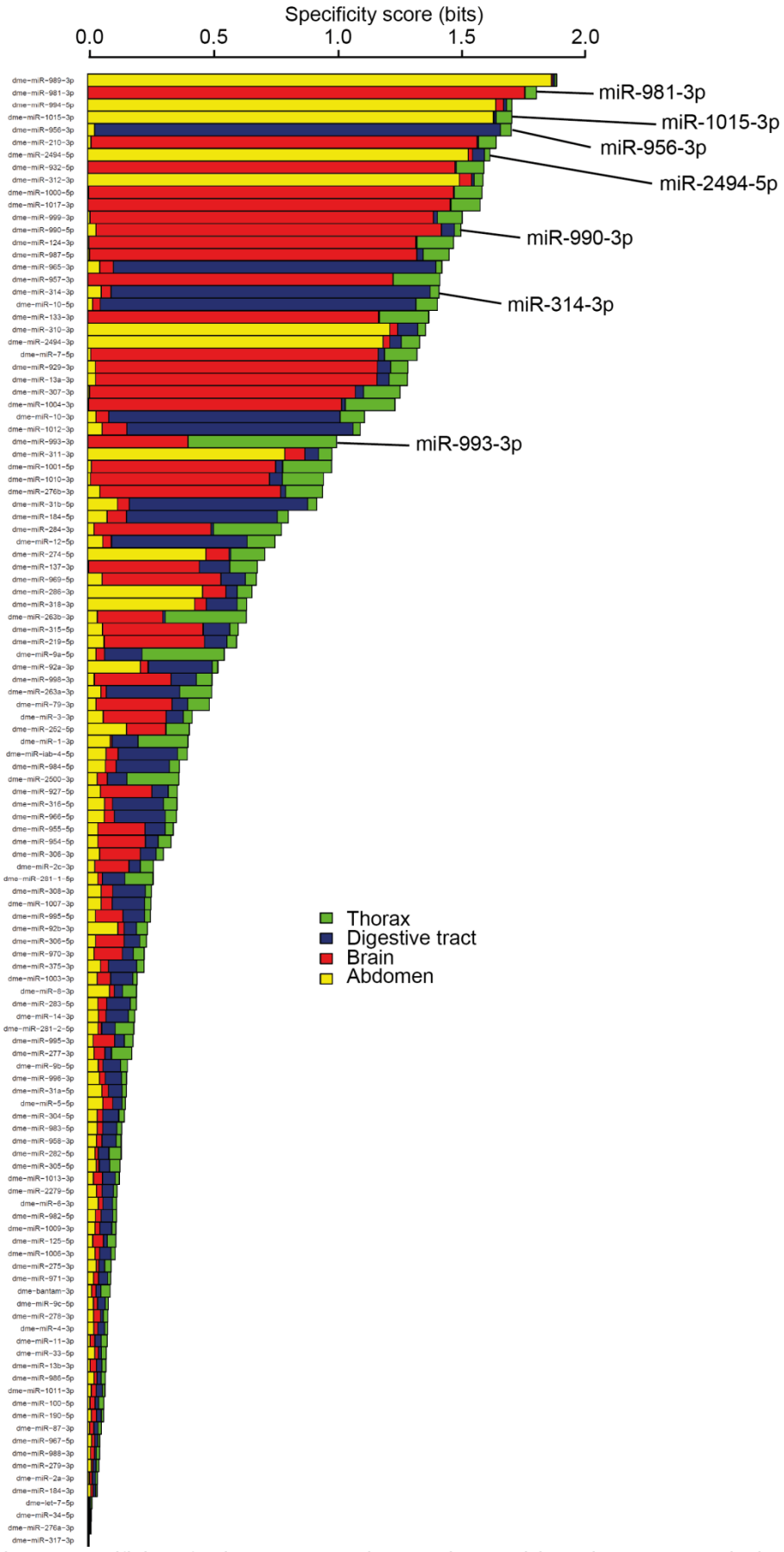

Figure 2.3: Tissue specificity of miRNA expression as detected by microarray analysis in wild type

flies. The total length of each bar represents the tissue specificity and the relative length for each of the tissues are proportional to miRNA expression in a given tissue type relative to all tissue types. Only miRNAs with an expression value of 15 or greater were included in the analysis.

2.1.4 Evolutionary conservation of microRNAs does not correlate with expression level as detected by microarray

In diverse species including *Drosophila* it was shown that evolutionarily conserved miRNAs normally have higher expression levels than non-conserved miRNAs (Ruby *et al*., 2006; Ruby *et al*., 2007; Bartel, 2004). In order to examine whether highly evolutionarily conserved miRNAs are stronger expressed than less conserved miRNAs in our microarray study, I compared the phylogenetic conservation of miRNAs with their expression level. miRNAs were ranked in five classes according to the degree of evolutionary conservation. I distinguished between miRNAs that were found to be unique for *Drosophila melanogaster*, or conserved in Drosophilidae, insects, Ecdysozoa and Bilateria. To assign a miRNA to a conservation class, I searched for miRNA family members in other species as annotated on miRBase and examined the phylogenetic relation to *D. melanogaster*. In contrast to the previous studies, with a Pearson correlation coefficient of 0.03 I found no correlation between expression level and evolutionary conservation in our microarray data set (Figure 2.4 A).

2.1.5 Expression level as detected by microarray does not correlate with tissue specificity

Previous studies have suggested that miRNAs that are highly evolutionarily conserved tend to be ubiquitously expressed, while non-conserved miRNAs are expressed in a tissue-specific manner (Ruby *et al*., 2007). To analyze whether a similar trend was present in our microarray data set, I analyzed the correlation between evolutionary conservation and tissue specificity. Among tissue-specifically expressed miRNAs we found conserved as well as non conserved miRNAs (Figure 2.4 B). Expression of conserved miRNAs as well as non-conserved miRNAs was also found to be evenly distributed across tissues. Thus, with a Pearson correlation coefficient of -0.14, no correlation between degree of conservation and breadth of expression was found in adult tissues of *Drosophila* as detected by microarray.

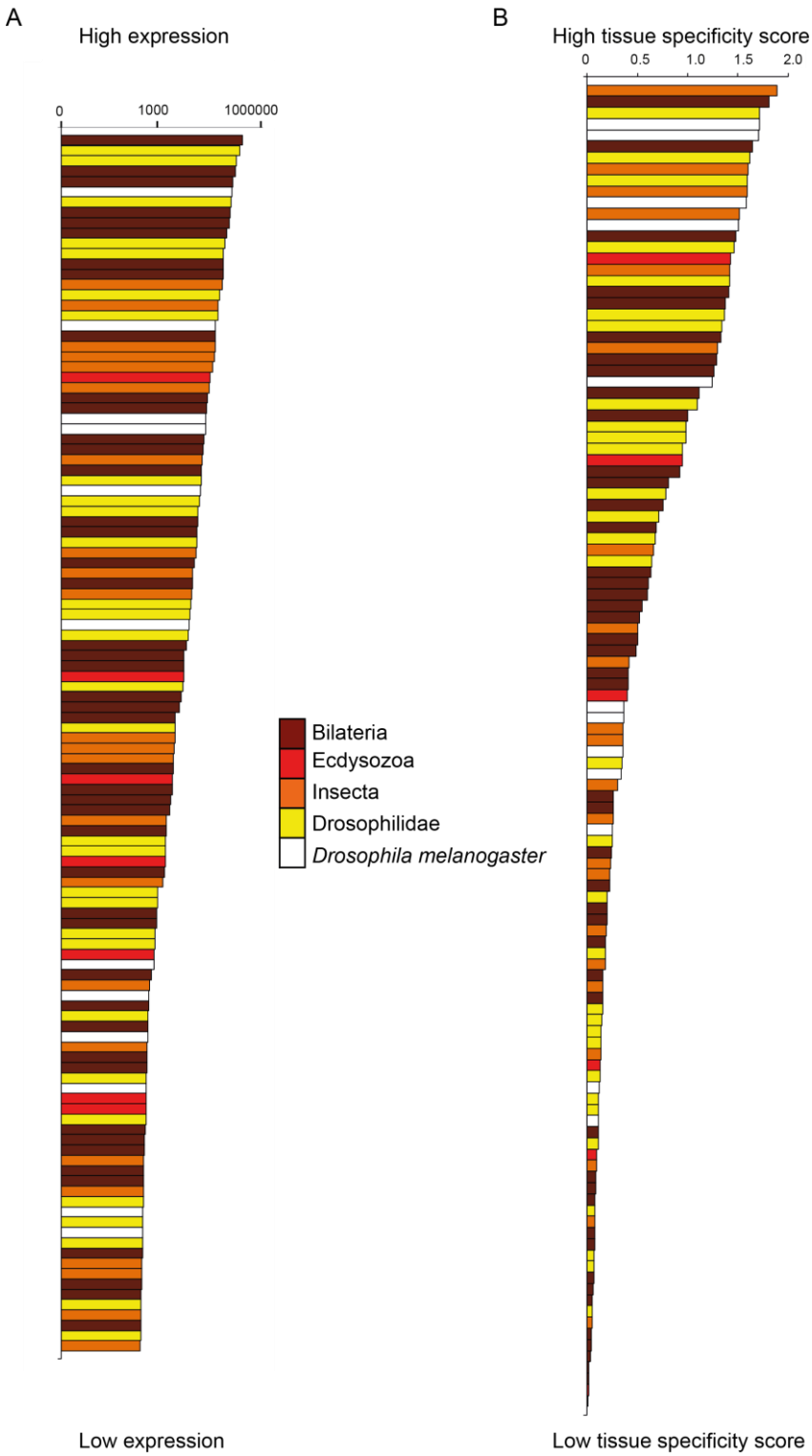

Figure 2.4: Correlation of evolutionary conservation and tissue specificity or absolute expression of miRNAs, respectively. For both comparisons no correlation was observed. (A) Relationship between absolute expression and evolutionary conservation of miRNAs. (B) Relationship between tissue specificity and evolutionary conservation of miRNA expression as detected by microarray analysis.

2.1.6 Identification of differentially expressed microRNAs in four tissues of *dilp2-3,5* mutants

In order to identify differentially expressed miRNAs in *dilp2-3,5* tissues, the expression of single miRNAs was compared with the expression in wild type tissues. Differentially expressed miRNAs were detected in all tissues (Table 2-5). When assessed by row wise t-test, in the brain 6 miRNAs were significantly down-regulated and 5 were up-regulated. 2 miRNAs were found to be down-regulated in the thorax and 11 were found to be up-regulated. In the digestive tract of *dilp2-3,5* flies 7 miRNAs were down-regulated while 4 were up-regulated. In the abdomen 4 miRNAs were down-regulated and also 4 miRNAs were up-regulated. In total, 40 miRNAs were found to be differentially expressed in *dilp2-3,5* mutant flies. 7 miRNAs had a fold change over 1.5 or under 0.5, respectively. mir-986-5p had the highest fold change with 3.26 in the thorax. The strongest down-regulated miRNA was miR-2500-5p in the brain. Most miRNAs had a moderate fold change and were regulated tissue-specifically, however miRNAs like miR-986-5p and miR-978-3p were differentially regulated in more than one tissue. Some miRNAs like miR-285-3p or miR-1000-5p were down-regulated in one tissue, but up-regulated in other tissues, suggesting complex tissue-specific miRNA regulation in response to reduced insulin signaling. However, a table-wide statistical test could not confirm significance for differential expression.

Brain					
miRNA	Mean wt	Mean *dilp2-3,5*	FC	p-value	p-value (adjusted)
dme-miR-2500-5p	77.83	39.54	0.51	0.00	0.19
dme-miR-285-3p	32.87	20.41	0.62	0.02	0.52
dme-miR-998-3p	1751.55	1142.64	0.65	0.02	0.52
dme-miR-1014-3p	19.48	14.46	0.74	0.01	0.52
dme-miR-2497-5p	14.96	11.86	0.79	0.01	0.52
dme-miR-308-3p	18.98	16.41	0.87	0.05	0.78
dme-let-7-5p	8804.45	10297.69	1.17	0.05	0.78
dme-miR-9b-5p	13.44	18.25	1.36	0.02	0.52
dme-miR-960-5p	13.82	18.78	1.36	0.01	0.52
dme-miR-10-3p	1535.48	2109.08	1.37	0.04	0.78
dme-miR-986-5p	59.28	141.32	2.38	0.02	0.52

Table 2: Differentially expressed miRNAs in *dilp2-3,5* brains as detected by microarray. Mean represents miRNA expression in three independent replicates of each genotype. P-values are calculated by Student's t-test and adjusted by Benjamini-Hochberg procedure. FC, fold change; wt, wild type

Thorax					
miRNA	Mean wt	Mean *dilp2-3,5*	FC	p-value	p-value (adjusted)
dme-miR-992-3p	17.52	13.34	0.76	0.05	0.44
dme-miR-307b-5p	19.60	15.75	0.80	0.05	0.44
dme-miR-276a-3p	36760.54	39592.58	1.08	0.05	0.44

dme-miR-2501-3p	16.24	18.12	1.12	0.03	0.44
dme-miR-303-5p	18.17	22.50	1.24	0.02	0.44
dme-miR-4-3p	14.98	18.72	1.25	0.01	0.44
dme-miR-985-3p	16.77	22.34	1.33	0.04	0.44
dme-miR-3-3p	42.06	59.84	1.42	0.03	0.44
dme-miR-263b-3p	11030.76	15713.83	1.42	0.04	0.44
dme-miR-1000-5p	224.59	332.69	1.48	0.04	0.44
dme-miR-210-3p	659.88	1292.84	1.96	0.00	0.44
dme-miR-954-5p	122.38	240.41	1.96	0.03	0.44
dme-miR-986-5p	92.04	300.04	3.26	0.00	0.35

Table 3: Differentially expressed miRNAs in *dilp2-3,5* thoraces as detected by microarray. Mean represents miRNA expression in three independent replicates of each genotype. P-values are calculated by Student's t-test and adjusted by Benjamini-Hochberg procedure. miRNAs that were detected as differentially regulated in the pre-test are highlighted in bold. FC, fold change; wt, wild type

Digestive tract

miRNA	Mean wt	Mean *dilp2-3,5*	FC	p-value	p-value (adjusted)
dme-miR-2494-5p	17.14	12.40	0.72	0.05	0.66
dme-miR-12-5p	9301.95	6747.07	0.73	0.03	0.66
dme-miR-1012-3p	35.93	27.56	0.77	0.02	0.66
dme-miR-985-3p	24.38	20.20	0.83	0.02	0.66
dme-miR-1004-3p	20.63	17.38	0.84	0.01	0.66
dme-miR-1000-5p	16.75	14.15	0.84	0.03	0.66
dme-miR-309-3p	15.88	13.81	0.87	0.05	0.66
dme-miR-1011-3p	12.77	14.35	1.12	0.02	0.66
dme-miR-927-5p	13.19	15.04	1.14	0.04	0.66
dme-miR-978-3p	11.96	14.46	1.21	0.01	0.66
dme-miR-2280-3p	13.98	17.88	1.28	0.05	0.66

Table 4: Differentially expressed miRNAs in *dilp2-3,5* digestive tracts as detected by microarray. Mean represents miRNA expression in three independent replicates of each genotype. p-values are calculated by Student's t-test and adjusted by Benjamini-Hochberg procedure. FC, fold change; wt, wild type

Abdomen

miRNA	Mean wt	Mean *dilp2-3,5*	FC	p-value	p-value (adjusted)
dme-miR-308-3p	19.34	14.74	0.76	0.05	0.90
dme-miR-iab-4-3p	16.76	13.33	0.80	0.01	0.75
dme-miR-14-3p	17.15	13.81	0.81	0.00	0.75
dme-miR-274-5p	27157.96	23190.94	0.85	0.01	0.75
dme-miR-1004-3p	15.39	18.14	1.18	0.03	0.90
dme-miR-1009-3p	14.99	18.46	1.23	0.02	0.75
dme-miR-285-3p	15.19	23.84	1.57	0.04	0.90
dme-miR-978-3p	15.57	41.03	2.64	0.03	0.90

Table 5: Differentially expressed miRNAs in *dilp2-3,5* abdomen as detected by microarray. Mean represents miRNA expression in three independent replicates of each genotype. p-values are calculated by Student's t-test and adjusted by Benjamini-Hochberg procedure. FC, fold change; wt, wild type

2.1.7 MicroRNA expression in the thorax as detected by microarray is reproducible

2.1.7.1 Verification of differentially expressed microRNAs in independent thorax samples

To assess whether data are reproducible between independent sample preparations, results from manually dissected thoraces were compared with the results of the pre-test where mechanically dissected thoraces were used. Only miRNAs with probe sets on both chips were analyzed. Consistent with the observation from the pre-test that most differentially expressed miRNAs were up-regulated in the thorax, in manually dissected thoraces only two miRNAs were down-regulated and 11 miRNAs were up-regulated (Table 3). In comparison with the pre-test, we detected less miRNAs to be significantly differentially expressed in the thorax with the new chips. Due to technical problems with these chips, two of three replicates for *dilp2-3,5* thoraces had to be hybridized for a second time with the same RNA. To check whether the second hybridization influences miRNA profiles, we analyzed correlation of the chips by Pearson. Indeed, profiles from chips which were hybridized twice were most distinct from the other profiles (Figure 2.5 A).

To test whether this technical variation affected the identification of differentially expressed miRNAs, we used Pearson correlation to compare detected fold changes of the pre-test and the manually dissected thoraces. The fold change profiles had a relative low Pearson correlation index of 0.36 (Figure 2.5 B). However, miRNAs which were significantly differentially expressed, were to a large extend congruent between the two chips (Table 3) Thus, the second hybridization did affect the sensitivity of detection of fold changes of miRNAs, but it had minor effects on the identity of differentially expressed miRNAs. Therefore, thorax miRNA expression data are consistent and reproducible between independent sample preparations and additionally, between different types of microarray.

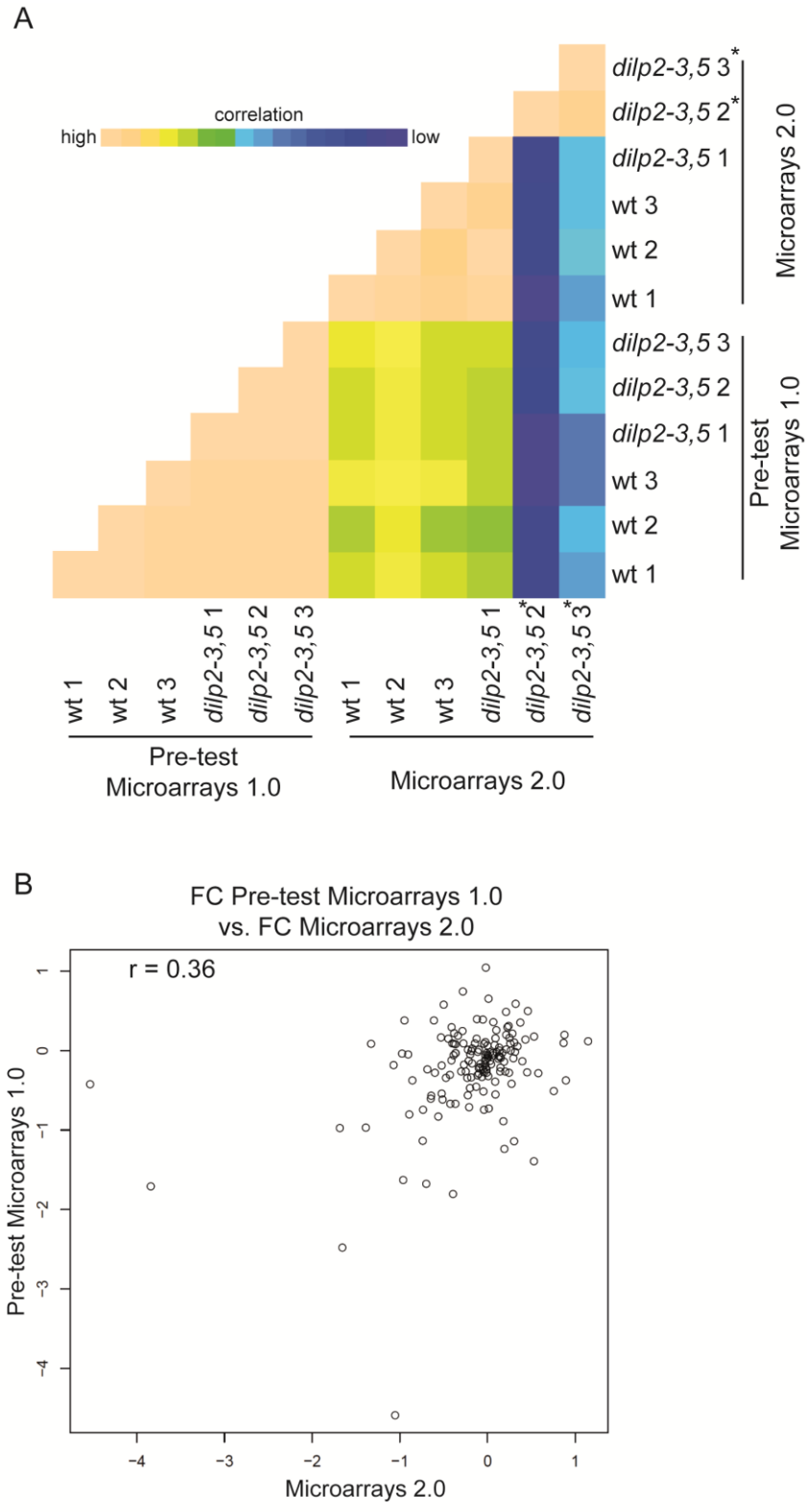

Figure 2.5: Comparison of thorax profiles of microarray 1.0 (pre-test) and microarray 2.0. (A) Absolute expression profiles. Pearson correlation coefficient for all pairwise comparisons was computed and the values are depicted color-coded. Only miRNAs with probe sets on both chips are analyzed. Samples from the same chip-type cluster. Chips that were hybridized twice due to technical reasons are marked with asterisks. Notably, profiles from chips that were hybridized for a second time, show strong clustering and were most distinguishable from other profiles. (B) Comparison of fold change data as detected by microarrays 1.0 (pre-test) and microarrays 2.0. Pearson correlation coefficient of fold change data was computed and revealed low correlation. FC, fold change; wt, wild type.

2.1.7.2 Verification of differentially expressed microRNAs by quantitative RT-PCR

In order to verify the results from the microarray analysis, expression of selected miRNAs was tested by quantitative Real-time-PCR (q-RT-PCR). Due to limited availability of dissected tissue, the same RNA samples that were used for microarray experiments were also used for the qRT-PCR analysis.

Upregulation of miR-986-5p and downregulation of 2500-5p in the brain was confirmed by qRT-PCR (Figure 2.6 A). In contrast, downregulation of miR-285-3p as measured by microarray, could not be confirmed by qRT-PCR. miR-986-5p, miR-210-3p and miR-1000-5p were all up-regulated by microarray analysis in the thorax. Although upregulation did not reach significance, similar tendencies were observed in the qRT-PCR analysis (Figure 2.6 B).

Additionally, differential expression of miR-2500-5p, which was significantly down-regulated in the brain, was tested in the thorax. By microarray miR-2500-5p showed a non-significant tendency to be down-regulated. However, qRT-PCR revealed a significant down-regulation in this tissue. Because we could verify differential expression of selected miRNAs in the brain and in the thorax, we tested whether those miRNAs were also differentially expressed in digestive tract and abdomen. By microarray, miR-210-3p, miR-285-3p, miR-986-5p and miR-2500-5p tended to be differentially expressed in the digestive tract (Figure 2.6 C). This tendency was reproduced by qRT-PCR. In the abdomen upregulation of miR-285-3p by microarray was observed. By qRT-PCR a tendency of upregulation of miR-285-3p was confirmed, although this was not significant (Figure 2.6 D). Microarrays could not detect differential expression of miR-210-3p in the abdomen and this was confirmed by qRT-PCR. However, miR-986-5p, which had a tendency of up-regulation by microarray was confirmed to be up-regulated significantly by qRT-PCR. miR-2500-5p expression was not changed as detected by microarray. However, qRT-PCR revealed that it is down-regulated by trend in the abdomen, like in every other tissue analyzed.

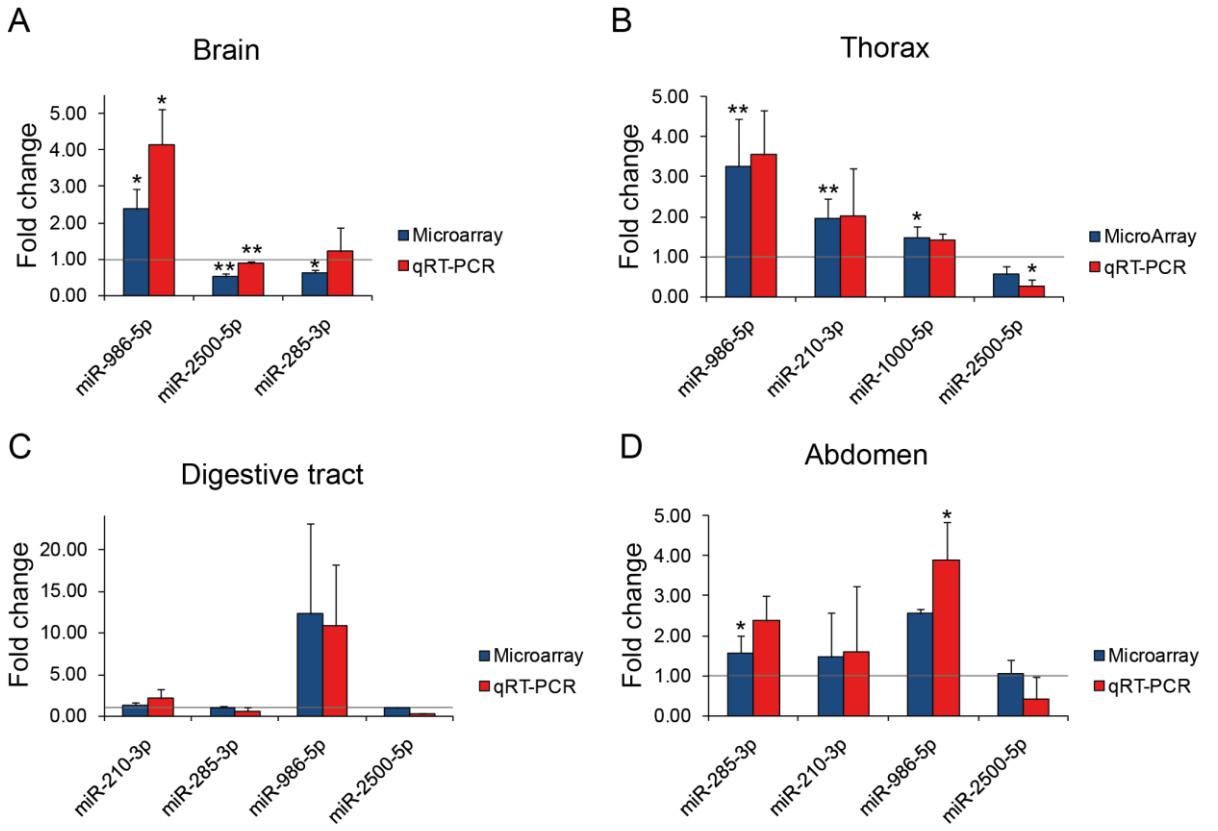

Figure 2.6: qRT-PCR analysis verifies differential expression of most miRNAs in *dilp2-3,5* tissues as detected by microarrays. Fold change in (A) brain, (B) thorax, (C) digestive tract and (D) abdomen from microarray and qRT-PCR analysis are compared. * p<0.05; ** p<0.01,Student's t-test for qRT-PCR, Benjamini-Hochberg for microarray data. miRNA transcript level was normalized to wild type samples, which by default was set to 1.

Taken together, miRNAs are tissue-specifically expressed in *Drosophila*. Tissue-specificity or expression level did not correlate with evolutionary conservation, when assessed by microarray. Differentially expressed miRNAs in *dilp2-3,5* mutants were found by microarray. By qRT-PCR differential expression for most miRNAs was confirmed. Interestingly, differentially expressed miRNAs, such as miR-2500-5p and miR-986-5p, which by microarray were found to be differentially expressed in brain and thorax, were also regulated in digestive tract and abdomen of *dilp2-3,5* flies. These results suggest that the sensitivity of microarrays may be limiting for some miRNAs to detect differential expression and demonstrates that verification by qRT-PCR is essential to conclude about tissue-specific regulation.

2.2 Functional *in vivo* characterization of differentially expressed microRNAs

By microarray, differentially expressed miRNAs were identified. These miRNAs might execute functions that mediate phenotypes observed for *dilp2-3,5* flies such as lifespan extension, reduced organismal growth, reduced fecundity and increased development time. MiRNAs with significant expression fold change of >1.5 or <0.5 were selected to analyze their role in IIS related phenotypes (Fig. 2.7 A). These included miR-986, miR-210, miR-954, miR-285 and miR-978. Although, miR-7 did not match the selection criteria, it was included in the analysis to represent a differentially expressed miRNA in the digestive tract. Additionally, miR-2500 was added to the analysis because of a consistent and reproducible down-regulation in every tissue also in other *Drosophila* IIS mutants and under different food conditions (Supplemental Figure S1).

A

	miRNA	FC
Brain	miR-986-5p	2.38
	miR-2500-5p	0.51
Thorax	miR-210-3p	1.96
	miR-986-5p	3.26
	miR-954-5p	1.96
Digestive tract	miR-7-5p	0.57
Abdomen	miR-285-3p	1.57
	miR-978-3p	2.64

B

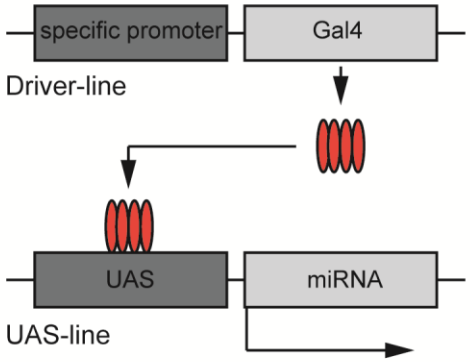

C

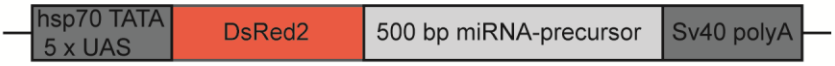

Figure 2.7: Overexpression of candidate miRNAs is achieved by the Gal4/UAS system. (A) Candidate miRNAs as detected by microarray in *dilp2-3,5* tissues of *Drosophila* melanogaster. Shown are miRNAs with a significant expression fold change of more than 1.5 or less than 0.5 in comparison to wild type tissues with $p<0.05$, Student's t-test. (B) The Gal4/UAS system for miRNAs in *Drosophila melanogaster*. In flies generated by the cross of a driver-line to an UAS-line, Gal4 is expressed in a promoter-dependent manner and can activate transcription of the miRNA by binding to upstream activation sites (UAS). (C) Transgene construct used to generate UAS lines. Transgenic flies contain 500 bp of the genomic region of the miRNA precursor under the control of the hsp70 TATA UAS (5x). The construct also includes DsRed2 and a SV40 polyadenylation (polyA) signal. UAS-lines were kindly provided by Dr. Eric Lai.

To study their function, candidate miRNAs were overexpressed *in vivo* using the Gal4/UAS system (Figure 2.7 B). For each miRNA UAS-overexpression lines were kindly provided by Dr. Eric Lai from the Sloan Ketterin Institute, New York. The inserted overexpression transgene included approximately 500 bp of the genomic region including the miRNA precursor cloned into a vector containing the hsp70 promoter with 5 UAS sites and DsRed for visualization of overexpression (Figure 2.7 C).

2.2.1 Organismal growth and development time of flies overexpressing microRNAs

dilp2-3,5 mutants have a reduced body weight due to decreased organismal growth and a severely increased development time (Grönke *et al*., 2010). In order to investigate a putative role of the candidate miRNAs in the regulation of body size and developmental timing, body weight and egg to adult development time of flies with ubiquitous overexpression of miRNAs during development were determined. Overexpression of miR-2500 and miR-954 did not affect body weight (Figure 2.10 A) nor development time (Figure 2.10 B), suggesting that those miRNAs do not play an important role during development. Overexpression of miR-986 also had no effect on body weight, but these flies were slightly developmental delayed. The delay of male flies was stronger than of female flies, suggesting that miR-986 might regulate development time in a gender-specific manner.

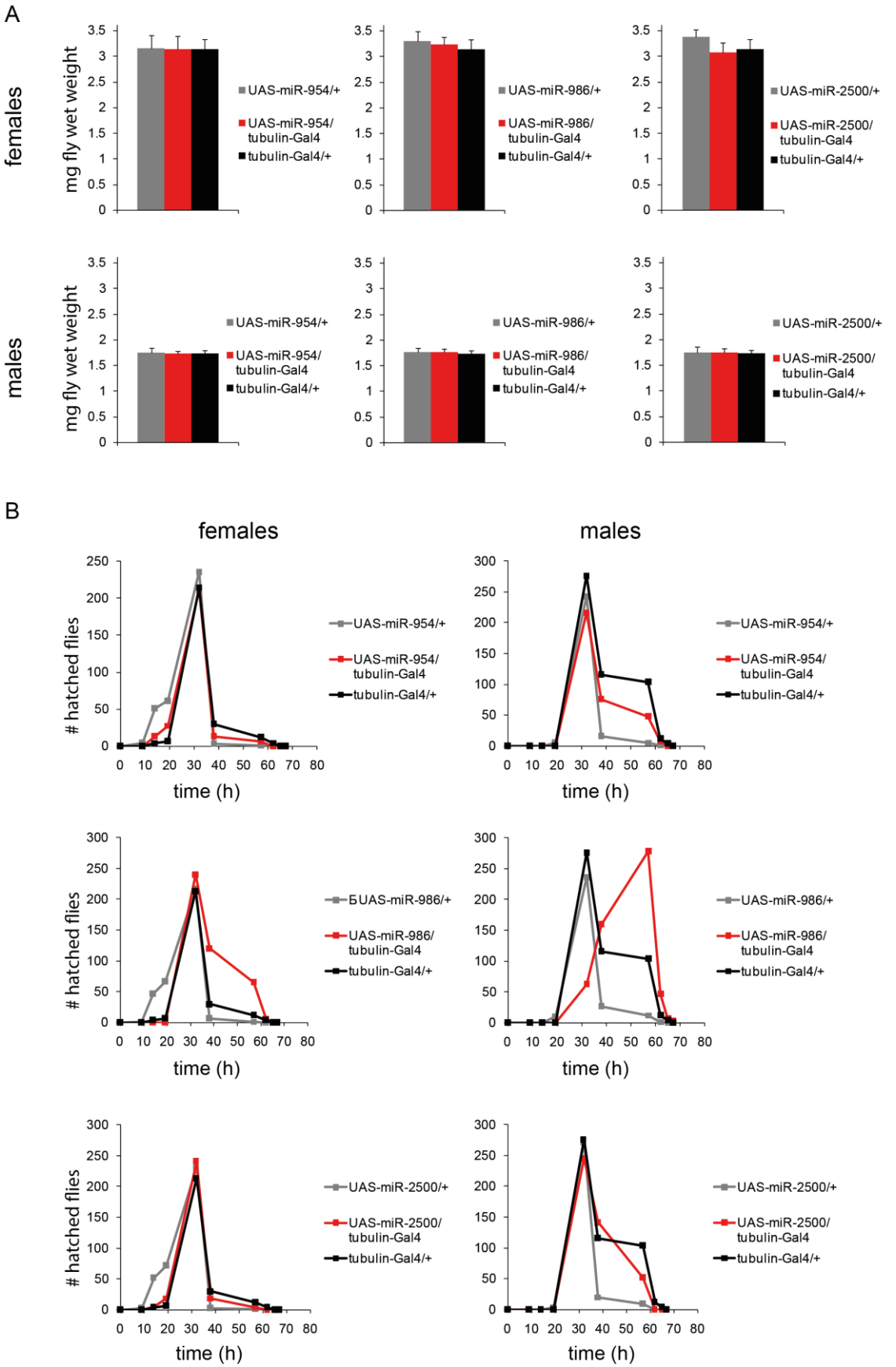

Figure 2.8: Body weight and development time of flies overexpressing miR-986, miR-2500 or miR-954. (A) Body weight of flies overexpressing miR-986, miR-2500 or miR-954 was not changed in both sexes. Flies were measured in pairs, therefore results reflect the mean body weight of two flies. n=20 flies per genotype and sex. (B) Overexpression of miR-986, but not miR-2500 or miR-954 did increase development time in both sexes.

2.2.2 Lifespan and fecundity of strongly ubiquitously overexpressed microRNAs

In order to analyze whether selected candidate miRNAs might play a role in lifespan regulation, these miRNAs were overexpressed and lifespan of overexpressing flies was measured. For overexpression we used the constitutive tubulin-Gal4 driver line, which drives strong ubiquitous expression both during development and adulthood. Overexpression of miR-978 and miR-7 caused embryonic lethality, suggesting toxic effects during development. To bypass developmental lethality, both miRNAs were overexpressed using an inducible tubulin-GeneSwitch (tubulinGS) driver, which allows expression to be restricted to adulthood (Osterwalder *et al*., 2001). Degree of induced overexpression was measured by qRT-PCR. Overexpression of miR-285 was not detected; therefore miR-285 was excluded from further analysis (Supplemental Figure S2). In all other tested miRNA lines, strong overexpression ranging from 26.71- to 791.24-fold was detected (Figures 2.9 and 2.10). Adult-specific overexpression of miR-978 and miR-7 resulted in a severe reduction of median lifespan by 22.14 % (Figure 2.10 A) and 71.43 % (Figure 2.10 B), respectively. This reduction in adult lifespan is consistent with their detrimental role upon overexpression during development. Overexpression of miR-986 and miR-954 caused moderate but significant reduction in lifespan (Figure 2.9 A, C) while overexpression of miR-2500 did not significantly affect lifespan compared to controls (Figure 2.9 B).

In order to analyze the role of selected miRNAs in the regulation of fecundity, egg production of miRNA overexpressing flies was measured. Adult-specific overexpression of miR-978 (Figure 2.10 A) and miR-7 (Figure 2.10 B) resulted in severe reduction in fecundity. In contrast, egg production of flies overexpressing miR-986, was only slightly reduced (Figure 2.9 A) and fecundity of miR-2500 or miR-954 overexpressing flies was not changed compared to controls (Figure 2.9 B, C).

In summary, tubulin-Gal4/GS mediated overexpression of miRNAs negatively affected lifespan and fecundity, suggesting that strong ubiquitous overexpression of the selected miRNAs is detrimental for fly health.

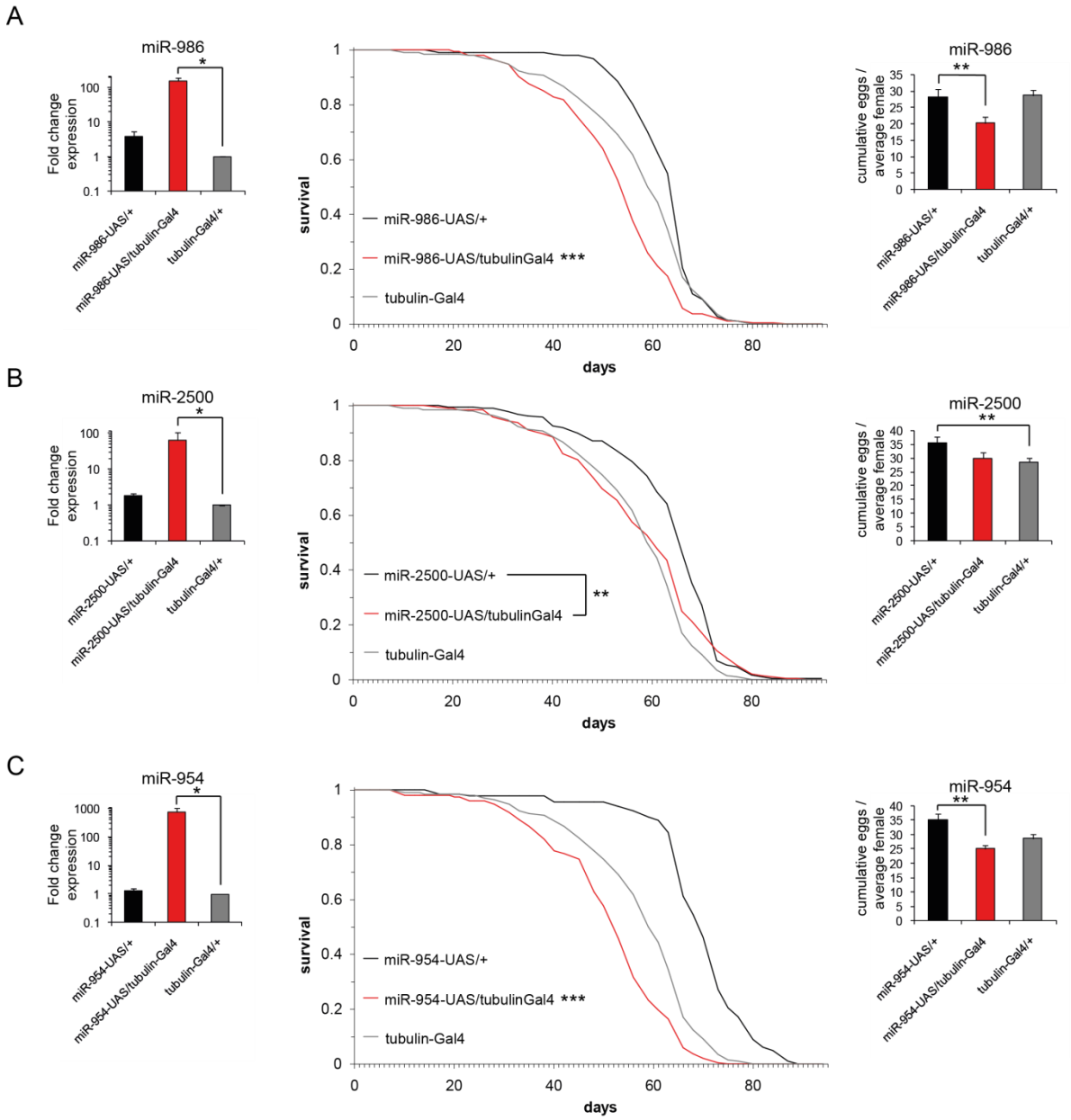

Figure 2.9: Expression level, lifespan and fecundity of flies overexpressing miRNAs with a strong ubiquitous driver. Overexpression of (A) miR-986, (B) miR-2500 and (C) miR-954 with tubulin-Gal4 was confirmed by qRT-PCR. * p<0.05,Kruskal-Wallis test, Dunn's test for multiple comparisons. Lifespan of miR-986 or miR-954 overexpressing flies were shortened compared to both controls, respectively (*** p<0.001, log-rank test). Survival of miR-2500 overexpressing flies was not changed compared to the tubulin-Gal4 control. Fecundity of miR-986 and miR-954 overexpressing flies was reduced and not changed for flies overexpressing miR-2500. ** p<001, Kruskal-Wallis test, Dunn's test for multiple comparisons.

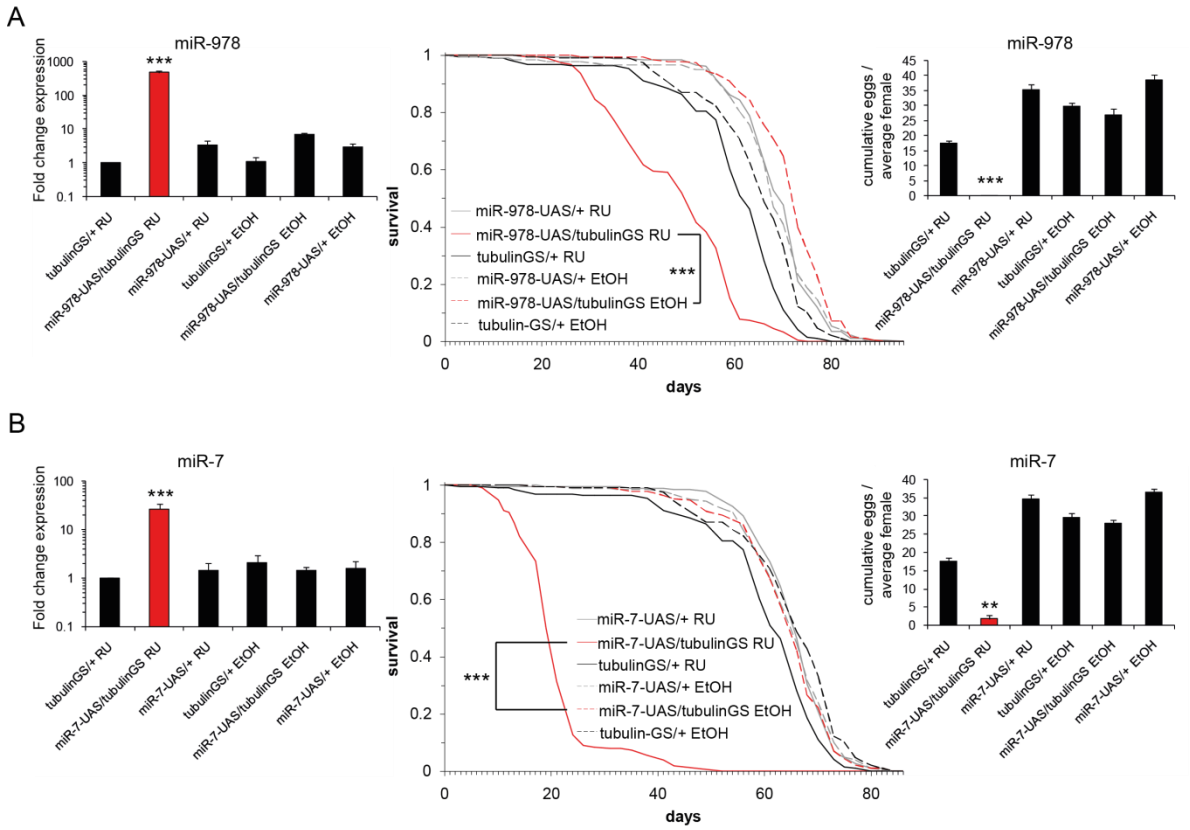

Figure 2.10: Expression level, lifespan and fecundity of flies overexpressing miRNAs with a strong ubiquitous inducible driver. Overexpression of (A) miR-978 and (B) miR-7 with tubulin-GS was confirmed by qRT-PCR. ***p<0.001, Kruskal-Wallis test, Dunn's test for multiple comparisons. Lifespan of miR-978 or miR-7 overexpressing flies is shortened (*** p<0.001, log-rank test). Fecundity of miR-978 and miR-7 overexpressing flies was dramatically reduced. *** p<001, Kruskal-Wallis test, Dunn's test for multiple comparisons.

2.2.3 Lifespan of mildly ubiquitously overexpressed microRNAs

In contrast to the very strong overexpression achieved by the tubulin-Gal4 driver (Figures 2.9 and 2.10) miRNAs that were identified in the microarray analysis only showed small fold changes in the range of 1.5-14 fold induction in the *dilp2-3,5* mutants compared to controls (see chapter 2.1.6). As strong overexpression was detrimental to flies, we reasoned that induction that resembles more the physiological conditions might cause different, beneficial effects on lifespan. In order to achieve low-level overexpression of specific miRNAs we used the UAS-miRNA lines in combination with the inducible daughterless-GeneSwitch (da-GS) driver (Figure 2.11). To determine the right induction conditions, i.e. concentration of RU486, for the lifespan analysis, flies were fed with increasing concentrations of RU486 (10, 25 and 50 µM) and miRNA induction was analyzed by qRT-PCR. As shown in Figure 2.11 expression level of miRNA increased with increasing amounts of RU486 and overall expression induction was smaller than when using the tubulin-Gal4 or tub-GS driver lines (compare Figure 2.11 with 2.9 and 2.10). Accordingly, lifespan was not decreased upon mild

overexpression of miR-986, miR-954 or miR-978, however, lifespan was also not increased. Ubiquitous overexpression of miR-210 with the da-GS driver still resulted in decreased median lifespan, demonstrating that even mild overexpression of this miRNA is detrimental for survival. In summary, none of the tested miRNAs caused lifespan extension upon moderate ubiquitous overexpression.

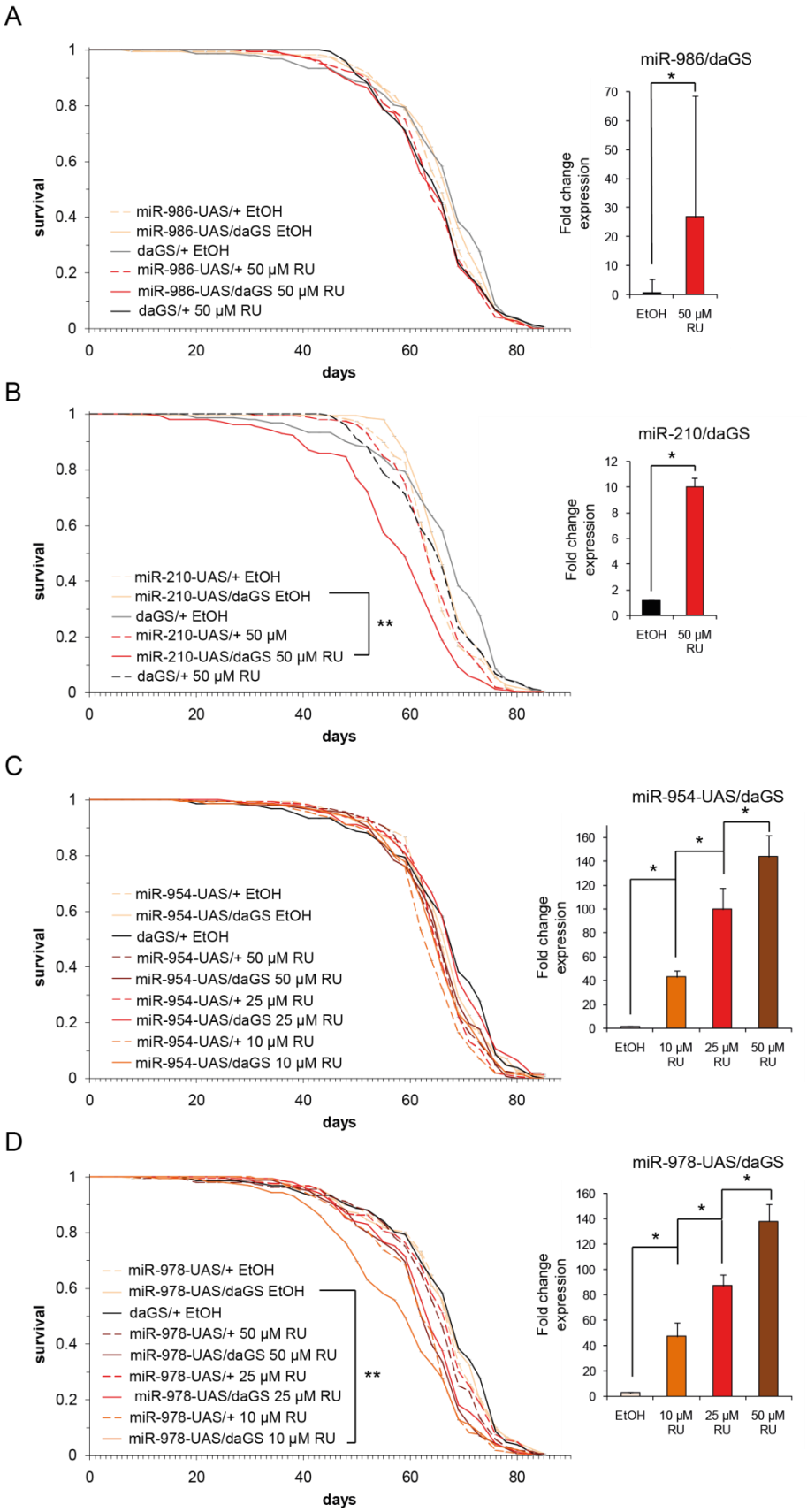

Figure 2.11: Survival and expression level of flies overexpressing miRNAs with the ubiquitous da-GS driver line. Overexpression using different RU-concentrations of (A) miR-986, (B) miR-210, (C) miR-954 and (D) miR-978 with da-GS was confirmed by qRT-PCR. * p<0.05, Kruskal-Wallis test, Dunn's test for multiple comparisons. Expression of miRNAs was directly correlated to RU486 (RU) concentration in the food. Overexpression of miR-986 or miR-954 did not affect lifespan, overexpression of miR-210 decreased lifespan (** p<0.01, log-rank test).

2.2.4 Lifespan analysis upon tissue-specific overexpression of microRNAs

miRNAs were up-regulated in specific tissues of *dilp2-3,5* mutants and maybe tissue-specificity is important for lifespan regulation. In order to test this hypothesis, we overexpressed the miRNAs in a tissue-specific manner according to which tissue they were up-regulated in the *dilp2-3,5* mutant flies (Figure 2.12). miR-210 and miR-954 were differentially expressed in the thorax, which consists to a large extend of muscle tissue. However, overexpressing miR-210 or miR-954 specifically in the muscle using the MHC-Gal4 driver did not change lifespan compared to the controls. Similarly, overexpression of miR-978, which was found to be differentially expressed in the abdomen, with the abdominal fat body specific driver S_{106}-GS had no effect on lifespan. Therefore, tissue-specific overexpression of the selected candidate miRNAs had no beneficial effect on lifespan.

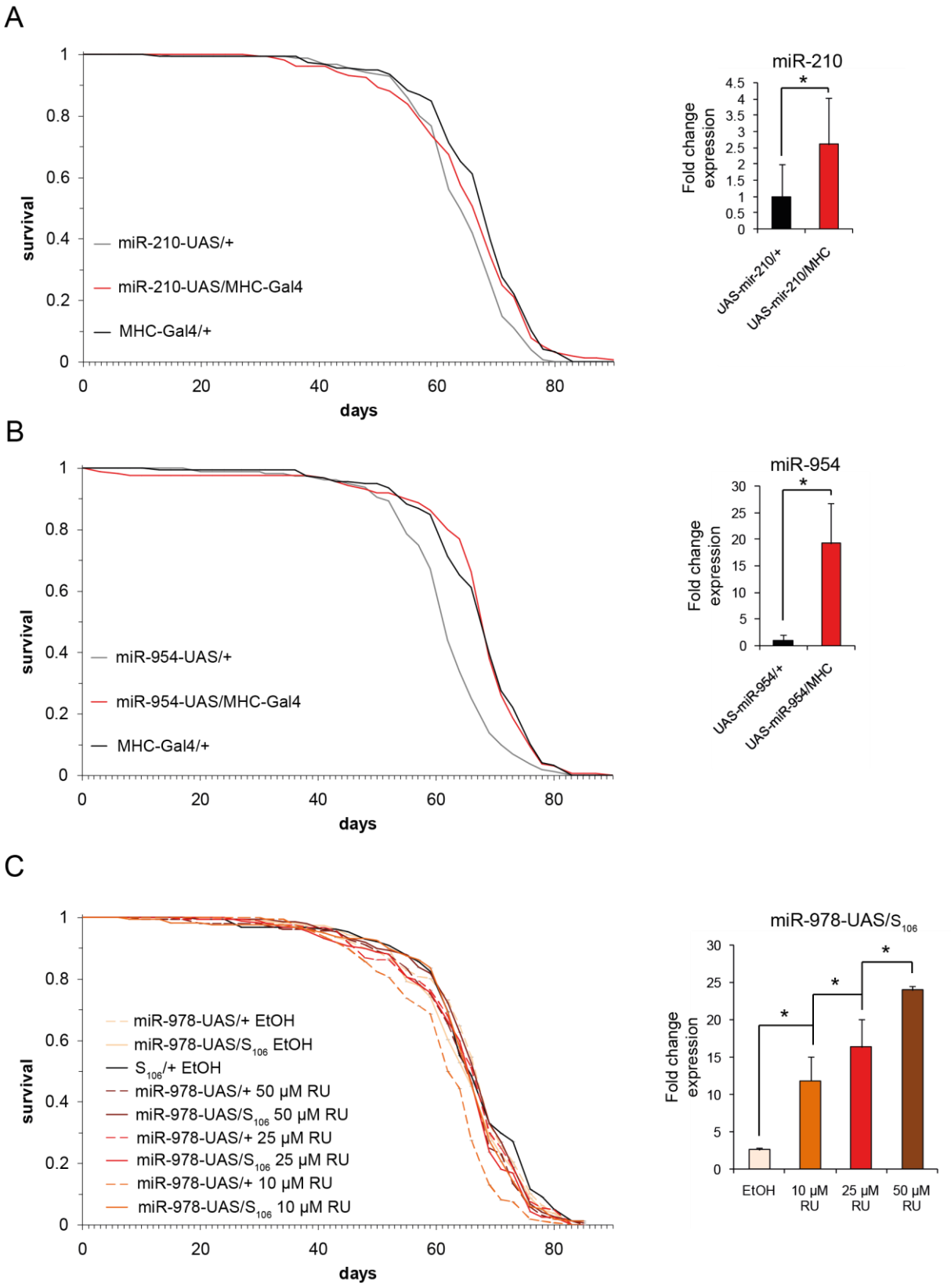

Figure 2.12: Survival and expression level of flies overexpressing miRNAs with tissue-specific drivers. Overexpression of (A) miR-210 and (B) miR-954 with the muscle-specific MHC-Gal4 driver and overexpression of (C) miR-978 with the fat-body specific S_{106}-GS driver using different RU-concentrations was confirmed by qRT-PCR (* $p<0.05$, Wilcoxon rank-sum test, Mann-Whitney for (A) and (B), Kruskal-Wallis test, Dunn's test for multiple comparisons for (C)) but did not change lifespan compared to controls.

2.3 The *Drosophila miR-986* knock-out mutant

2.3.1 Generation of a *Drosophila miR-986* knock-out mutant

miR-986 was one of the most strongly induced miRNAs in *dilp2-3,5* flies according to the microarray analysis, however, its function is currently unknown. Therefore I decided to study miR-986 *in vivo* function by generating a loss-of-function mutant. The *miR-986* precursor is located on the right arm of the 2nd chromosome, in sense orientation within the 3rd intron of the protein coding *Cyp4e2* gene (Fig. 2.13 A). *Cyp4e2* encodes for a cytochrome P450, an enzyme with oxidoreductase activity. Cytochrome P450s are suggested to be involved in the metabolism of insect hormones and the breakdown of insecticides (Chung *et al*., 2009). Cyp4e2 was recently identified as a putative methanol metabolizing enzyme (Wang *et al*., 2012).

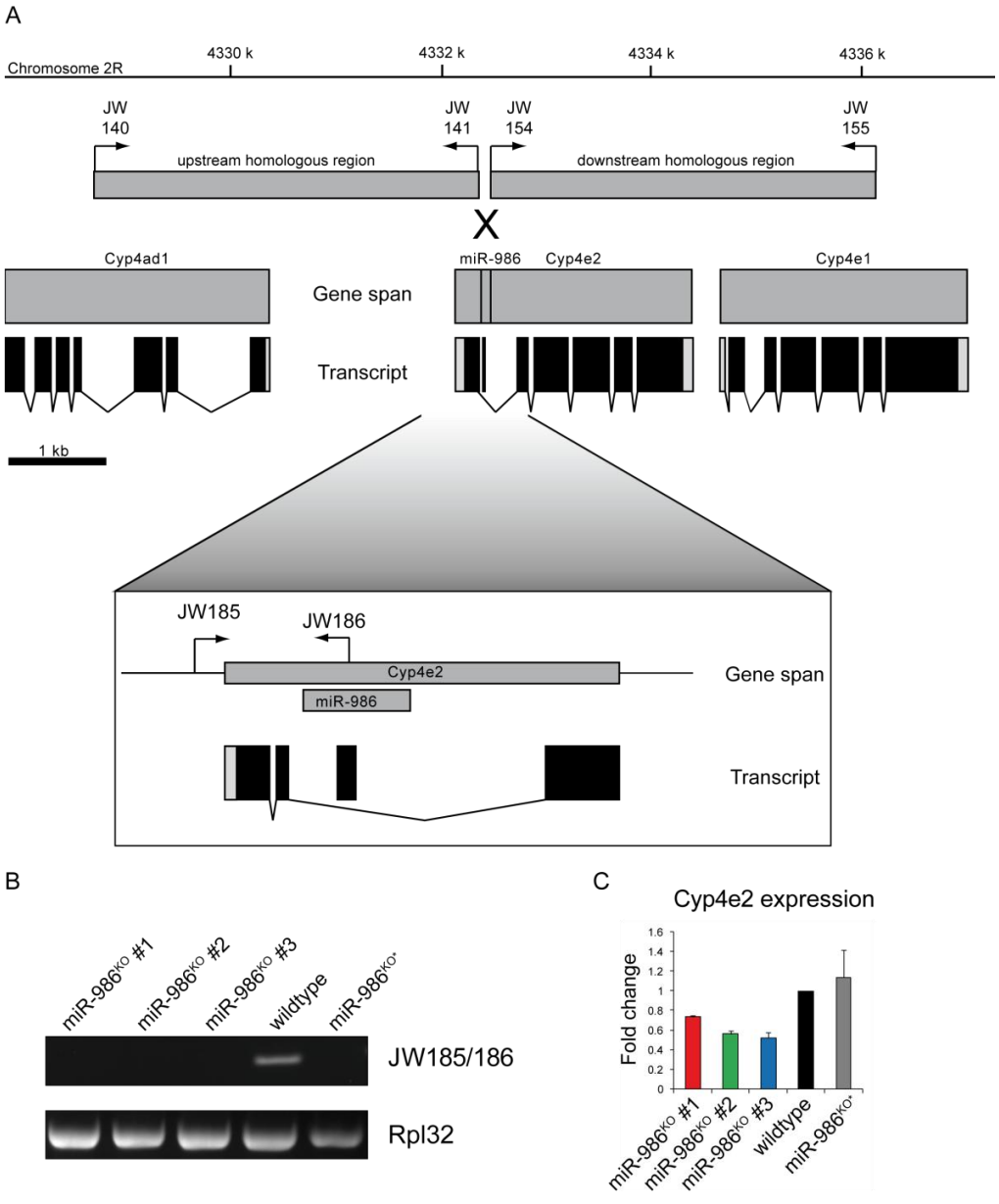

Figure 2.13: Generation of a *miR-986* knock-out mutant (*miR-986^{KO}*). (A) Ends-out homologous recombination was used to generate knock-out mutants of the *miR-986* gene which is located on the right arm of the 2nd chromosome, within the 3rd intron of *Cyp4e2*. (B) PCR verified the knock-out of *miR-986* in three independent targeting lines as well as in *miR-986^{KO*}* which excludes the mini-*white* gene. (C) Cyp4e2 expression was affected in *miR-986^{KO}* lines as tested by qRT-PCR and restored by removal of the mini-*white* marker.

In order to generate a *Drosophila mir-986* loss-of-function mutant (*miR-986^{KO}*) I used ends-out homologous recombination (Gong *et al*., 2003). In the first step, the *miR-986* precursor gene was replaced by homologous recombination with a mini-*white* marker gene. Knock-out of *miR-986* was verified by PCR with primers 185 and 186 (Figure 2.13 B). These primers produce a 535 bp fragment on wild type genomic DNA and no fragment on *mir-986* knock-out mutants. Three mutant lines from independent targeting events were verified and used for further analysis. In order to test whether Cyp4e2 expression was affected by insertion of the mini-*white* gene in these lines, qRT-PCR was performed (Figure 2.13 C). A slight but significant decrease in expression of Cyp4e2 was detected: line #1 showed 27 %, line #2 44 % and line #3 48 % reduction. Thus, Cyp4e2 is affected but still expressed in *miR-986^{KO}* mutants. In order to restore Cyp4e2 expression to wild type levels, the mini-*white* marker gene was removed from the *mir-986* locus by Cre recombinase-mediated excision for one of the three *miR-986^{KO}* lines. Excision of the marker gene was verified by eye color and deletion of *miR-986* was verified by PCR using primers 185 and 186. Removal of the *white* marker gene fully restored wild type expression levels of Cyp4e2 (Figure 2.13 C).

2.3.2 *In vivo* characterization of *miR-986^{KO}* mutants

For *in vivo* analysis three *miR-986^{KO}* lines including the *white* gene were used. Homozygous *miR-986^{KO}* mutant flies were viable and had no visible obvious phenotypes. Therefore, I analyzed their body weight, development time, lifespan, fecundity and stress resistance, all phenotypes that are affected by mutations in IIS (Figures 2.14 and 2.15).

Reduced IIS in flies causes reduced body size and a delay in development (Weinkove and Leevers, 2000; Rulifson *et al*., 2002; Grönke *et al*., 2010). Therefore, body weight and egg to adult development time of the three *miR-986^{KO}* mutants lines was assessed. *miR-986^{KO}* males and females had normal body weight, suggesting that miR-986 does not regulate organismal growth (Figure 2.14 A).

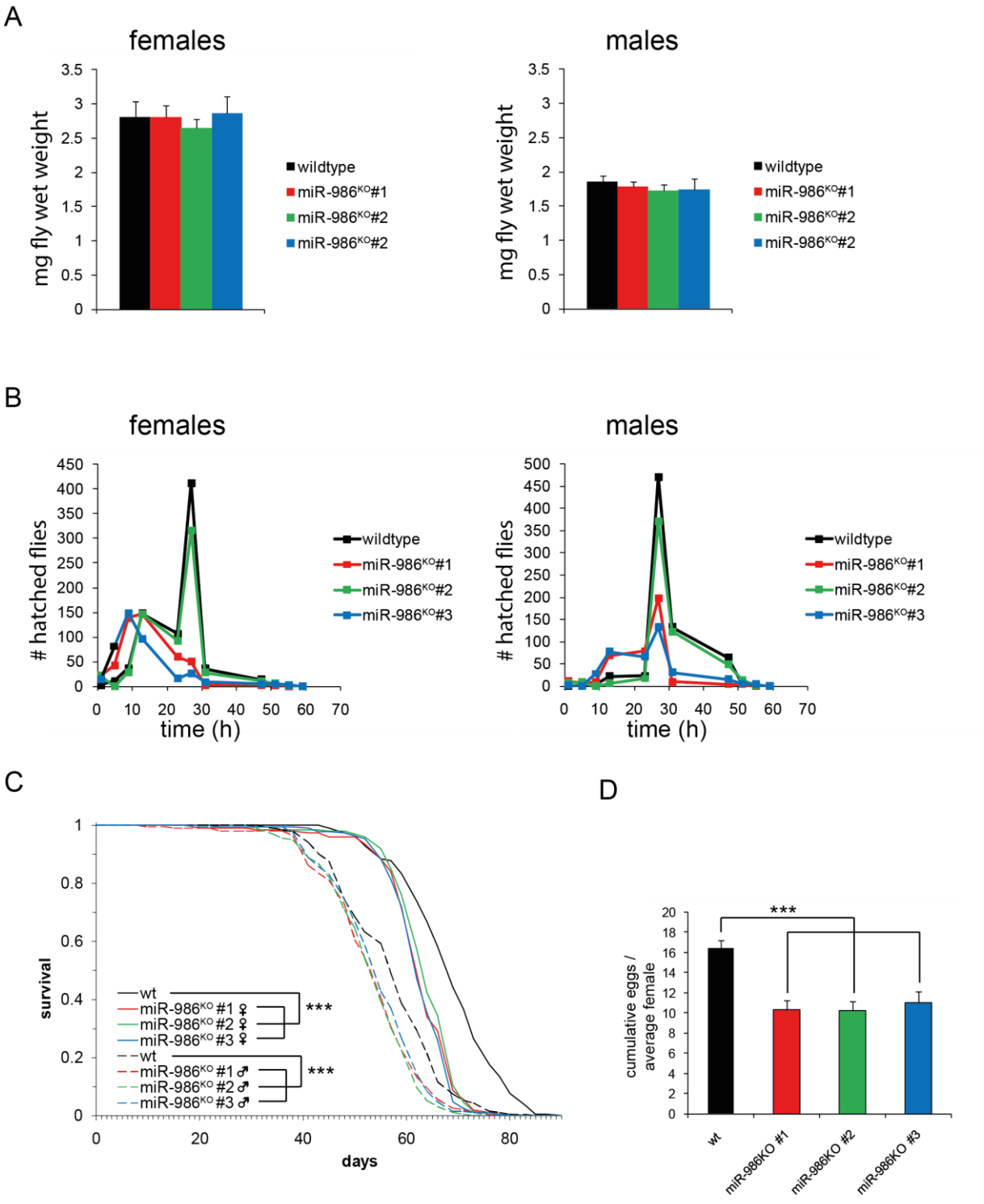

Figure 2.14: Body weight, development time, survival and fecundity of *miR-986*^{KO} mutants. (A) Body weight of *miR-986*^{KO} females and males was not changed. Flies were weighed in pairs. (B) Egg-to-adult development time of *miR-986*^{KO} mutant females and males. Only the hatching period of adult flies is shown. Two of three independent *miR-986*^{KO} lines hatched earlier than wild type flies. (C) Survival curves of *miR-986*^{KO} mutants. Female and male lifespan was decreased. *** p<0.001, log-rank test. (D) Fecundity of female *miR-986*^{KO} flies was decreased. *** p<0.001, Wilcoxon rank sum test.

Development time of two *miR-986*^{KO} strains was slightly shortened for males and for females (Figure 2.14 B). However, one strain had the same development time as wild type flies. Therefore, the shortened development time of the two other strains is likely to be a non-specific, miR-986-independent effect. Survival analysis of the three *miR-986*^{KO} lines revealed that lifespan of *miR-986*^{KO} males and females was reduced, suggesting that miR-986 is required for normal lifespan (Figure 2.14 C). Fecundity of *miR-986*^{KO} flies was also reduced as flies of all three *miR-986*^{KO} lines laid about 37 % less eggs than wild type flies suggesting that miR-986 might be involved in the regulation of fecundity (Figure 2.14 D).

dilp2-3,5 mutants were shown to be resistant to oxidative stress including paraquat and H_2O_2 (Grönke *et al*., 2010). If miR-986 mediates resistance to oxidative stress in *dilp2-3,5* mutants, *miR-986*^{KO} flies are expected to be sensitive to these stresses. In contrast, *miR-986*^{KO} flies survived significantly longer when exposed to paraquat (Figure 2.15 A). This suggests a putative role for miR-986 in the regulation of paraquat resistance but not in *dilp2-3,5* mediated paraquat resistance. When exposing *miR-986*^{KO} flies to H_2O_2 only one of three lines had reduced resistance (Figure 2.15 B). Therefore, miR-986 most likely does not account for H_2O_2 resistance.

Mutants with reduced IIS activity were shown to tolerate starvation conditions better than wild type flies as a result of suppressed nutrient storage and cell growth and the enabling of nutrient mobilization by energy storing tissues (Britton *et al*., 2002). *miR-986*^{KO} flies were sensitive to starvation, suggesting a putative role of miR-986 in the regulation of starvation response (Figure 2.15C). However, *dilp2-3,5* mutants do not have increased starvation resistance (Grönke *et al*., 2010). Therefore, it is likely that reduced starvation tolerance of *miR-986*^{KO} mutants is independent of IIS.

dilp2-3,5 mutants were shown to be resistant to the xenobiotic DDT (Grönke *et al*., 2010). Only one of three lines of *miR-986*^{KO} was significantly resistant to DDT (Figure 2.15 D). In the DDT assay *miR-986*^{KO} and wild type flies were kept separately on food containing the drug. Strikingly, over time the surface of the food of the mutants but not of wild type became smeary, most probably due to bacterial contamination. As this could affect the response to DDT, the assay was performed again, with wild type and *miR-986*^{KO} flies in same vials where flies were distinguished by eye color. When both genotypes were pooled, still only one of three *miR-986*^{KO} lines survived longer than wild type. Therefore, miR-986 does not mediate the response to DDT.

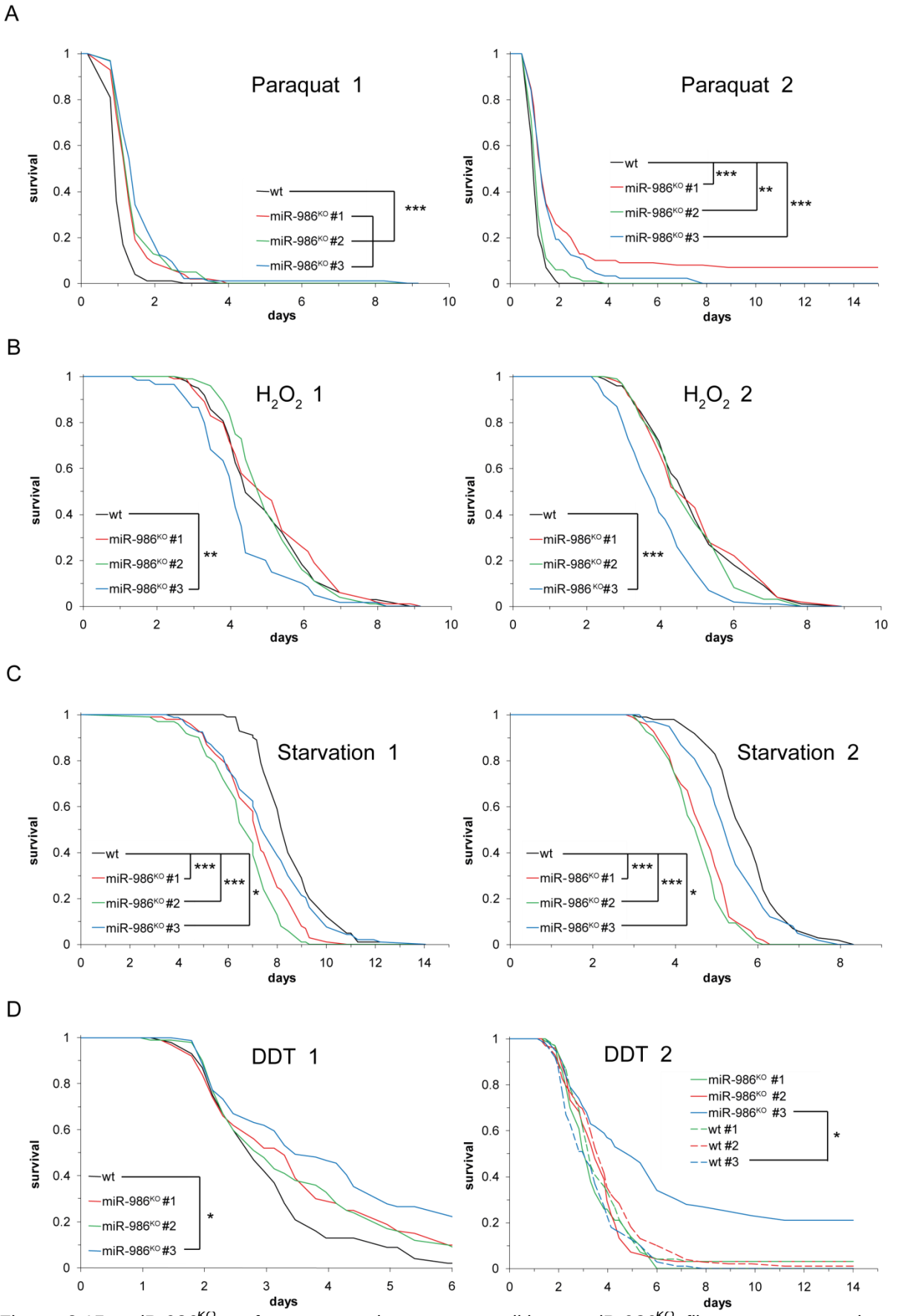

Figure 2.15: *miR-986*^{KO} performance under stress conditions. *miR-986*^{KO} flies were exposed to paraquat (A), H_2O_2 (B), starvation (C) and DDT (D). (A) Survival under H_2O_2 stress was decreased for one of three *miR-986*^{KO} lines. (B) Stress tolerance of *miR-986*^{KO} flies against paraquat was increased. (C) Starvation reduced the lifespan of *miR-986*^{KO} flies. (D) Only one *miR-986*^{KO} line had increased

lifespan in the first experiment. The second experiment was done with pooled wild type and *miR-986*^{KO} flies in same vials (for details see text). Still, only one of three *miR-986*^{KO} lines was longer-lived. For each drug treatment two replicate experiments are shown. * p<0.05; ** p<0.01; *** p<0.001, log-rank test.

2.3.3 Putative targets of miR-986

miRNAs regulate gene expression by silencing target mRNAs. To find putative targets of miR-986, the miRanda algorithm was used (Enright *et al*., 2003). This algorithm predicts targets based on sequence complementarity, free energies of RNA-RNA duplexes and evolutionary conservation of target sites. In order to rank predicted targets the mirSVR method was used (Betel *et al*., 2010). Using the miRNA.org source that combines miRanda algorithm with the mirSVR method (Betel *et al*., 2008), predicted targets of *miR-986* were identified (Table 6). The predicted miR-986 targets were shown to be involved in diverse functions including olfactory learning, dopamine secretion, mitosis, phagocytosis, histone actetylation, reproduction, notch signaling, glycogen biosynthesis, brain development and fatty acid biosynthesis. Targets involved in detoxification of superoxide were not predicted.

Putative Target	ID	mirSVR score	Biological function
klg	NM_079730	-1.85	homophilic cell adhesion; behavioral response to ethanol; long-term memory (olfactory learning); R7 cell differentiation.
CG10338	NM_136053	-1.7	unknown
Ih	NM_001038859	-1.59	determination of adult lifespan; positive regulation of circadian sleep/wake cycle, locomotor rhythm; transmembrane potassium ion transport; proboscis extension reflex; regulation of dopamine secretion.
larp	NM_080259	-1.57	spindle assembly involved in male meiosis; mitochondrion inheritance; salivary gland cell autophagic cell death; centrosome separation; mitotic chromosome condensation.
ATPsyn-b	NM_168365	-1.51	phagocytosis; ATP synthesis coupled proton transport.
CG10492	NM_136093	-1.48	unknown
msl-1	NM_057548	-1.41	histone H4-K16 acetylation; complex assembly involved in dosage compensation by hyperactivation of X chromosome.
CG10433	NM_137746	-1.36	reproduction; defense response.
CG32479	NM_167844	-1.34	positive regulation of Notch signaling pathway; ubiquitin-dependent protein catabolic process.
Glycogenin	NM_166432	-1.34	glycogen biosynthetic process.
CG2790	NM_138142	-1.31	unknown
fdl	NM_165908	-1.3	brain development; N-glycan processing
CG2781	NM_141497	-1.3	very long-chain fatty acid biosynthetic process.

Table 6: Putative miR-986 targets as predicted by miRDeep algorithm. Scores are calculated by mirSVR.

In summary, miR-986 did not modulate body size, development time and the response to H_2O_2 or DDT. However, miR-986 seemed to be required for normal lifespan, egg-production and starvation resistance, as *miR-986*^{KO} flies were short-lived, laid fewer eggs and were sensitive to starvation. Lack of miR-986 significantly increased paraquat resistance, suggesting that miR-986 might target genes involved in the detoxification of superoxide. However, currently we cannot exclude that down-regulation of Cyp4e2 expression in *miR-986*^{KO} flies might contribute to the observed phenotypes. The repetition of the experiments with the *miR-986*^{KO*} line without the white gene and fully restored Cyp4e2 expression will answer this question.

2.4 Next-generation sequencing of *Drosophila* tissues

2.4.1 Establishment of a small RNA preparation protocol for deep sequencing of *Drosophila* microRNAs

2.4.1.1 Standard microRNA library generation resulted in ribosomal RNA contamination

In addition to microarray analysis, miRNA expression can also be analyzed by next generation sequencing. Next generation sequencing offers several advantages over microarray analysis. Sequencing discriminates highly similar sequences and can distinguish miRNA family members and isoforms on the basis of single nucleotides. Furthermore, it allows the detection of editing events and even unknown small RNAs, e.g. of the 238 miRNAs currently annotated in MirBase, only 186 are represented on the Affymetrix GeneChip 2.0. Thus, in order to analyze miRNA expression by an independent method and to cover all possible expressed miRNAs, we used next generation sequencing to profile tissue-specific miRNA expression in adult flies.

In order to establish a protocol for RNA isolation that is compatible with next generation sequencing of miRNAs in *Drosophila*, we generated a test library from total RNA of the digestive tract of wild type flies. Total RNA, which was extracted and size-fractionated on a column to isolate small RNAs, served as input for the library. After adapter ligation the RNA was reverse transcribed and amplified by PCR. The generated library was then used for sequencing on an Illumina platform.

Sequencing of the gut library resulted in 20.83 million reads, however, only 1.94 % of the reads mapped to *Drosophila* miRNAs (Table 7). To identify the other 98.06 % non-miRNA sequences we performed a BLAST search on the *Drosophila* genome. This analysis revealed that most non-miRNA sequences matched to ribosomal RNAs, particularly 2S rRNA. The proportion of rRNA in the library amounted to 96.33 %, with 91.01 % identified as 2S rRNA. 1.73 % of all sequences failed to align to miRNAs or rRNAs. Thus, the standard protocol of library preparation was not suitable for deep sequencing of *Drosophila* miRNA expression.

	column fractionation	Protocol A	Protocol B	Protocol C
# x 10^6 reads analyzed	20.83	26.59	12.33	23.57
% reads mapped to *Drosophila* miRNA	1.94	3.84	1.01	4.31
% reads mapped to rRNA	96.33	33.22	66.20	29.27
% reads mapped to 2S rRNA	91.01	1.34	45.54	1.20
% reads not mapped to Drosophila rRNA or miRNA	1.73	62.94	32.79	66.42

Table 7: Comparison of different methods for miRNA library preparation.

2.4.1.2 Optimization of microRNA library preparation

Drosophila 2S rRNA is expressed at higher levels than miRNAs and with 30 nt has a similar size as miRNAs, which are on average 22 nt long. Thus standard column fractionation may not be sufficient to separate miRNAs from 2S rRNA. In order to generate miRNA next generation libraries with lower 2S rRNA contamination, three different approaches were tested: (A) gel purification of 15-27 nt small RNAs, (B) oligo-depletion of 2S RNA and (C) combination of A and B (Figure 2.16). To test the three methods, total RNA of digestive tracts of wild type flies was used consistent with the pre-test library (2.4.1.1).

Sequencing of library A resulted in 26.59 million reads. Importantly, the percentage of rRNA in the library was significantly reduced from 96.33 % to 33.22 % (Table 7), whereby 2S rRNA content was reduced from 91.01 % to 1.34 %, demonstrating that gel purification is an efficient method to avoid 2S rRNA contamination. Reads mapping to miRNA were increased from 1.94 % to 3.84 %. Noteworthy, the amount of reads which did not map to *Drosophila* miRNAs or rRNAs was increased from 1.73 % to 62.94 % (compare 2.4.3). Overall sequencing depth was lower in the oligo-depleted library B, resulting in only 12.33 million reads. rRNA and particularly 2S rRNA was reduced to 66.2 % and 45.54 %, respectively, demonstrating that oligo depletion was less efficient in removing rRNA contamination than gel purification. The amount of reads mapping to miRNA was decreased

to 1.01 % and therefore even lower than in the standard protocol. Reads that could not be mapped to miRNAs or rRNAs represented 32.79 % of all analyzed reads, which is lower than in protocol A and probably the result of less efficient rRNA depletion. Combined gel purification and oligo-depletion of library C resulted in 23.57 million reads, of which only 29.27 % mapped to rRNA and 1.2 % to 2S rRNA sequences. These values are just slightly lower than the results of just the gel purification. Consistent with this finding, 4.31 % of the reads mapped to miRNAs, which is only slightly more than the 3.83 % of gel purification alone. Reads which did not map to miRNA or rRNA accounted for 66.42 % of all analyzed reads. Thus, in summary, oligo depletion combined with size selection only marginally improved rRNA depletion and miRNA enrichment compared to gel purification alone. Therefore, we decided to use gel purification (method A) for the generation of the libraries for the tissues of wt and *dilp2-3,5* flies.

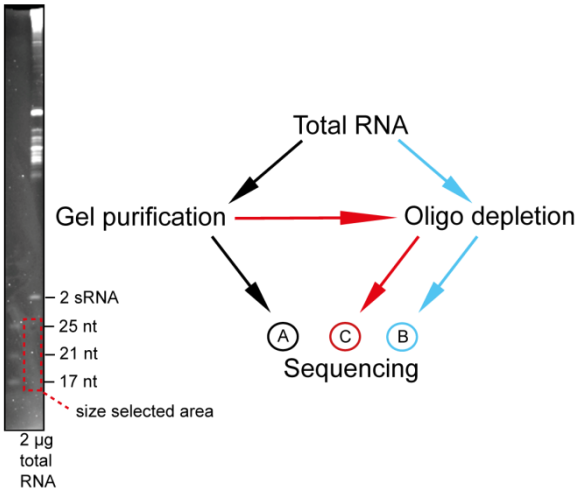

Figure 2.16: Optimization of miRNA library preparation. In protocol A total RNA was size-separated on an acrylamide-urea gel and miRNAs were isolated from 2S rRNA by size selection. Protocol B used oligonucleotide-coated beads with antisense oligonucleotides to deplete 2S rRNA identified in the pretest-library. In protocol C both protocols are combined; Total RNA is size-selected on a polyacrylamide-urea gel and 2S rRNA is then depleted using oligonucleotide-coated beads.

2.4.2 Next generation sequencing of *Drosophila* tissues

We used total RNA isolated from brain, thorax, digestive tract and abdomen of wild type and *dilp2-3,5* flies to generate 24 miRNA libraries (3 replicates per tissue and genotype). Libraries were sequenced using Illumina technology and the number of reads per library varied between 9 and 36 million reads (Table 8).

Gel purification of miRNAs (protocol A, see 2.4.1.2) resulted in low level of rRNA contamination in all libraries. Brain libraries contained on average 4 %, thorax libraries 6 % and abdomen libraries 4 % reads mapping to rRNA sequences. The digestive tract showed the highest rRNA contamination with 17.32 % of all reads. Thus, the used protocol successfully reduced the amount of rRNA in all tissues although to varying degree.

The percentage of analyzed reads that mapped to *Drosophila* miRNA varied between tissues. In libraries originating from brain, thorax and abdomen 82 %, 71 % and 73 % of the reads mapped to miRNAs, respectively. In contrast, libraries made from the digestive tract contained significantly less reads mapping to miRNA sequences, only 16 % of all reads mapped to miRNAs.

A miRNA was defined as detected when the normalized read count was more than 10. With this stringent criterion, between 109 and 159 distinct mature miRNAs were detected, on average 134 miRNAs per library. Among replicates the normalized sequencing read count for miRNAs was similar, suggesting that the sequencing data are reproducible. Given a total number of 426 annotated mature *Drosophila* miRNAs (miRBase release 20) the average amount of detected distinct mature miRNAs in all libraries was 30.95 %. The microarray chip contained probe sets for 186 distinct miRNAs. The average amount of miRNAs detected over background by microarray was 22.82 % compared to all annotated miRNAs. Thus, next generation sequencing resulted in the detection of more miRNAs compared to the microarray analysis despite the stringent detection criterion used in the sequencing analysis.

	Brain						Thorax					
	WT 1	*WT 2*	*WT 3*	*dilp2-3,5 1*	*dilp2-3,5 2*	*dilp2-3,5 3*	*WT 1*	*WT 2*	*WT 3*	*dilp2-3,5 1*	*dilp2-3,5 2*	*dilp2-3,5 3*
Sequencing												
# x 1000000 reads analyzed	21.07	20.24	19.72	16.40	14.98	17.79	15.19	12.75	13.40	35.89	17.50	10.46
% reads mapped to *Drosophila* miRNA	79.03	82.92	83.79	79.13	83.29	82.92	64.77	74.63	72.19	74.35	77.11	65.11
% reads mapped to rRNA	3.95	3.47	3.30	4.24	3.06	3.48	7.67	4.02	4.43	6.30	6.70	6.91
% reads not mapped to Drosophila rRNA or miRNA	17.02	13.60	12.91	16.63	13.64	13.60	27.56	21.35	23.38	19.36	16.20	27.98
% reads mapped to Wolbachia pipientis RNA	2.74	3.39	3.63	3.83	4.96	5.38	2.66	4.08	4.09	11.48	10.30	5.42
% reads mapped to yeast RNA	2.83	0.55	0.51	2.86	0.73	0.62	4.02	4.64	1.81	8.75	0.80	3.05
# detected distinct miRNAs	153	153	155	158	153	159	128	122	126	117	109	112
% detected distinct miRNAs of annotated and analysed miRNAs (detected: >10 normalized reads)	35.25	35.25	35.71	36.41	35.25	36.64	29.49	28.11	29.03	26.96	25.12	25.81
Microarray												
% detected distinct miRNAs of miRNAs with probe sets on microarray chip (detected over background)	56.45	62.90	58.06	61.83	53.76	58.60	55.38	53.76	58.06	56.99	53.76	51.08
% detected distinct miRNAs of all annotated miRNAs by microarray (detected over background)	24.65	27.46	25.35	27.00	23.47	25.59	24.18	23.47	25.35	24.88	23.47	22.30

Table 8: Sequencing and microarray results for brain, thorax, digestive tract and abdomen libraries. wt, wildtype

	Digestive tract						Abdomen					
	WT 1	WT 2	WT 3	*dilp2-3,5* 1	*dilp2-3,5* 2	*dilp2-3,5* 3	WT 1	WT 2	WT 3	*dilp2-3,5* 1	*dilp2-3,5* 2	*dilp2-3,5* 3
Sequencing												
# x 1000000 reads analyzed	27.23	33.00	17.13	13.74	33.78	8.96	34.22	17.12	17.67	20.36	32.38	12.09
% reads mapped to *Drosophila* miRNA	3.62	21.46	31.98	2.63	21.02	15.47	67.95	72.86	77.81	67.94	78.72	73.84
% reads mapped to rRNA	3.83	28.67	35.63	2.05	16.49	17.26	4.45	3.36	4.17	4.36	4.51	3.67
% reads not mapped to Drosophila rRNA or miRNA	92.55	49.87	32.38	95.31	62.48	67.27	27.60	23.78	18.02	27.70	16.76	22.48
% reads mapped to Wolbachia pipientis RNA	0.80	0.78	1.54	3.42	8.37	8.36	6.03	6.74	8.02	7.97	14.81	10.48
% reads mapped to yeast RNA	48.69	20.98	11.15	52.90	23.61	26.51	4.20	1.54	0.95	6.98	2.54	1.76
# detected distinct miRNAs	135	141	129	126	130	129	132	129	126	133	134	135
% detected distinct miRNAs of annotated and analysed miRNAs (detected: >10 normalized reads)	31.11	32.49	29.72	29.03	29.95	29.72	30.41	29.72	29.03	30.65	30.88	31.11
Microarray												
% detected distinct miRNAs of miRNAs with probe sets on microarray chip (detected over background)	52.15	46.77	46.24	46.24	46.24	44.62	48.92	49.46	47.85	47.85	48.92	48.39
% detected distinct miRNAs of all annotated miRNAs by microarray (detected over background)	22.77	20.42	20.19	20.19	20.19	19.48	21.36	21.60	20.89	20.89	21.36	21.13

Table 8 (continued)

2.4.3 Identification of non-microRNA reads

A large part of the library reads did not map to the *Drosophila* genome (Table 8). 14.57 % of brain, 22.64 % of thorax and 22.73 % of abdomen library sequences did not map to either *Drosophila* miRNA or rRNA. For digestive tract the amount of reads that did not map to *Drosophila* miRNA or rRNA was the highest with 66.65 %.

wDah and *wDah; dilp2-3,5* flies used for the next generation sequencing analysis contain the intracellular endosymbiont *Wolbachia pipientis* (Grönke *et al*., 2010). In order to test whether reads that could not be mapped to the *Drosophila* genome may be originating from *Wolbachia*, we mapped the library sequences onto the *Wolbachia* genome (see chapter 4.24.5). Indeed, in brain 0.36 %, thorax 1 %, digestive tract 1.13 % and in the abdomen 1.82 % of all analyzed reads mapped to *Wolbachia*. Interestingly, in all tissues, the amount of sequences that map to *Wolbachia* was much higher in *dilp2-3,5* flies than in wild type flies. Especially in the digestive tract the amount of reads corresponding to the *Wolbachia* genome was 11 times higher in *dilp2-3,5* flies than in wild type.

Since the food source of flies used in this experiment contained yeast, the library of digestive tract samples might be contaminated with yeast small RNA sequences. We therefore compared the analyzed sequences with the transcriptome of *Saccharomyces cerevisiae* by BLAST algorithm. Indeed, the amount of reads mapping to yeast sequences was low in brain (1.35 %), thorax (3.84 %) and abdomen (3 %), while with 30.64 % it was high in digestive tract. Thus, dietary yeast affected the digestive tract library composition.

2.4.4 Tissue-specific microRNA expression profiles

We used Pearson correlation analysis to analyze whether global miRNA expression profiles differs between tissues and genotypes and whether tissue dissection was consistent between replicates (Figure 2.17). miRNA profiles of the same tissue type showed strong correlation indicating high similarity. Consistent with the microarray data, this indicated that *Drosophila* tissues have a characteristic miRNA expression profile. Furthermore, these results show that tissue preparation was consistent between the replicates and that profiles from wild type and *dilp2-3,5* tissues showed strong correlation.

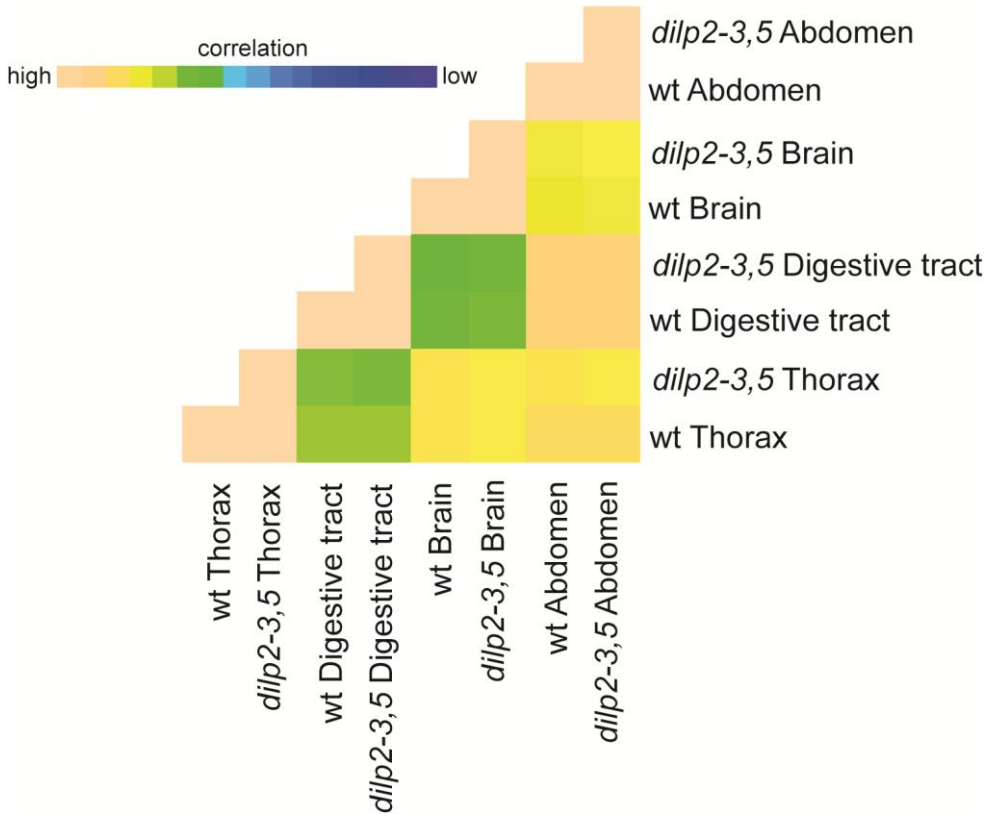

Figure 2.17: Comparisons of miRNA tissue profiles generated by next-generation sequencing. Pearson correlation coefficient for all pairwise comparisons was computed and the values are depicted color-coded. Samples of the same tissue cluster, indicating high quality of tissue preparation and tissue-specific miRNA expression.

2.4.5 Identification of tissue-specific microRNAs by sequencing

In order to analyze tissue specificity of miRNAs that were detected by next generation sequencing, a tissue specificity score was calculated as before for microarray data (see chapter 2.1.3). miRNAs with less than 10 normalized reads were not included in the analysis. Sequencing data for tissue specificity highly correlated with microarray data with a Pearson coefficient of 0.72. Thus similar tissue specificity as for microarray data was found by sequencing data. We found ubiquitously expressed miRNAs and tissue-specific miRNAs (Figure 2.18). Consistent with the microarray results, miRNAs specific for the digestive tract included miR-314-3p and miR-956-3p. In the abdomen among others miR-2494-5p and miR-1015-3p were specifically expressed. Also by sequencing we found that most tissue-specific miRNAs were expressed in the brain, like mir-981-3p and 990-5p. As observed before, miR-993-3p was specifically expressed in the thorax. While by microarray 30 miRNAs were detected as tissue-specific, by sequencing 75 miRNAs had a tissue specificity score of more than 1.0. Thus by sequencing we were able to extend the information about tissue specificity to more miRNAs. For example miR-4916-3p is a miRNA with no probe set

on the array but by sequencing we found it to be highly specific for the brain. Also we found miRNAs, which were evenly expressed in all tissues, like let-7-5p. Tissue specificity of *dilp2-3,5* miRNAs was altered compared to wild type (Supplemental Figure S3), suggesting differential regulation of spatial miRNA expression in *dilp2-3,5* mutants.

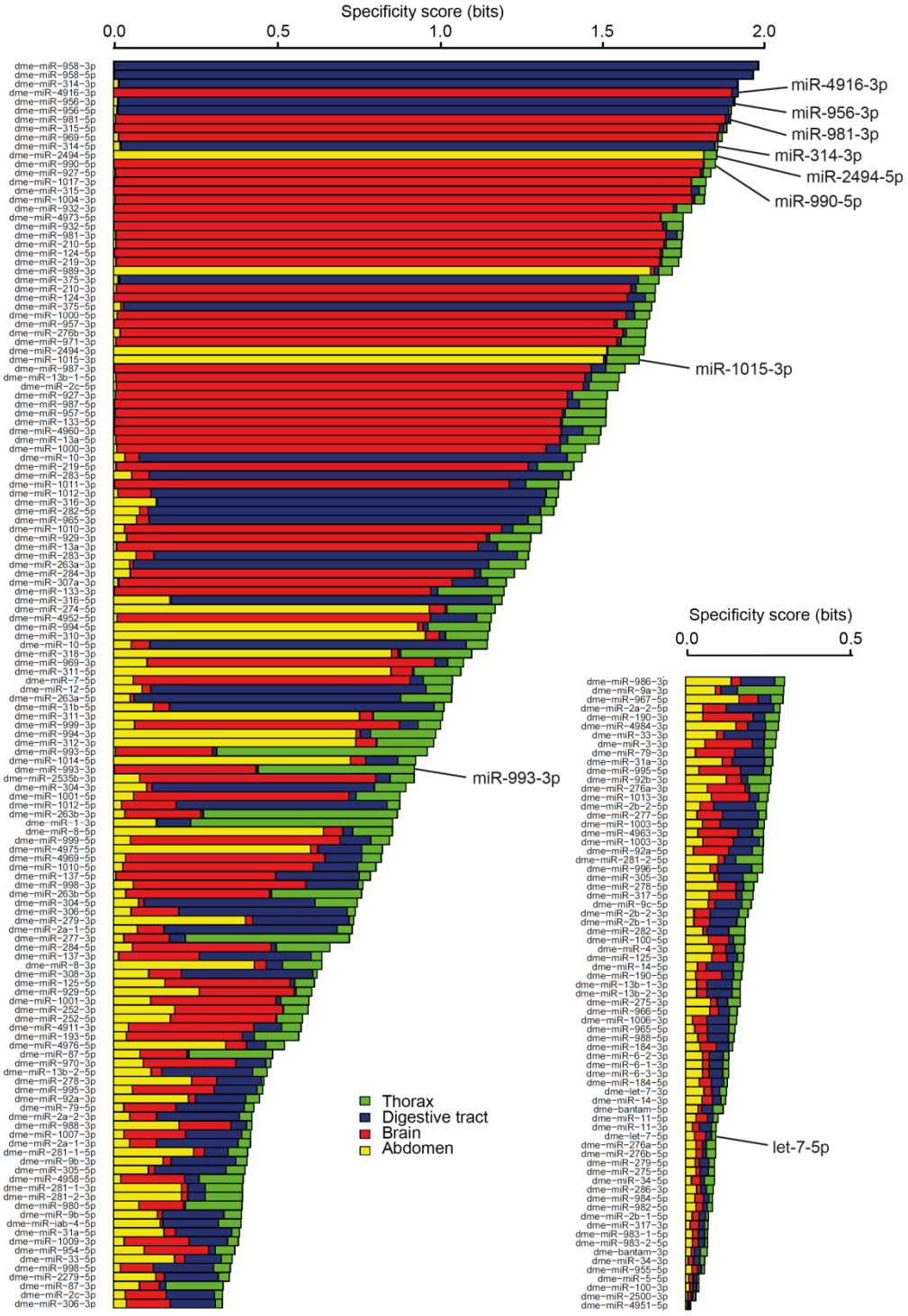

Figure 2.18: Tissue specificity of miRNA expression as detected by next-generation sequencing in wild type flies. The total height of each bar represents the tissue specificity and the relative heights for each of the tissues are proportional to miRNA expression in a given tissue type relative to all tissue types. miRNAs with at least 10 reads are included in the analysis.

2.4.6 Evolutionary conservation of microRNAs correlates with expression level as detected by sequencing

Although it was shown in previous studies, that miRNA expression level correlates with degree of evolutionary conservation (Ruby *et al*., 2007), we could not verify this observation by microarrays (see chapter 2.1.4). In order to test whether in contrast our sequencing results can confirm the observation of previous studies we compared miRNA read number with degree of evolutionary conservation. By sequencing we found that the majority of miRNAs with high read number are highly evolutionary conserved whereas miRNAs with low read number are not conserved. Thus with a Pearson coefficient of 0.3 expression level of miRNAs correlated with evolutionary conservation. (Figure 2.19 A)

2.4.7 Expression level as detected by sequencing does not correlate with tissue specificity

It was published that highly expressed miRNAs are evenly distributed across tissues whereas low expressed miRNAs show higher tissue specificity (Ruby *et al*., 2007). I did not observe the same correlation in my microarray analysis (see chapter 2.1.5). In order to re-analyze this correlation on my next generation sequencing dataset, we compared miRNA tissue specificity with sequencing read count (Figure 2.19 B). As for microarrays, with a Pearson coefficient of -0.13 we found no correlation between evolutionary conservation and specificity of expression in adult tissues of *Drosophila* flies.

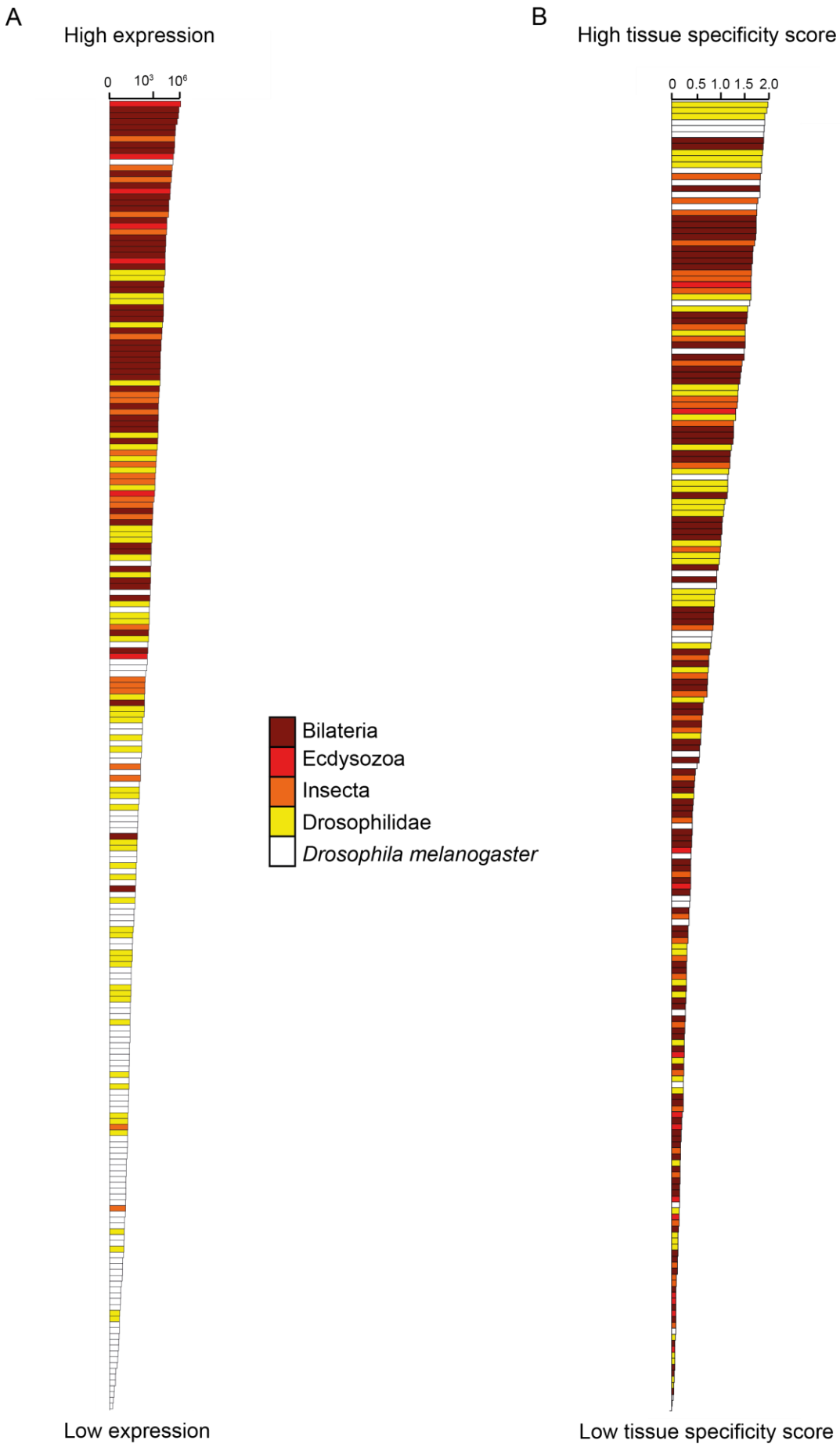
A
High expression
0
10³
10⁶
Low expression
B
High tissue specificity score
0
0.5
1.0
1.5
2.0
Low tissue specificity score
Bilateria
Ecdysozoa
Insecta
Drosophilidae
Drosophila melanogaster

Figure 2.19: Correlation of evolutionary conservation of miRNAs and tissue specificity or absolute expression, respectively. Sequencing data was used for the analysis. (A) Relationship between absolute expression and evolutionary conservation of miRNAs. Strong correlation was observed as evolutionary conserved miRNAs are highly expressed. For a detailed list see supplemental table 1. (B) Relationship between tissue specificity of miRNA expression as detected by sequencing and evolutionary conservation. No correlation between tissue specificity and conservation was observed. Only miRNAs with a read number of >10 were included in the analysis..

2.4.8 Identification of differentially expressed microRNAs in *dilp2-3,5* tissues by sequencing

Global miRNA expression was highly similar between wt and *dilp2-3,5* tissues (Figure 2.17). However, single miRNAs might be differentially expressed yet not significantly alter global miRNA expression profiles. To identify differentially expressed miRNAs in the brain, thorax, digestive tract and abdomen of *dilp2-3,5* flies, we used the Bioconductor package DESeq (Anders and Huber, 2010). For the detection of differentially expressed miRNAs, this package uses a negative binominal distribution and a shrinkage estimator for the distribution's variance to test for differential expression. In the brain and in the thorax significance of differential expression was supported by multiple testing. Considering this test, in the brain 2 miRNAs were up-regulated and 3 down-regulated (Table 9), while in the thorax, 4 miRNAs were up-regulated and 15 down-regulated (Table 10). In the digestive tract and abdomen miRNAs were differentially expressed but not significant at the significance level of a multiple comparison test. As tested by single comparisons one miRNA was up-regulated in the digestive tract (Table 11), while in the abdomen 3 miRNAs were up-regulated and one was down-regulated (Table 12). Thus, miRNAs were differentially expressed in *dilp2-3,5* tissues.

Brain					
miRNA	Mean wt	Mean *dilp2-3,5*	FC	p-value	p-value (adjusted)
dme-miR-4911-3p	193.90	91.21	0.47	7.28×10^{-5}	0.01
dme-miR-980-5p	296.92	156.47	0.53	7.96×10^{-5}	0.01
dme-miR-986-5p	10211.99	6201.73	0.61	0.00003	0.02
dme-miR-92a-5p	1913.62	3855.52	2.01	4.8×10^{-7}	0.0002
dme-miR-375-3p	1400.82	5411.37	3.86	2.06×10^{-6}	0.0004

Table 9: Differentially expressed miRNAs in *dilp2-3,5* brains as detected by next generation sequencing. Mean represents miRNA expression in three independent replicates each genotype. Fold changes are calculated by DeSeq algorithm. p-values are calculated by Student's t-test and adjusted by Benjamini-Hochberg procedure. FC, fold change; wt, wild type

Thorax					
miRNA	Mean wt	Mean *dilp2-3,5*	FC	p-value	p-value (adjusted)
dme-miR-929-5p	353.71	38.89	0.11	1.41×10^{-07}	2.37×10^{-05}

dme-miR-219-3p	37.16	4.33	0.12	0.0002	0.006
dme-miR-9b-3p	99.14	16.60	0.17	2.17×10^{-05}	0.001
dme-miR-14-3p	217439.69	37063.70	0.17	4.43×10^{-08}	1.49×10^{-05}
dme-miR-998-3p	62.62	11.22	0.18	0.0002	0.005
dme-miR-277-5p	594.03	124.79	0.21	1.04×10^{-06}	0.0001
dme-miR-33-3p	281.87	61.55	0.22	3.88×10^{-05}	0.002
dme-let-7-3p	496.89	111.23	0.22	6.74×10^{-05}	0.002
dme-miR-317-5p	5848.93	1486.28	0.25	5.93×10^{-05}	0.002
dme-miR-33-5p	15512.60	4130.58	0.27	3.17×10^{-05}	0.002
dme-miR-981-3p	269.10	75.00	0.28	0.0005	0.01
dme-miR-988-3p	107.33	30.29	0.28	5.75×10^{-05}	0.002
dme-miR-274-5p	3038.69	1053.38	0.35	0.001	0.02
dme-miR-927-5p	581.19	201.82	0.35	0.0009	0.02
dme-miR-9c-5p	16398.16	5749.61	0.35	0.001	0.02
dme-miR-1010-3p	676.09	1807.25	2.67	0.001	0.03
dme-miR-124-5p	43.48	132.16	3.04	0.002	0.04
dme-miR-1016-5p	14.44	62.94	4.36	0.0003	0.007
dme-miR-316-3p	76.45	691.14	9.04	4.34×10^{-06}	0.0004

Table 10: Differentially expressed miRNAs in *dilp2-3,5* thoraces as detected by next generation sequencing. Mean represents miRNA expression in three independent replicates each genotype. Fold changes are calculated by DeSeq algorithm. p-values are calculated by Student's t-test and adjusted by Benjamini-Hochberg procedure. FC, fold change; wt, wild type

Digestive tract

miRNA	Mean wt	Mean *dilp2-3,5*	FC	p-value	p-value (adjusted)
dme-miR-312-3p	1.04	21.60	20.75	0.005	> 0.99

Table 11: Differentially expressed miRNAs in *dilp2-3,5* digestive tracts as detected by next generation sequencing. Mean represents miRNA expression in three independent replicates each genotype. Fold changes are calculated by DeSeq algorithm. p-values are calculated by Student's t-test and adjusted by Benjamini-Hochberg procedure. FC, fold change; wt, wild type

Abdomen

miRNA	Mean wt	Mean *dilp2-3,5*	FC	p-value	p-value (adjusted)
dme-miR-10-5p	36310.82	20477.72	0.56	0.03	> 0.99
dme-miR-133-3p	155.46	297.28	1.91	0.01	> 0.99
dme-miR-263b-5p	3948.61	8055.09	2.04	0.04	> 0.99
dme-miR-87-5p	27.39	66.44	2.43	0.02	> 0.99

Table 12: Differentially expressed miRNAs in *dilp2-3,5* abdomen as detected by next generation sequencing. Mean represents miRNA expression in three independent replicates each genotype. Fold changes are calculated by DeSeq algorithm. p-values are calculated by Student's t-test and adjusted by Benjamini-Hochberg procedure. FC, fold change; wt, wild type

2.4.9 qRT-PCR analysis of differential expressed microRNAs

In order to verify differentially expressed miRNAs in *dilp2-3,5* brain and thorax, qRT-PCR on selected miRNAs was performed. Independent biological samples were used. In agreement with sequencing results, up-regulation of miR-92a-5p in *dilp2-3,5* brains was detected, although it was not significant (Figure 2.20). However, differential expression of selected miRNAs in thorax and for two of three tested miRNAs in the brain was not detected by qRT-PCR. Thus, only differential up-regulation of miR-92a-5p in *dilp2-3,5* brains could be confirmed by qRT-PCR analysis.

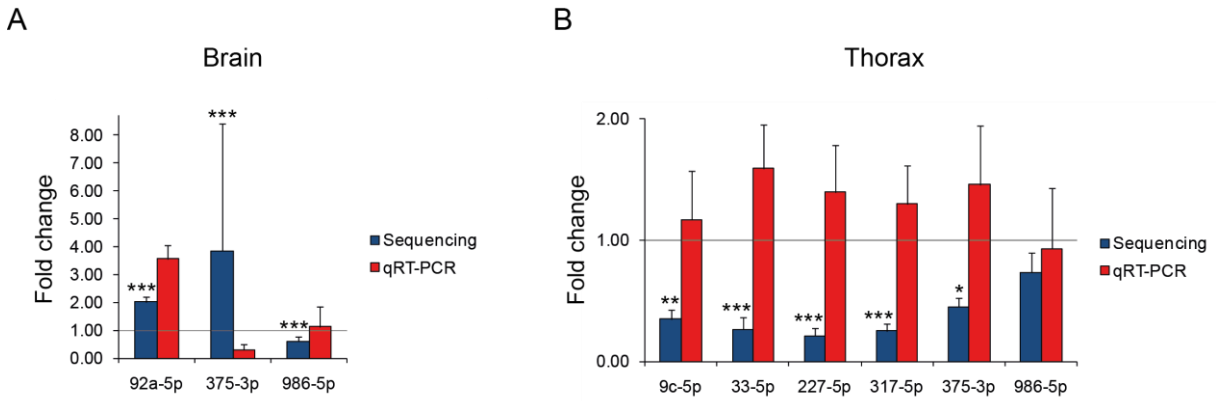

Figure 2.20: qRT-PCR analysis verifies differential expression of miR-92a-5p in *dilp2-3,5* brains as detected by next-generation sequencing. Fold change in (A) brain and (B) thorax from next-generation sequencing and qRT-PCR analysis are compared. Differential expression of miR-92a-5p as detected by sequencing was verified by tendency of up-regulation as measured by qRT-PCR. miRNA transcript level was normalized to wild type samples, which by default was set to 1. * $p<0.05$, ** $p<0.01$; *** $p<0.001$, Benjamini-Hochberg test.

2.5 Comparison of microarray with next-generation sequencing data

2.5.1 Comparison of absolute expression datasets between next-generation sequencing and microarrays

To assess whether the miRNA next generation sequencing data were consistent with the miRNA microarray data, correlation between absolute expression profiles of all tissues of wild type flies was examined by comparing sequencing density to expression metrics from microarray intensities. Raw data were normalized to total number of reads or quantile normalization, respectively, to obtain absolute expression profiles. To exclude miRNAs that were not detected by either microarray or sequencing, miRNAs with an expression value > 15 or with less than 10 sequencing reads were filtered out, respectively. The congruency between sequencing and microarray expression data was relatively low (Figure 2.21 A). Pearson coefficients varied between 0.46 for thorax libraries and 0.56 for brain libraries.

There can be several reasons for the difference between the sequencing and microarray data. The differences could be caused by the use of total RNA for microarrays while for sequencing miRNAs were isolated by gel purification ahead of library preparation. Furthermore, for both techniques different RNA samples were used, thus biological variation may account for the low correlation between sequencing and microarray profiles. Also, the fact that sequencing and microarrays are different detection techniques may account for the differences in the expression data. To experimentally differentiate whether low correlation of both datasets was due to differences in miRNA isolation, biological variation or due to technical reasons between the two platforms, we used the same RNA, which was used for sequencing also for hybridization to microarrays. Although we used the same gel purified miRNA source, the congruency between microarray and next generation sequencing data was not significantly increased (Pearson coefficient of 0.5). However, when we compared this newly generated microarray data with the microarray data that were generated from total RNA, we observed strong correlation between the two datasets (Pearson coefficient 0.9, Figure 2.21 C). Therefore, biological variation between samples and miRNA purification methods were not underlying the differences in absolute expression between sequencing and microarrays, and these differences are most likely caused by technical differences between the two platforms.

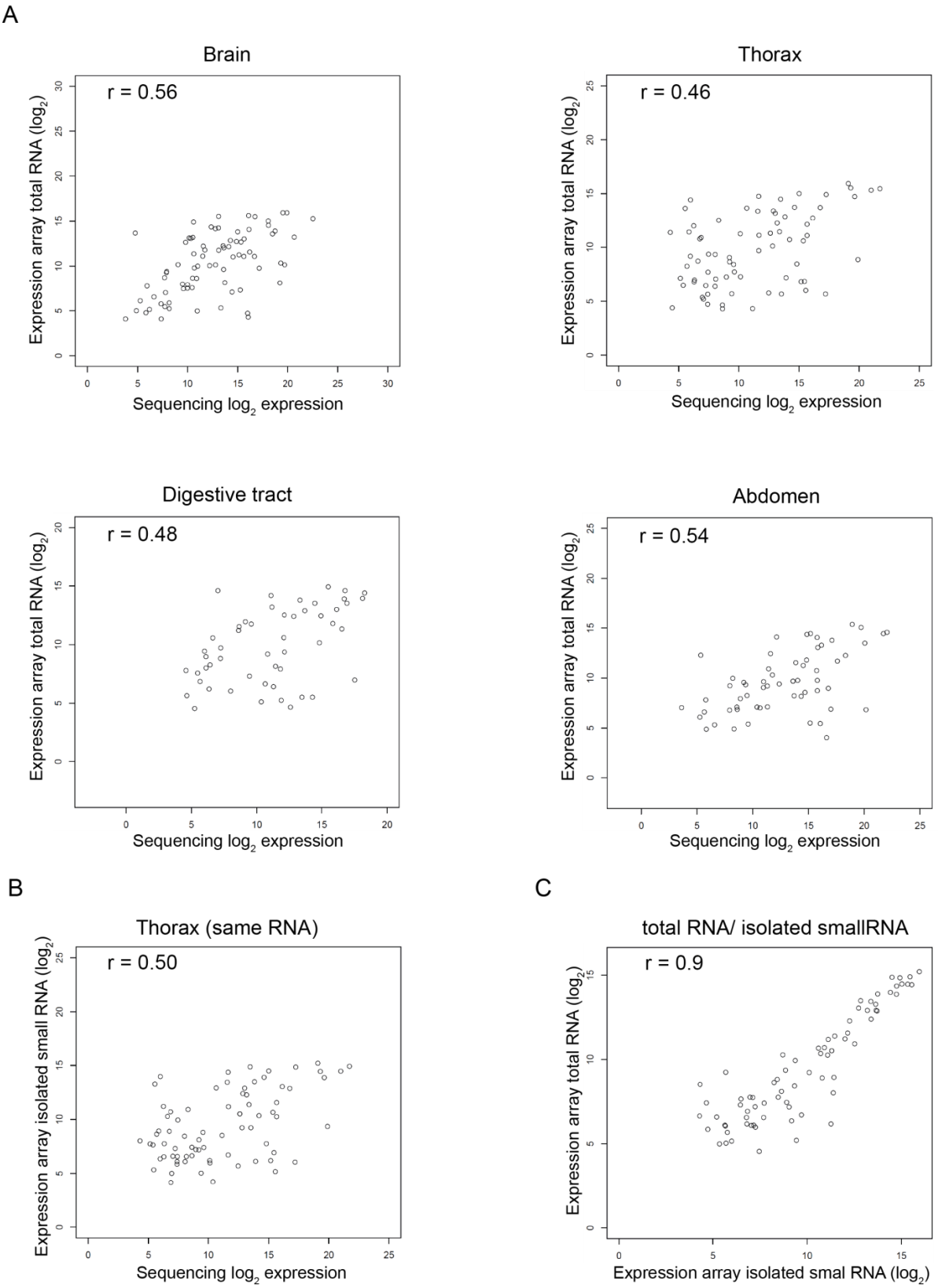

Figure 2.21: Comparison of wild type absolute expression data of microarrays and next generation sequencing. (A) Comparison of expression data in brain, thorax, digestive tract and abdomen as detected by microarray hybridized with total RNA and sequencing of libraries generated from isolated small RNA. Pearson correlation coefficient of fold change data was computed. (B) Comparison of expression of sequencing datasets and datasets from microarrays hybridized with the same isolated RNA as used for sequencing. Using the same RNA for both platforms does not increase correlation. (C) Comparison of datasets from microarrays hybridized with total RNA and isolated RNA show strong correlation. r = Pearson correlation coefficient.

2.5.2 Analyzed microRNAs have different calculated hybridization affinities to microarray chips

One technical difference between sequencing and microarrays is that the latter is based on hybridization affinity of miRNAs to complementary sequences on microarrays. Hybridization affinity does not only depend on sequence similarity but also on the melting temperature (Tm) of the miRNAs and therefore might be affected by the temperature used during the microarray hybridization step. As the GC content varies between miRNAs, we calculated and compared Tms of individual miRNAs that had probe sets on the chip (see supplemental table 2). The mean calculated Tm of those miRNAs was 57.64 °C but several miRNAs had a Tm over 65 °C or under 50 °C respectively. The temperature used for the hybridization step was 48 °C. Tm is the approximated temperature when half of the molecules are bound to complementary sequences on the chip. At temperatures below Tm binding of non-specific miRNAs is increased, at temperatures higher than Tm less miRNAs bind to complementary sequences of the correspondent probe set. It is likely that miRNAs with low Tm bind to their corresponding probe sets at 48 °C with lower affinity than miRNAs with high Tm, and that miRNAs with high Tm are prone to bind to non specific probe sets. This might interfere with quantification of absolute expression levels.

2.5.3 Comparison of differential expression datasets between sequencing and microarrays

Although normalized absolute expression data between sequencing and microarrays showed low correlation, both platforms might give similar results when analyzing differential expression between wild type and *dilp2-3,5* tissues. To test this hypothesis we compared differential expression measurements between both platforms. However, fold changes of miRNA expression as detected by sequencing did not correlate with differential expression as detected by microarray (Pearson coefficient between 0.24 for abdomen and -0.38 for thorax, Figure 2.22 A). To assess whether biological differences account for the discrepancy in fold change detection of genotypes, we compared fold changes as detected by microarray with fold changes as detected by sequencing using the same RNA input. When using the same biological sample, the fold changes of both techniques showed strong correlation with a Pearson coefficient of 0.82 (Figure 2.23 B). In contrast, a Pearson coefficient of -0.4 for the comparison of two microarray datasets which were generated using different biological RNA samples showed no correlation of fold changes (Figure 2.23 C), suggesting that the

differences in differential expression between microarray and next generation sequencing data is caused by biological variation between samples.

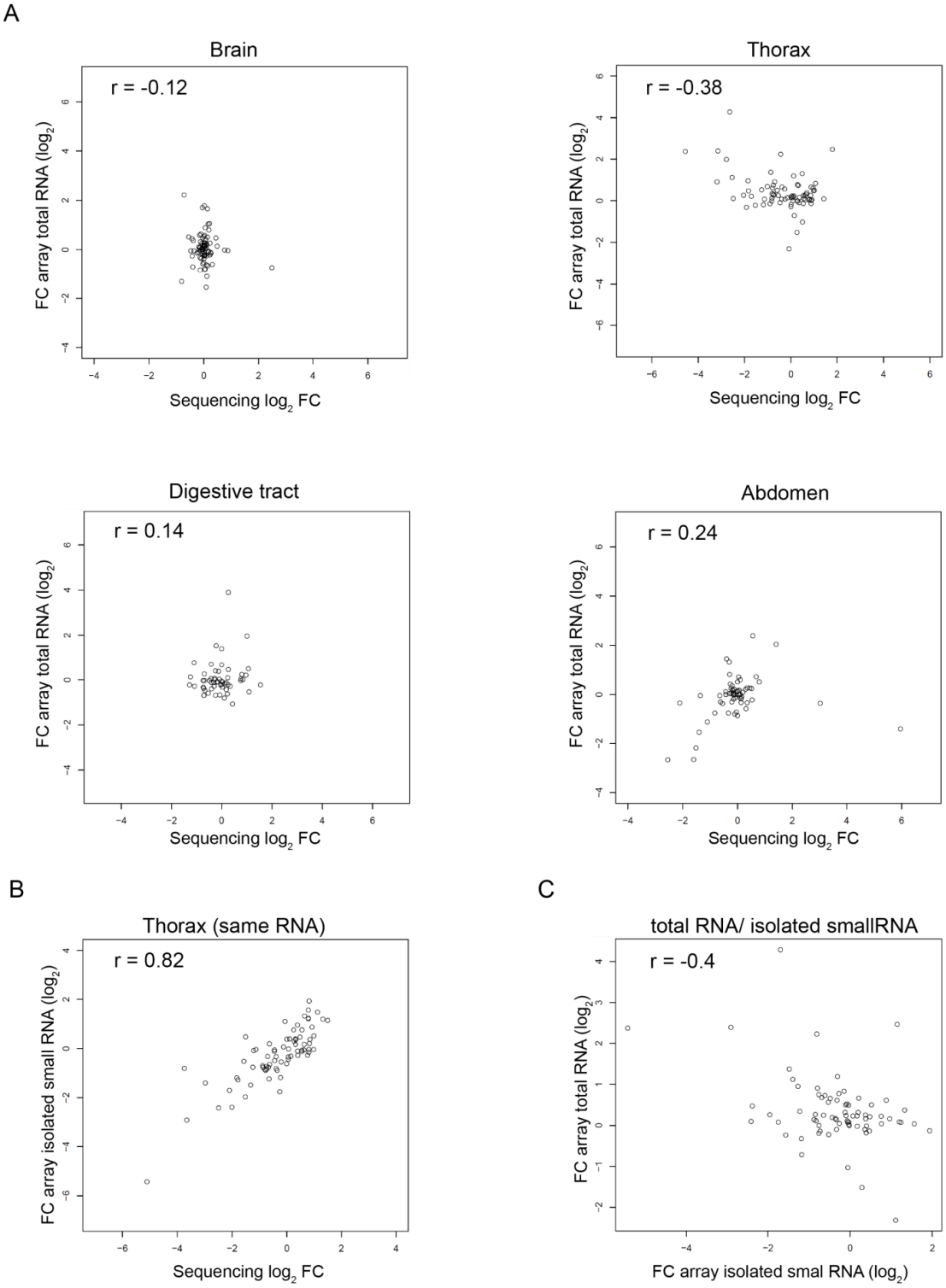

Figure 2.22: Comparison of fold change data as detected by microarrays and next generation sequencing. (A) Comparison of fold change data in brain, thorax, digestive tract and abdomen as detected by microarray hybridized with total RNA and sequencing of libraries generated from isolated small RNA. Pearson correlation coefficient of fold change data was computed and revealed low correlation (B) Comparison of fold change of sequencing datasets and datasets from microarrays hybridized with the same isolated RNA as used for sequencing. Using the same RNA for both platforms revealed strong correlation (C) Comparison of datasets from microarrays hybridized with total RNA and isolated RNA show low correlation. r = Pearson correlation coefficient.

2.5.4 Correlation between expression level and fold change in differentially expressed microRNAs

Differential expression of lowly expressed miRNAs is prone to be affected by small aberrations in expression. Accordingly, small variations in expression do not considerably contribute to expression differences of strongly expressed miRNAs. In order to investigate whether correlation of fold changes between microarray and sequencing of strongly expressed miRNAs is higher than of lowly expressed miRNAs, miRNA expression level as detected by microarray was color labeled in the comparison of differential expression between microarray and sequencing (Figure 2.23). Indeed, low expressed miRNAs showed the strongest fold change difference between experiments. Therefore, fold changes of lowly expressed miRNAs might be an artefact generated by small variations in expression and not caused by genotype.

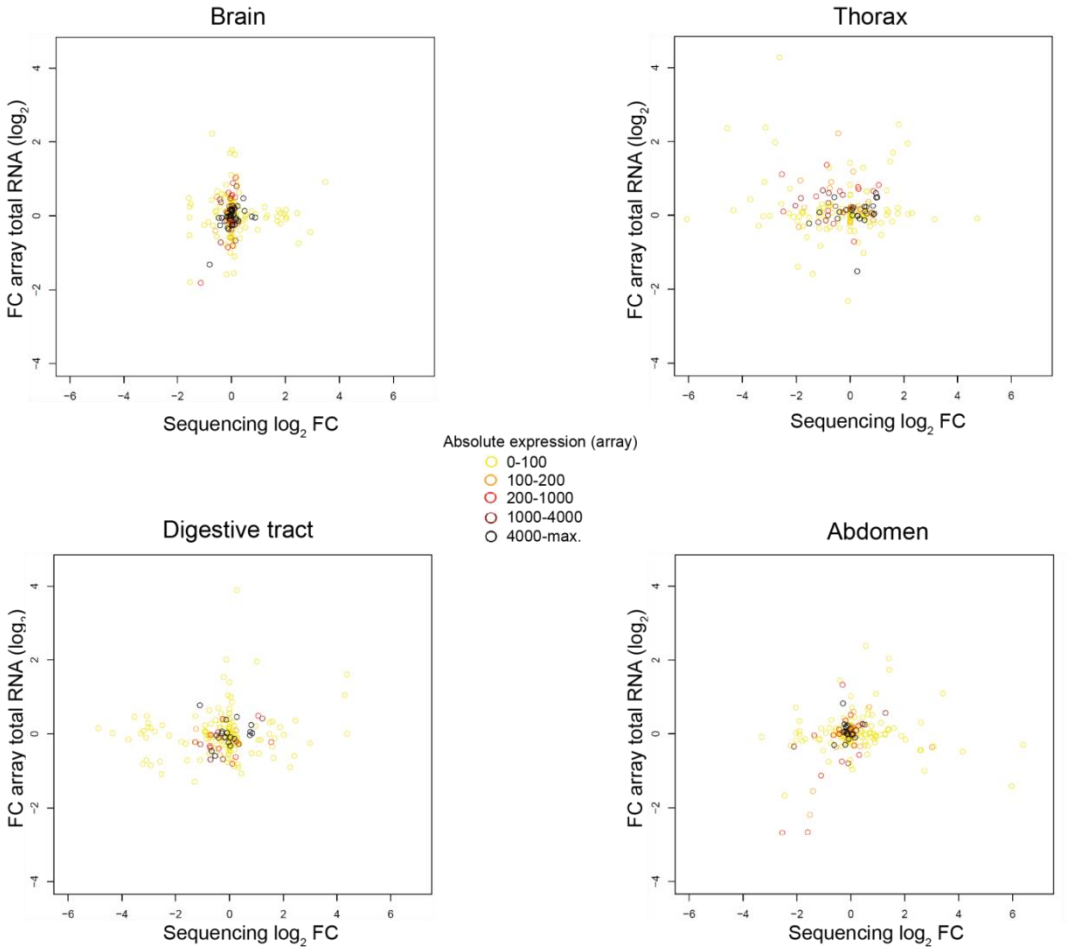

Figure 2.23: MiRNAs, which are expressed at low levels, show higher variation in fold change between microarrays and next-generation sequencing. Comparison of fold change data as detected by microarrays and next generation sequencing in brain, thorax, digestive tract and abdomen. Microarrays were hybridized with total RNA and next-generation sequencing libraries were generated from isolated small RNA. Degree of absolute expression in microarrays is depicted color-coded.

In summary, absolute expression levels were dependent on the technical platform used for analysis, whereas fold change differences were more affected by variation between different biological samples. MiRNAs that were detected to be expressed at low levels account for the majority of miRNAs which were detected to be differentially expressed.

3 Discussion

3.1 Next generation sequencing of *Drosophila* tissues

I used next generation sequencing to generate tissue-specific miRNA expression profiles of adult wild type and *dilp2-3,5* mutant *Drosophila* flies. In a first test library, which was isolated by a standard column fractionation protocol, most reads mapped to ribosomal RNA, particularly 2S rRNA. With a size of 30 nucleotides *Drosophila* 2S rRNA is very similar in length to miRNAs and therefore column fractionation was not sufficient to remove 2S rRNA from the library. In addition, 2S rRNA is expressed at very high levels compared to miRNAs, which explains the high number of reads mapping to 2S rRNA and the low number of miRNAs detected in the test library. In order to optimize library preparation, I tested three different miRNA enrichment methods, (A) gel purification, (B) oligo-depletion of 2S rRNA and (C) a combination of A and C. Gel purification of miRNAs was more efficient than oligo-depletion in removing 2S rRNA from the library and the combination of both methods did not improve the enrichment of miRNA significantly beyond gel purification alone. Therefore, all next generation sequencing of adult *Drosophila* miRNAs was done using gel purification of miRNAs as input for library preparation. By this method the amount of sequences that mapped to rRNA was reduced to 4-6 % in the brain, thorax and abdomen and to 17 % in the digestive tract. With an average of 12 million the number of reads per library mapping to miRNAs was very high. Although libraries from the digestive tract contained four times less miRNA reads than the libraries of the other tissues, in all libraries the amount of reads that mapped to *Drosophila* miRNAs, was sufficient for analysis. Three replicates were used for each condition and miRNA read counts were reproducible within independent biological replicates.

In the digestive tract only 16 % of all reads mapped to *Drosophila* miRNAs, which is significantly less than in the other tissues, where 70-80 % of all reads mapped to miRNAs. Furthermore, 67 % of the reads of the digestive tract library did not map to any *Drosophila* sequence. The digestive tract differs from the other tissues in the fact, that it contains the food the fly is eating but also serves as a habitat for the gut microbiota (Wong *et al*., 2011). Yeast is a main component of the fly food and alignment of the reads to the yeast genome showed that more than 30 % of all reads of the digestive tract libraries mapped to yeast sequences. Thus, the high amount of reads not mapping to *Drosophila* sequences in the digestive tract libraries is at least partially due to small yeast RNAs. Whether these small yeast-derived RNAs have any functional role in *Drosophila* or are just degradation products of digestion is

currently unknown. Interestingly, in humans and various animals cross-species regulation of gene expression by miRNAs taken up with the food have been reported. For example, mir-186 is a very abundant miRNA in rice that was shown to be enriched in the blood serum of Chinese people. In mice, rice mir-186 was able to regulate expression of the low-density lipoprotein receptor adaptor protein 1, demonstrating that a plant-derived miRNA can regulate gene expression in mammals (Zhang *et al*., 2012). However, as miRNAs are not annotated in yeast, it is currently unknown whether these yeast-derived RNAs have similar function in flies.

The wild type and *dilp2-3,5* mutant flies used in this study both carry the endosymbiontic bacterium *Wolbachia pipientis*. Accordingly, reads mapping to the genome of *Wolbachia* were identified in all analyzed tissues, ranging from 0.4 % of all reads in the brain up to 1.8 % of all reads in the abdomen. Even though the detailed molecular interaction between *Wolbachia* and its host are still elusive, *dilp2-3,5* mutants are only long-lived in the presence of this bacterium (Grönke *et al*., 2010). Interestingly, the amount of reads mapping to the *Wolbachia* genome is increased in *dilp2-3,5* flies. This is in agreement with the observation, that in *dilp2-3,5* flies the amount of *Wolbachia* bacteria is increased (Sebastian Grönke, personal communication). The influence of increased *Wolbachia* load in *dilp2-3,5* flies is still elusive. In mosquitos, *Wolbachia* changes the expression of host miRNAs to increase its density in the host (Hussain *et al*., 2011). Profiling and comparing miRNA expression of *dilp2-3,5* mutants with and without *Wolbachia* could explore a putative role of *Wolbachia* in the regulation of miRNA expression in *dilp2-3,5* flies.

3.2 Comparison of absolute expression datasets between sequencing and microarrays

I could show in this study that absolute miRNA expression data between microarray and next generation sequencing only show low level of correlation between the two platforms. This was also evident on the level of individual miRNAs. For example, miR-14 was one of the strongest expressed miRNAs as detected by sequencing, but miR-14 was not detected at all by microarray analysis. Using the same RNA source for both platforms did not increase correlation of absolute expression values. In contrast, two microarray expression datasets from independent biological RNA samples showed strong correlation, demonstrating that the observed differences are not caused by biological variation between samples. Therefore,

differences in absolute expression data between the two platforms are likely caused by differences between microarray and next generation sequencing technologies. One technical difference might be hybridization bias of microarrays, which can have several reasons. First, hybridization affinity of miRNAs on the microarrays is dependent on the similarity to the complementary sequence of the probe set. Many miRNAs share high sequence similarities. For example miR-2a and miR-2c mature miRNAs only differ in a single nucleotide. Thus, differences between miRNA expression data might be due to miRNAs binding to probe sets of closely related miRNAs. Second, the Affymetrix 2.0 GeneChip used in this study contains probe sets for more species in addition to the *Drosophila melanogaster* probe sets. Thus, miRNAs may bind these non-*Drosophila melanogaster* probe sets, which could affect their absolute expression levels. Third, the GC content varies substantially among miRNAs resulting in different melting temperatures for each miRNA. As hybridization temperature is constant, miRNAs with low melting temperatures might bind to the chip with lower affinity while others with high melting temperatures bind with high affinity. Thus differences between miRNA expression data might be caused by different GC content and consequently different affinity of miRNAs in binding to complementary sequences on the chip. Library preparation for next generation sequencing might also introduce expression bias for certain miRNAs. In a comparison of different miRNA profiling methods Linsen *et al.* (Linsen *et al.*, 2009) observed, that different methods for miRNA library preparation caused differences in absolute expression profiles for specific miRNAs. Biases caused by RNA ligation preferences, reverse transcriptase and PCR amplification could also contribute to the difference between microarrays and sequencing in the ability to detect absolute expression levels of miRNAs in our study. It has been shown that it is not possible to conclude from detection signal of microarrays to biological expression levels (Chen *et al*., 2009). The results of my study are in agreement with the observation that absolute miRNA expression measurements are dependent on the used detection technique. NGS can distinguish between very similar sequences, which differ only in a single nucleotide. Additionally, since NGS is not dependent on *a priori* information it allows the detection of unknown miRNAs as well as miRNA isoforms resulting from post-transcriptional modification. Additionally, it allows the detection of more miRNAs than by microarray. Therefore, further studies should be based on sequencing results.

3.3 Adult *Drosophila* microRNA expression atlas

The function of most *Drosophila* miRNAs is still unknown. An important step in comprehending miRNA function is to understand miRNA tissue specificity. However, for most *Drosophila* miRNAs adult expression level and tissue specificity are still elusive. To close this gap we generated miRNA expression profiles of four adult *Drosophila* tissues, namely brain, thorax, digestive tract and abdomen, by microarray and next generation sequencing.

3.3.1 Tissue-specific microRNA expression profiles

Pairwise comparison of miRNA expression profiles of the four tissues confirmed that the quality of tissue preparation was constant and indicated that each tissue inhered a unique and characteristic miRNA expression pattern. Tissue specificity from sequencing and microarrays were mostly consistent between both platforms as revealed by Pearson correlation analysis. We identified ubiquitously expressed miRNAs and many miRNAs that are expressed specifically in a certain tissue. Most miRNAs with a high tissue specificity score were expressed in the brain. This could indicate that particularly brain function is highly specialized and needs to be regulated by specific miRNAs. However, this could also represent the purity of dissected brains.

3.3.2 Tissue specificity of microRNAs is in agreement with published data

Our *Drosophila* miRNA atlas is in agreement with published data. miRNAs like miR-981, miR-969, miR-927 or miR-990 were shown to be expressed in *Drosophila* heads (Ruby *et al*., 2007). Accordingly, we found these miRNAs to be specifically expressed in the brain. Neuronal expression of miR-124 is evolutionarily conserved between flies, nematodes, and vertebrates and a function of miR-124 in *Drosophila* neurons has been reported (Sun *et al*., 2012). In agreement, we found specific expression of miR-124 in the brain. Another brain-specific miRNA, miR-219, was shown to be specific for brain cells in vertebrates, and to control oligodendrocyte differentiation (Zhao *et al*., 2010). In contrast to the analysis of total head miRNA expression (Ruby *et al*., 2007), our analysis detected expression more precisely in the brain and in addition identified up to now unknown brain specificity for some miRNAs. For example, miR-315 was found to be specifically expressed in fly imaginal discs (Ruby *et al*., 2007), but we could show specific expression of miR-315 in the adult brain. Data about tissue specificity of novel miRNAs is still limited. Our study provides detailed information

about tissue specificity of novel miRNAs such as miR-4960, which we assigned to be a brain specific miRNA.

miR-1 has been shown in diverse species including *Drosophila* to be specifically expressed in muscles (Zhao *et al*., 2007; Simon *et al*., 2008; Sokol and Ambros, 2005). In our study miR-1 expression was enriched in the thorax, although with a relative low tissue-specificity score compared to the brain-specific miRNAs. Similarly, miR-277 was previously shown to be expressed in the thorax (Esslinger *et al*., 2013), which we could verify in our analysis. However, as for *miR-1*, the tissue specificity score was relatively low. The dissected thorax does not only consist of muscle tissue, but also includes epidermal tissue, fat tissue and parts of the nervous system. Different tissues types in thorax samples might limit the detection of specificity. Indeed, only few miRNAs had a high tissue specificity score for the thorax.

miRNAs like miR-314, miR-958 or miR-956 were previously shown to be expressed in adult fly bodies (Ruby *et al*., 2007). Our study shows that these miRNAs are not ubiquitously expressed throughout the whole adult fly, but specifically in the digestive tract. Another example for a digestive tract-specific miRNA is miR-10. During embryogenesis miR-10 is expressed in the posterior midgut and the anal pad (Aboobaker *et al*., 2005) and we show that in the adult, expression of miR-10 remains specific for the digestive tract. miR-2494, miR-1015, miR-994 and miR-274 are examples of miRNAs, which expression was previously detected in whole adult bodies (Ruby *et al*., 2007) and we could now show that they are specifically expressed in abdomen. In summary, the observed tissue-specific miRNA expression profiles are consistent with previous reports and significantly extend our knowledge about miRNA expression in adult *Drosophila* flies.

Expression and function of miR-993 was unknown so far. miR-993 belongs to the well characterized and conserved *miR-10* miRNA family. *miR-10* is one of two miRNA genes of the *Drosophila* Hox clusters and it has been shown to be expressed in ventral nerve cord, posterior midgut and hindgut in *Drosophila* embryos (Aboobaker *et al*., 2005). miR-10 was shown to regulate Hox genes in zebrafish (Woltering and Durston, 2008) and humans (Han *et al*., 2007). However, in *Drosophila* the targets of miR-10 are unknown. Although *miR-993* belongs to the *miR-10* family, it is not predominantly expressed in the gut. Instead, it is expressed in the thorax and also to a minor extent in the brain, suggesting that its function is different to miR-10. Therefore, miRNAs which belong to the same miRNA family do not necessarily have same expression patterns.

3.3.3 Strong microRNA expression increases reliability in the detection of tissue specificity

For few miRNAs tissue specificity differs between microarrays and sequencing. miRNAs, which were determined as tissue-specific by microarray but not by sequencing, are usually expressed at low levels as detected by sequencing and high levels as detected by microarray. For example miR-184-5p had a strong signal on microarrays, whereas by sequencing this miRNA had only few reads. Reciprocally, miRNAs, which were determined to be tissue-specific by sequencing, but not by microarray are barely detected by microarrays, but detected to be highly expressed by sequencing. For example miR-958-3p had a high number of reads in the digestive tract whereas this miRNA was not detected by microarray analysis to be tissue-specific. Thus, assigning tissue specificity to a miRNA can depend on the platform used to detect its expression and is more reliable if the miRNA expression is detected at significant levels on both platforms.

3.3.4 Evolutionary conservation of microRNAs does not correlate with breadth of expression

Evolutionary conserved miRNAs were more ubiquitously expressed across libraries of different *Drosophila* developmental stages, heads and adult bodies than non-conserved miRNAs (Ruby *et al*., 2007). In contrast, we found no correlation between evolutionary conservation of miRNAs and breadth of expression across tissues of adult *Drosophila* flies. Non-conserved miRNAs might define profile specificity only of developmental stages but not of adult tissues. However, our finding could also reveal that there is indeed no correlation between tissue specificity and conservation level of a miRNA in adult flies.

3.3.5 Evolutionary conservation of microRNAs correlates with expression level

Highly expressed miRNAs tend to be more evolutionarily conserved than miRNAs with low expression levels (Ruby *et al*., 2006; Ruby *et al*., 2007; Bartel, 2004). In agreement with this hypothesis, we also found a positive correlation between expression level and evolutionary conservation in our next generation sequencing data set. However, some miRNAs deviate from this rule, e.g. miR-956 is only present in *Drosophila* but highly expressed. On the other hand, expression level of some conserved miRNAs might be underestimated due to a very tissue- or cell type-specific expression. These miRNAs would have low read counts in libraries of complex tissues samples. For example, miR-285 was found to be expressed at low levels in all analyzed tissues although it belongs to the conserved *miR-29* family. In

mammals, miR-29 expression is enriched in astrocytes (Ouyang *et al*., 2013). Astrocyte-like glia account for a subset of brain cells in *Drosophila* and other cells of the dissected brain may mask high astrocyte-specific expression of miR-285. Like miR-285, other conserved miRNAs, which were found to be lowly expressed could be restricted to a certain tissue or cell type not analyzed in this study. Although sequencing analysis revealed a clear correlation between miRNA expression level and evolutionary conservation, no correlation was observed using microarrays. On the Affymetrix microarray only a limited number of miRNAs are present, excluding many miRNAs with low expression. Sensitivity of microarrays might be limiting, whereas sequencing was able to detect a non-random correlation between expression level and evolutionary conservation.

3.4 Differentially expressed microRNAs in *dilp2-3,5* mutants

In *Drosophila,* tissue-specific down-regulation of IIS signaling is sufficient to increase lifespan (Grönke *et al*., 2010; Giannakou *et al*., 2004; Hwangbo *et al*., 2004; Demontis and Perrimon, 2010). However, it is currently unknown whether miRNAs mediate pathway activity and gene expression downstream of the insulin receptor. We identified differentially expressed miRNAs in all four analyzed tissues of the *dilp2-3,5* mutant by microarray analysis and confirmed the expression changes for selected miRNAs by qRT-PCR. qRT-PCR analysis also showed that miRNAs such as miR-2500-5p and miR-986-5p, which by microarray analysis were only found to be regulated in the brain and thorax, were also differentially regulated in the digestive tract and the abdomen. These results suggest that the sensitivity of microarrays may be limiting for some miRNAs to detect differential expression and demonstrates that qRT-PCR verification is important. Some miRNAs were found to be up-regulated in one tissue and down-regulated in other tissues, demonstrating complex tissue-specific changes in miRNA expression upon down-regulation of the IIS pathway. The number of miRNAs that were up- and down-regulated was comparable in the brain and in the abdomen. In the digestive tract most miRNAs were down-regulated and in the thorax most miRNAs were up-regulated in *dilp2-3,5* mutants. This observation was independent of the tissue preparation method and the microarray chip version and was reproducible, because it was observed for both mechanically and manually dissected thoraces. Less miRNAs were detected to be differentially expressed in manually dissected thoraces due to variation in samples, which affects the sensitivity to detect differentially expressed miRNAs.

By sequencing of independent biological tissue samples we found a different set of miRNAs to be up- and down-regulated than by microarray. In the brain and in the thorax miRNAs were

found to be significantly differentially expressed. At the significance level of single comparisons, differentially expressed miRNAs were also found in the abdomen and digestive tract. In contrast to microarray results, we found the majority of differentially expressed miRNAs in the thorax to be down-regulated. Malone and Oliver (Malone and Oliver, 2011) reported that sequencing and microarrays show similar performance in detecting differential mRNA expression. We could show that the detection of differentially expressed miRNAs in *dilp2-3,5* mutants correlated only if the same RNA input was used for both techniques. Comparison of differential expression of microarray and sequencing data using independent RNA samples showed no correlation. Thus, detection of differential expression levels in *dilp2-3,5* mutants is independent of the technique used though only consistent when the same RNA is used for both techniques. miRNAs with the strongest fold change in expression were usually detected at low levels. The signal of differentially expressed miRNAs like miR-303-5p was even close to the detection threshold. Strongly expressed miRNAs are usually evolutionary conserved and the expression was less changed in the mutant than the expression of low expressed miRNAs. One possible explanation is that conserved miRNAs could execute essential functions and are therefore under stringent control to keep constant expression levels. Another explanation is that the fold change of barely expressed miRNAs is caused by variations in expression attributable to the influence of small variations on FC of low expressed miRNAs. This could account for the different results of microarray, sequencing and qRT-PCR in the detection of differentially expressed miRNAs using independent biological samples.

3.4.1 MicroRNA candidates and their role in regulation of lifespan

The function of most miRNAs that were detected as differentially expressed in *dilp2-3,5* mutants is not known in *Drosophila* or any other species. However, some of those miRNAs have been shown to play a role in aging or aging-modulating pathways.

miR-210 is highly evolutionarily conserved between flies and mammals. In mammals, miR-210 is induced by hypoxia and is a direct targeted of the hypoxia-inducible factor (HIF-1α) (Liu *et al*., 2011), a transcription factor involved in lifespan regulation. Interestingly, HIF-1α is activated by the insulin pathway in *Drosophila* (Dekanty *et al*., 2005). Thus, it would be expected that miR-210 abundance is reduced in *dilp2-3,5* mutants. In contrast, we showed by microarray that miR-210 is up-regulated in *dilp2-3,5* flies. This might indicate an inherent compensatory effect. However, to discover the role of elevated miR-210 levels in *dilp2-3,5* mutants, functional analysis of this miRNA in *Drosophila* is required.

miR-285 is down-regulated in *dilp2-3,5* mutants. *Drosophila miR-285* belongs to the conserved *miR-29* family. In mammals, upregulation of miR-29 correlates with aging and miR-29 is up-regulated in a progeroid mouse model most likely in response to DNA damage (Ugalde *et al*., 2011). The function of *Drosophila* miR-285 is not known, yet. However, if the function of miR-29 is conserved, *dilp2-3,5* mutants might have less DNA damage, which in consequence results in the down-regulation of miR-285. Further studies are needed to test this hypothesis.

miR-375 expression was found to be up-regulated in *dilp2-3,5* brains by sequencing. miR-375 is highly evolutionarily conserved and its function has been extensively characterized. miR-375 is specifically expressed in secretory pituitary brain cells in zebrafish (Kapsimali *et al*., 2010). In mammals, miR-375 is specifically expressed in pancreatic islets (Poy *et al.*, 2009), where it is involved in regulation of glucose homeostasis. miR-375 knockout mice are hyperglycemic, have decreased numbers of pancretic β-cells and reduced insulin levels (Poy *et al.*, 2009). Furthermore, in obese mice, which are insulin resistant and have an increased insulin demand, miR-375 is up-regulated to compensate this state by promoting β-cell expansion (Poy *et al.*, 2009). The function of *Drosophila* miR-375 is currently unknown. However, its role in glucose homeostasis in mammalian pancreatic cells, and its differential expression in *dilp2-3,5* flies, might indicate a role of miR-375 in *Drosophila* insulin producing cells (IPCs).

Our sequencing analysis reveals that miR-33 is down-regulated in the thorax of *dilp2-3,5* mutant flies. miR-33 is evolutionarily conserved and in mammals it targets the insulin receptor substrate 2 (IRS2) in liver cells (Dávalos *et al*., 2011). Overexpression of miR-33 not only reduces IIS, it also reduces fatty acid oxidation, whereas reduction of miR-33 increases both pathways (Dávalos *et al*., 2011). Furthermore, miR-33 was shown to regulate cholesterol levels in mice (Rayner *et al*., 2010). miR-33 might be a putative regulator of metabolic pathways in the fly, since *dilp2-3,5* flies have altered lipid levels. However, so far miR-33 was not functionally characterized in *Drosophila* and it role in IIS or fatty acid metabolism needs to be further investigated.

miR-277, which is specifically expressed in the thorax was down-regulated in *dilp2-3,5* mutant flies. We could show that overexpression of miR-277 in fly thoraces shortens lifespan, which would suggest down-regulation of miR-277 as a putative mechanism of IIS-mediated lifespan extension. However, inhibition of miR-277 also shortens lifespan in flies and

miR-277 has been reported to be down-regulated with age (Esslinger *et al*., 2013). Thus the role of miR-277 in IIS-dependent lifespan extension is currently unclear.

let-7 miRNA is highly evolutionarily conserved between species including worms, flies and mammals. In mammals let-7 was shown to target components of the insulin pathway including insulin-like growth factor 1 receptor (IGF1R), insulin receptor (INSR) and IRS2 (Zhu *et al*., 2011). In worms let-7 family members miR-84 and miR-241 were also shown to regulate insulin/IGF signaling and metabolism. Additionally, these two miRNAs are required for germline mediated longevity through DAF-16/FOXO (Shen *et al*., 2012). let-7 family members miR-84 and miR-241 are not annotated in *Drosophila* or more complex species. let-7-3p was shown to be down-regulated in *dilp2-3,5* thoraces as detected by sequencing. However, this miRNA is lowly expressed and there is no evidence that it has a biological function. let-7-5p is highly expressed, its expression was validated by northern blot and its function was characterized (Sokol *et al*., 2008). In contrast to let-7-3p let-7-5p was not detected to be differentially regulated in *dilp2-3,5* flies suggesting that the conserved miRNA let-7 might not regulate IIS mediated phenotypes in *Drosophila*.

miR-14 was shown to control insulin production in IPCs in the fly brain. Overexpression of miR-14 in the IPCs resulted in lean flies possibly as consequence of elevated insulin levels. Similar to IIS mutants, *miR-14* mutants have elevated fat levels. Furthermore, dILP2, dILP3 and dILP5 levels in the brain are decreased in *miR-14* mutants (Varghese *et al*., 2010). miR-14 expression was not only detected in the brain, but also in all other analyzed tissues. We found miR-14 to be down-regulated in *dilp2-3,5* thoraces. Since miR-14 was shown to regulate dILP levels and we showed that miR-14 expression in turn is dependent on dILPs, this miRNA could be part of a feedback loop regulating IIS. Interestingly, miR-14 was reported to play a role in the positive autoregulatory loop of ecdysone signaling (Varghese and Cohen, 2007), a pathway which was shown to play a role in lifespan (Gáliková *et al*., 2010). Further studies are needed to address the regulatory role of miR-14 in endocrine signaling and its putative connection to lifespan.

If differentially expressed miRNAs contribute to phenotypes of the *dilp2-3,5* mutant remains to be investigated. By microarray and sequencing in each tissue of the long-lived *dilp2-3,5* mutant differentially regulated miRNAs which are highly conserved even up to humans were found. Since many molecular mechanisms of IIS are similar between organisms, a comparison of our data with tissue-specific miRNA expression profiles of long-lived mutants from other organisms could provide information about conserved regulation of miRNAs in

processes associated with IIS-mediated phenotypes such as longevity. As *Drosophila* provides excellent genetic tools to study the role of miRNAs in aging *in vitro* and *in vivo*, studies in this model organism could provide new insights into mechanisms, which could be relevant for other organisms.

3.4.2 The microRNA 6~309 cluster is up-regulated in *dilp2-3,5* abdomen

Tissue specificity of *dilp2-3,5* miRNAs is altered compared to wild type. Interestingly, analysis of tissue specificity was able to identify miRNAs, which tissue specificity was altered but not significantly differentially expressed. miRNAs with altered tissue specificity involve miR-5-5p, miR-286-3p, miR-6-1-3p/miR-6-2-3p/miR-6-3-3p and miR-4-3p. Expression of these miRNAs is evenly distributed across tissues in wild type. In *dilp2-3,5* mutants, expression of these miRNAs becomes enriched in the abdomen. It was shown that clustered miRNAs are often co-expressed in an operon-like manner (Ruby *et al*., 2007; Lau *et al*., 2001; Sempere *et al*., 2004). Indeed, all identified miRNAs are located within the same genomic cluster, indicating that these miRNAs are concerted up-regulated in *dilp2-3,5* abdomen. Verification and functional analysis by knock-out or overexpression is necessary to unravel the putative role of this cluster in phenotypes of the *dilp2-3,5* mutant.

3.5 The *miR-986^{KO}* mutant

In this study a *miR-986^{KO}* mutant was successfully generated by homologous recombination and analyzed for IIS-associated phenotypes. Homozygous *miR-986^{KO}* mutant flies were viable and had no obvious developmental defects, indicating that miR-986 is not essential for viability and growth. Moderate overexpression of miR-986 did not affect lifespan. In contrast, lack of *miR-986* significantly reduces lifespan. Therefore, correct miR-986 expression is required for normal lifespan. Fecundity of *miR-986^{KO}* flies was reduced and mutants were prone to starvation, indicating that normal miR-986 expression is required for long term health.

Tolerance towards DDT or hydrogen peroxide was not changed in *miR-986^{KO}* mutants compared to wild type flies. In contrast, *miR-986^{KO}* mutants were more resistant to paraquat treatment. Toxicity of paraquat involves the production of superoxide. Increased paraquat resistance of flies lacking *miR-986* suggests that miR-986 might target mRNAs responsible for superoxide resistance. However, a target prediction algorithm did not reveal genes involved in superoxide detoxification. The production of superoxide by reduction of paraquat is mainly mediated by P450 oxidoreductases (Han *et al*., 2006). *miR-986* resides within an

intron of the P450 cytochrome gene *Cyp4e2*. Cyp4e2 expression is down-regulated in *miR-986*^{KO} flies. Therefore, increased tolerance of *miR-986*^{KO} flies to paraquat might be caused by a reduced expression of Cyp4e2 and hence reduced generation of superoxide in these mutants and not by a direct effect of loss of *miR-986*.

To differentiate whether reduced Cyp4e2 or the lack of *miR-986* causes the observed phenotypes further studies are needed. In order to test whether observed phenotypes can be assigned to the lack of *miR-986*, a *miR-986* mutant without white-marker and with rescued expression of Cyp4e2 was successfully generated and is available for phenotyping. Further, genomic rescue experiments are necessary to study the *in vivo* function of miR-986.

3.6 Functional characterization of differentially expressed microRNAs by overexpression

Overexpression of miR-7 and miR-978 during development caused lethality, suggesting that misexpression of those miRNAs has toxic effects early in development. Conserved miRNAs might execute essential functions and their precise regulation might be pivotal for the organism. Although miR-7 is conserved and causes lethality when artificially overexpressed, overexpression of the non-conserved miR-978 did also cause lethality. Therefore, toxicity upon overexpression is independent on evolutionarily conservation of the overexpressed miRNA. miRNAs are expressed at different levels in *Drosophila*. Upregulation of miRNAs that are normally expressed at low levels might have more severe impacts on health than upregulation of miRNAs that are highly expressed in wild type flies. Both, miR-7 and miR-2500 are expressed at relative low levels. While overexpression of miR-7 causes lethality and adult specific expression of miR-7 severely impacts lifespan, miR-2500 overexpressing flies are viable. Thus, toxicity of overexpression is independent on the degree of induced differential expression.

Adult specific strong ubiquitous overexpression with the tubulin-Gal4 or tubulin-GS driver of most miRNAs resulted in shortened lifespan. This could be a specific effect due to toxicity of the particular miRNA, possibly caused by expression in tissues where this miRNA is usually not or not as highly expressed resulting in the down-regulation of pivotal genes in these tissues. Alternatively, this could be a general effect of increased miRNA load in the cells, which becomes toxic over time. Strong overexpression may also affect miRNA target specificity so that genes are down-regulated, which are not normally a target of a given miRNA.

Strong overexpression of candidate miRNAs did not increase lifespan. However, this does not exclude that overexpression of other miRNAs could be beneficial for survival. Indeed, mild overexpression of miR-34 by genomic insertion constructs increased lifespan, while Gal4/UAS mediated expression of miR-34 during development caused lethality (Liu *et al*., 2012). By usage of a mild daGS driver, toxicity of overexpression of analyzed miRNAs was reduced. A lifespan extending effect of miRNA overexpression could be dosage-dependent with strong miRNA expression resulting in toxicity. In congruence, miRNAs in *dilp2-3,5* flies showed only small differential expression. Overexpression level of miRNAs can be fine tuned by the concentration of RU486 in the food. Therefore, miRNA expression that mimic the fold change in long-lived mutants were used to investigate lifespan phenotypes. Mild overexpression of selected miRNAs prevented toxic effects on lifespan, suggesting that toxicity of up-regulation is dosage dependent. However, lifespan was not increased upon various levels of mild overexpression, suggesting that ubiquitous up-regulation of the selected candidate miRNAs is not beneficial for survival. In *dilp2-3,5* flies miRNAs were differentially expressed in specific tissues. In order to test whether lifespan depends on tissue-specific overexpression of selected miRNAs, miR-210, miR-954 and miR-978 were overexpressed in specific tissues. Neither overexpression affected lifespan, suggesting that selected miRNAs do not mediate lifespan extension. Other miRNAs still could mediate IIS dependent lifespan, which were not identified to be differentially expressed by microarray. Sequencing revealed a different set of differentially expressed miRNAs in *dilp2-3,5* mutants, which should be analyzed for their role in lifespan extension.

Although there is no evidence for differentially expressed miRNAs which were identified by microarray to regulate lifespan extension, those miRNAs could play a role in other IIS mediated phenotypes and were therefore analyzed for phenotypes of *dilp2-3,5* flies. *dilp2-3,5* flies have a reduced body weight, increased development time and reduced fecundity (Grönke *et al*., 2010). However, flies overexpressing miR-986, miR-2500 or miR-954 had normal body weight, suggesting that these miRNAs do not regulate organismal growth. Overexpression of selected miRNAs reduced egg production. Because increased expression of miRNAs also reduced lifespan, it is unlikely that reduced egg production as a result of overexpression is a specific effect. Instead, decreased fecundity seems to be an unspecific effect caused by toxicity of overexpression. Overexpression of miR-2500 or miR-954 did not change development time, suggesting that those miRNAs do not regulate developmental timing. In contrast, miR-986 overexpression caused a delay in development. The effect was stronger in

males than in females, suggesting gender-specific functions of miR-986. Consistently, development time of two of three independent fly strains lacking *miR-986* was shortened.

Further analysis of IIS-related phenotypes of flies overexpressing miRNAs that are differentially regulated in *dilp2-3,5 flies* is needed. Differentially expressed miRNAs should also be investigated by knockout or RNAi in order to distinguish between specific and unspecific effects and to verify functions in IIS related phenotypes. In addition to the analysis of differentially expressed miRNAs that might be putative mediators of IIS depending phenotypes, miRNAs that are expected to target components of lifespan modulating pathways such as the IIS pathway, should be investigated for longevity by overexpression or down-regulation in order to explore upstream mechanisms and to get a comprehensive overview of the role of miRNAs in lifespan regulating pathways.

4 Material and methods

4.1 Bacterial media

All bacterial media were autoclaved to assure sterility. Antibiotics were added to media after autoclaving and cooling to 60 °C.

Lysogeny broth (LB) medium	1% NaCl pH 7.0 1 % (w/v) Trypton 0.5 % yeast extract

Bacterial plates consisted of LB medium with 1.5 % bacto-agar.

S.O.C medium	20 mM glucose 10 mM $MgSO_4$ 10 mM $MgCl_2$ 2.5 mM KCl 10 mM NaCl 0.5 % yeast extract 2 % bactotryptone

4.2 Solutions

TAE (1x)	40mM Tris 20mM acetic acid 1mM EDTA
TBE (5x)	445 mM boric acid 445 mM Tris 10 mM EDTA
PBS	145 mM NaCl 7.5 mM Na_2HPO_4 2.5 mM NaH_2PO_4 pH adjusted to 7.4
Squishing buffer	10 mM Tris-HCl 1 mM EDTA 25 mM NaCl 200 µg/ml Proteinase K pH adjusted to 8.2
Saline-sodium citrate buffer (SSC; 20x), RNAse-free	3 M sodium chloride 300 mM trisodium citrate pH adjusted to 7.0 with HCl
MyOne C1 dynabead B&W buffer + 0.01% Tween (2x)	10 mM Tris-HCl (pH 7.5) 1 mM EDTA 2M NaCl 0.01% Tween

MyOne C1 dynabead B&W buffer + 0.01% Tween (1x)	5 mM Tris-HCl (pH 7.5) 500 µM EDTA 1M NaCl 0.01% Tween
MyOne C1 dynabead Solution A	0.1 M NaOH 0.05 M NaCl
MyOne C1 dynabead Solution B	0.1 M NaCl

4.3 *Drosophila* food media

All *Drosophila* food and media were boiled to dissolve agar. Nipagin was added to media after boiling and cooling to 60 °C.

SYA food	5 % sugar 10 % yeast 1.5 % agar 0.3 % Nipagin (20 % in EtOH)
Starvation media	1 % agarose in H_2O
H_2O_2 media	1 % agarose (w/v) 5 % H_2O_2 10 % sugar (w/v) in H_2O
Dichlorodiphenyltrichloroethane (DDT) media	275 mg/l DDT in SYA food
Paraquat media	20 mM paraquat in SYA food
Grape medium	grape juice 1.5 % agar 1 % nipagin (20 % in EtOH)

4.4 Fly stocks, genetic background and general animal husbandry

The wild type stock used was w^{Dah} Wol+, carrying the intracellular bacterium *Wolbachia*. This stock is maintained in large population cages to reduce inbreeding. All fly lines were backcrossed for at least 9 generations into the w^{Dah} background. Backcrossed fly lines were kept in bottles (13.5 cm x 6 cm diameter) on standard food in order to maintain them in large cohorts. Backups of non-backcrossed stocks were kept in plastic vials (9.5 cm x 2.5 cm

diameter). All stocks were kept on a 12:12 light:dark cycle at 18°C and 65% humidity in a controlled temperature (CT) room.

Table 13: Fly stock list.

Name	Genotype	source
wild type	w^{Dah} Wolbachia +	Groenke *et al*., 2010
dilp2-3,5	w^{Dah}*; dilp2-3,5*	Groenke *et al*., 2010
#6934	y^1, *w**; *P{70FLP}11*, *P{70I-SceI}2B*, sna^{Sco}*/CyO*, S^2	Bloomington *Drosophila* Stock Center
#766	$y^1 w^{67c23} P\{Crey\}1b$; sna^{Sco}*/CyO*	Bloomington *Drosophila* Stock Center
#3938	w^{1118}*; P{70FLP}10*	Bloomington *Drosophila* Stock Center
miR-986^{KO}	w^{Dah}*; miR-986*^{KO}	Jennifer A. Werner, this study
miR-986^{KO*}	w^{Dah}*; miR-986*^{KO*}	Jennifer A. Werner, this study
UAS-miR-986	w^{1118}*; UAS-miR-986*	Bejarano *et al*., 2012
UAS-miR-210	w^{1118}*; UAS-miR-210*	Bejarano *et al*., 2012
UAS-miR-7	w^{1118}*; UAS-miR-7*	Bejarano *et al*., 2012
UAS-miR-954	w^{1118}*; UAS-miR-954*	Bejarano *et al*., 2012
UAS-miR-978	w^{1118}*; UAS-miR-978*	Bejarano *et al*., 2012
UAS-miR-2500	w^{1118}*; UAS-miR-2500*	Eric C. Lai, PhD
UAS-miR-285	w^{1118}*; UAS-miR-285*	Bejarano *et al*., 2012
Tubulin-Gal4	y^1 w^**; P{tubP-GAL4}LL7/TM3,* Sb^1	Bloomington *Drosophila* Stock Center
MHC-Gal4	w^**; P{Mhc-RFP.F3-580}2, P{Mhc-GAL4.F3-580}2/SM6b*	Bloomington *Drosophila* Stock Center
Tubulin-GS	w^{Dah}; Tubulin-GeneSwitch	Fernandez *et al*., 2009
Da-GS	w^{Dah}; Daughterless-GeneSwitch	Tricoire *et al*., 2009
$S1_{106}$-GS	w^{Dah}; $S1_{106}$-GeneSwitch	Roman *et al*., 2001

4.5 Collecting males and virgins and setting up crosses

Virgin females were collected in the morning from bottles which were cleared the day before and kept at 18 °C over night for a maximum of 16 h to ensure virginity. Parental flies for crossings were anesthetized by CO_2 and collected. Collected males and females were kept in bottles at 25 °C on a 12:12 light:dark cycle and 65 % humidity for 48 h to mate and were then transferred into cages with grape plates.

4.6 Egg collections for experiments

In order to assure standard larval density for experimental flies, parental flies were kept on grape agar plates to allow egg laying for 6 h. Eggs were washed of the plates with PBS using a brush. Eggs were then transferred into falcon tubes and allowed to settle down. PBS supernatant was removed and 20 µl eggs were pipetted per bottle using a cut pipette tip. Bottles with standardized amount of eggs were kept at 25 °C on a 12:12 light:dark cycle and 65 % humidity.

4.7 Mapping of transgene insertions

Male flies with unknown transgene insertion site, which contains the mini-*white* marker, were crossed to the female balancer lines CyO/+ and Tm3Sb/+. If all female F1 flies had red eyes and male flies had white eyes, the insertion is located on the X-Chromosome. If not, red-eyed F1 flies containing the respective balancer were intercrossed. F2 offspring flies were screened for red eyes. The insertion was mapped to the second chromosome, if all flies containing CyO had red eyes and all flies containing Tm3Sb had white or red eyes. The insertion was mapped to the 3rd chromosome if all flies containing Tm3 Sb had red eyes and all flies containing CyO had white or red eyes.

4.8 Expression of genes with the UAS/Gal4 System

In *Drosophila*, overexpression of a specific gene can be achieved by the binary Gal4/UAS system (Brand and Perrimon, 1993). The method is based on the activation of transcription by the yeast transcription activator Gal4 that binds to the upstream activation sequence (UAS) fused to sequences of the gene of interest (Figure 2.7 B). Flies expressing Gal4 (driver lines) are crossed to flies harbouring the UAS-transgene. F1 flies will express the gene of interest in a manner depending on the used Gal4 promoter. Modification of this system allows temporal expression induced by RU486 (Osterwalder *et al*., 2001), which is achieved by a RU486-dependent GAL4 protein (GeneSwitch).

4.9. Fly stress assays

Flies reared at standard density (see chapter 4.6) were allowed to mate after eclosing for 48 h in bottles at 25 °C on a 12:12 light:dark cycle and 65 % humidity. Flies were then sorted according to gender into plastic vials with SYA food. 5 x 20 flies per vial were used per treatment. Flies were transferred into new vials every 2 days, before starting the assay at the age of 10 days. For the stress assay flies were transferred into vials containing the stress media, which was prepared freshly on the day of the experiment (see chapter 4.3). Dead flies were counted in regular time intervals.

4.10 Lifespan assay

Experimental flies were reared at standard density (see chapter 4.6) and transferred into new bottles after eclosing. After a mating period of 48 h, 10 flies per glass vial (7.5 cm x 2.55 cm diameter) with standard SYA food and 20 flies per plastic vial (9.5 cm x 2.5 cm diameter) with food containing RU486 were allocated. Flies were transferred into new vials three times

a week and kept at 25 °C on a 12:12 light:dark cycle and 65 % humidity. The number of dead flies per vial was counted on the day of transfer.

4.11 Fecundity assay

The number of eggs laid was counted as readout for fecundity. Lifespan flies at the age of 10 days were kept on fresh food for 12-16 h and then transferred to new vials. The number of eggs laid over this time period was counted for each vial. Data represent cumulative number of eggs laid per female.

4.12 Development time assay

For measurement of development time parental flies were allowed to lay eggs for 3 h on grape plates. Eggs on the plate were kept on 25 °C until first instar larvae hatched. First instar larvae were hand-picked and transferred into glass vials at a density of 50 larvae per vial on standard food. The number of eclosing adults flies was recorded at regular time points.

4.13 Body weight

For body weight measurements, flies were anesthetized on ice and then weighted in pairs on a semi-microbalance (ME235S, Sartorius Mechantronics).

4.14 Tissue dissection

All tissues were manually dissected using fine forceps on silicone plates with PBS. The brain includes the optical lobes and attaching connective tissue as well as residual fat tissue from the head. The thorax includes the wings and legs and excludes the gut. Thus the dissected thorax mainly consists of muscle tissue. The digestive tract is the midgut excluding malpighian tubules. The whole abdomen is dissected, excluding ovaries, digestive tract and malpighian tubules. Thus, what is referred to as abdomen consists of the abdominal carcass with adhering fat tissue. Tissues were dissected in 1x PBS, snap frozen in tubes on dry ice and stored at -80 °C. RNA from dissected tissues was used for next generation sequencing and for microarrays.

4.15 Mechanic separation of thoraces and heads

Flies were frozen in liquid nitrogen and heads, thorax as well as abdomen were separated by vortexing in a reagent tube. First, heads were separated from thorax and abdomen through a sieve. Thoraces were then separated from abdomen by intensive vortexing and manual selection on dry ice using a fine brush.

4.16 General cloning techniques and molecular biology

4.16.1 Polymerase chain reaction (PCR)

PCR is a widely common technique used to amplify DNA molecules (Saiki *et al*., 1988). PCR reactions for cloning or genotyping were carried out in a Veriti 96 well thermal cycler (Applied Biosystems). Oligonucleotide primers for PCR reactions were purchased from MWG-Biotech. For a complete list of oligos used in this study see supplemental table 3.

4.16.1.1 Genotyping of flies by PCR

For genotyping of flies the HotStarTaq *Plus* DNA Polymerase (Qiagen) was used. 150 ng DNA and 0.5 µl of each primer at the concentration of 10 µM were mixed with 10 µl of HotStarTaq Plus Master Mix (2x) and water was added to adjust the total volume to 20 µl.

The cycler was programmed as follows:	Step 1	95 °C	5 min
	Step 2	94 °C	30 sec
	Step 3	50–68 °C	30 sec
	Step 4	72 °C	1 min
	Step 5	72 °C	7 min
	Step 6	4 °C	∞

Steps 2-4 were repeated 35 times.

4.16.1.2 Amplification of cloning constructs

For the amplification of DNA fragments used for cloning, the Phusion® High-Fidelity DNA Polymerase (Thermo Fisher Scientific) was used. 150 ng DNA, 0.4 µl dNTPs (10 mM), 1 µl of each primer (10 µM) and 0.2 µl Phusion DNA Polymerase were mixed with 4 µl of Phusion HF buffer (5x) and water was added to adjust the total volume to 20 µl.

The cycler was programmed as follows:	Step 1	98 °C	30 sec
	Step 2	98 °C	10 sec
	Step 3	50–68 °C	30 sec
	Step 4	72 °C	30 sec
	Step 5	72 °C	7 min
	Step 6	4 °C	∞

Steps 2-4 were repeated 35 times.

4.16.1.3 Quantitative real-time reverse transcription-PCR (qRT-PCR)

4.16.1.3.1 qRT-PCR of miRNAs

qRT-PCR of miRNAs was conducted using the TaqMan® Universal PCR Master Mix No AmpErase® UNG (Applied Biosystems). 1.5 µl cDNA was mixed with 7.5 µl H_2O, 10 µl TaqMan® Mastermix and 1 µl miRNA-specific TaqMan® assay. PCR was done using the 7900HT Fast Real-Time PCR System (Applied Biosystems). Raw data were analyzed using the sequence detection systems software 2.3 (Applied Biosystems). Data were analyzed using the ΔΔCt method and normalized to small nucleolar (sno) RNA that was shown to produce more reliable results than the 2S rRNA control (Supplemental Figure S5).

PCR was done using the 7900HT Fast Real-Time PCR System (Applied Biosystems) with following program:

Step 1	95 °C	10 min
Step 2	95 °C	15 sec
Step 3	60 °C	1 min

Steps 2 and 3 were repeated 40 times.

4.16.1.3.2 qRT-PCR of mRNAs

qRT-PCR of mRNAs was conducted using the TaqMan® Gene Expression Master Mix (Applied Biosystems). 2 µl diluted cDNA (1:1) was mixed with 7 µl H_2O, 10 µl TaqMan® Gene Expression Master Mix (2x) and 1 µl mRNA-specific TaqMan® Gene Expression Assay (20x). The internal Rpl32 control reaction mix consisted of 10 µl TaqMan® Master Mix (2x), 0.8 µl Primer SOL268 and SOL269 (10 µM), 0.4 µl FAM-Probe (10 µM) and 6.8 µl H2O.

PCR was done using the 7900HT Fast Real-Time PCR System (Applied Biosystems) with following program:

Step 1	95 °C	10 min
Step 2	95 °C	15 sec
Step 3	60 °C	1 min

Steps 2 and 3 were repeated 40 times.
Raw data were analyzed using the sequence detection systems software 2.3 (Applied Biosystems). Data were analyzed using the ΔΔCt method and normalized to Rpl32.

4.16.2 Agarose gel electrophoresis

DNA fragments of samples were separated by size by agarose gel electrophoresis. A molecular weight marker (HyperLadder™ II, Bioline) and samples mixed with DNA loading buffer (6x, thermo scientific) were applied on a gel consisting of 0.5 x TAE with 1 % agarose

and 0.5 µg/mL EtBr submerged in 0.5 x TAE. DNA fragments were separated by applying constant 5 V/cm with 400 mA and 400 W to the tank until adequate separation occurred.

4.16.3 Gel elution

In order to recover DNA from agarose gels, the appropriate DNA band was cut out with a clean scalpel. The DNA was eluted from the gel piece using the QIAquick® Gel Extraction Kit (Qiagen) following the manufacturers instructions.

4.16.4 cDNA synthesis by reverse transcription of miRNAs

cDNA from miRNA was produced using the NCode™ VILO™ miRNA cDNA synthesis kit (Invitrogen) with miRNA specific TaqMan® primers (Applied biosystems). 5 µl containing 300 ng RNA was mixed with 0.15 µl dNTPs (100 mM), 1 µl MultiScribe™ Reverse Transcriptase, 1.5 µl reverse transcriptase buffer (10 x), 0.19 µl RNase Inhibitor (20 U/µl), 4.16 µl H_2O and 3 µl specific primer. Reverse transcription was conducted using a Veriti 96 well thermal cycler (Applied Biosystems) with following cycle program:

16°C 30 min
42°C 30 min
85°C 5 min
4°C ∞

4.16.5 cDNA synthesis by reverse transcription of total RNAs

cDNA from total RNA was produced using the Superscript® VILO™ cDNA synthesis kit (Invitrogen). 1 µg total RNA in 14 µl H_2O was mixed with 4 µl VILO™ Reaction Mix (5x) and 2 µl SuperScript® Enzyme Mix (10x). cDNA was synthesized by incubation at 25 °C for 10 minutes and incubation at 42 °C for 60 minutes in a thermal cycler. The reaction was terminated by incubation at 85 °C for 5 minutes.

4.16.6 Restriction digest

For the cleavage of DNA at specific sites, restriction endonucleases from New England Biolabs were used. Usually, for analytical restriction 1 µg DNA was cleaved by mixing it with 0.5 µl restriction enzyme (5 U) and 2.5 µl appropriate NEB buffer (10x) in a total volume of 25 µl. The reaction was incubated for 1 h at an enzyme-dependent temperature. For cloning purpose 10 µg DNA were digested.

4.16.7 In-Fusion® cloning

In-Fusion® cloning is a fast method for cloning based on recombination between fragment and vector. The In-Fusion® HD Cloning (Clontech Laboratories) was conducted following the procedure for Spin-Column Purification of PCR fragments. For the In-Fusion® reaction cloning primers for the fragment were designed according the manufacturers protocol and used for amplification by PCR. The PCR fragment was purified and the target vector was linearized by restriction digest (see 4.16.6). 200 ng PCR fragment was mixed with 200 ng vector and 2 µl In-Fusion HD Enzyme Premix (5x) in a total reaction volume of 10 µl. The reaction was incubated for 10 minutes at 50 °C, placed on ice and used for transformation of chemically competent *E. coli.*

4.16.8 Transformation of chemically competent *E. coli*

For transformation of chemically competent cells One Shot® TOP10 cells (Invitrogen) were used. After thawing frozen cells on ice, 1 µl (50 ng DNA) was added, gently mixed and incubated on ice for 30 minutes. Transformation was induced by heat shock for 30 seconds at 42 °C. Bacteria were placed on ice for two minutes before 250 µl pre-warmed S.O.C medium was added. The cells were incubated at 37 °C for 1 h at 225 rpm in a shaking incubator and 50 µl was spread on pre-warmed selective plates containing the appropriate antibiotic. The plates were inverted and incubated overnight at 37 °C. Bacterial colonies were used for inoculation of LB media.

4.16.9 Plasmid DNA purification

Small amounts of plasmid DNA was purified from 2 ml overnightbacterial cultures, which were produced by the inoculation of antibiotics containing LB medium with single colonies at 37 °C. Bacteria were harvested by centrifugation at room temperature and 8000 rpm for 10 minutes. For purification of plasmid DNA the QIAprep® Spin Miniprep kit (Qiagen) was used according to the protocol of the manufacturer.

4.16.10 Plasmid DNA purification for generation of transgenic flies

In order to obtain high quality DNA for injections to generate transgenic fly lines, the QIAGEN Plasmid Midi Kit was used according to manufacturers protocols. Single bacterial colonies were used to inoculate a starter culture of 2 ml of LB medium with appropriate antibiotics. Bacterial cultures were grown for 8 hours at 37 °C and 300 rpm. 50 µl starter culture was used to inoculate 100 ml LB medium with appropriate antibiotics which was

incubated overnight at 37 °C and 300 rpm. The bacterial cells were harvested by centrifugation at 6000 g for 15 min at 4 °C.

4.16.11 Conventional Sanger sequencing of cloned constructs

DNA sequencing was done in house by Regina Dirksen on a 3730 DNA Analyzer sequencer (Applied Biosystems) at the Max-Planck-Institute for Biology of Aging.

4.16.12 Genomic DNA preparation from whole flies

A single fly was placed into a tube and homogenized in 50 µl squishing buffer using a pipette tip and incubated at 37 °C for 20 minutes. Proteinase K was inactivated by heating to 95 °C for 2 minutes and then the homogenate was briefly centrifuged. 1 µl of the supernatant containing the DNA was used for PCR analysis.

4.16.13 RNA extraction

Tissues or whole flies were homogenized in 700 µl QIAzol Lysis Reagent using FastPrep™ Lysing Matrix tubes and the FastPrep®-24 instrument at maximum speed for 20 seconds. RNA was extracted using the miRNeasy Mini Kit (Qiagen) following the protocol for purification of total RNA including small RNAs, from animal tissues. Purified RNA was eluted in 30 µl elution buffer.

4.16.14 Determination of RNA concentration

RNA concentration was measured using the Qubit® 2.0 Fluorometer and the Qubit™ RNA BR Assay Kits (Invitrogen). Quantification of RNA by the Qubit system is based on a comparison with a standard curve generated with kit-included standard concentrations.

4.16.15 Polyacrylamide RNA gel electrophoresis

RNA gel electrophoresis was conducted using a PROTEAN® II xi Cell (Bio-Rad) with a 15 % polyacrylamide/urea gel in 0.5 x TBE buffer. The polyacrylamide/urea gel was prepared as follows: 18 g urea was dissolved in 14.075 ml acrylamide solution (40 %, 29:1) and 3.75 ml TBE (10x) by stirring at 37 °C. 6.33 ml water was added. For polymerization 187.5 µl ammonium persulfate (APS; 10 %) and 18.75 µl TEMED was added. The solution was mixed and the gel was poured avoiding the introduction of air bubbles. Polymerization was complete after 45 minutes. The gel was pre-run at 275 Volt for 30 minutes and remaining non-polymerized acrylamide was rinsed off the wells using a small pipette tip. Samples were

mixed 1:1 with RNA loading dye (2x; 89.75 % Formaldehyde, 10 % TBE (5x), 0.05 % sodium dodecyl sulfate (SDS), 0.05 % bromophenol blue) and miRNA marker (NEB) and denatured at 95 °C for 2 minutes before loading on the gel. The gel was run at 300 Volt for 300 minutes with permanent cooling of the buffer by connecting the gel running apparatus to a GD120 water bath (Grant). For visualization the gel was incubated in an 1 % EtBr solution for 30 minutes and viewed under UV light. The invisible band containing small RNAs was cut out at the size between 19 and 26 bases.

4.16.16 RNA gel elution and precipitation

The excised polyacrylamide gel containing small RNAs was crushed with a RNA-free pistol and RNA was eluted using 528 µl elution buffer (17.96 µl H_2O, 2 µl NaOac (3M), 40 µl EDTA (0.5 M), 3 µl RNase Inhibitor) with agitation overnight at 4°C. The sample was centrifuged at 4 °C at 10000 rpm and the gel-free supernatant was mixed with 70 µl 3M Sodium Acetate pH 5.5, 2 µl GlycoBlue™ and 600 µl isopropanol and placed at -80 °C for 30 minutes for precipitation. The sample was centrifuged at 4 °C and 20000 g for 30 minutes. The supernatant was discarded and the pellet was washed with cold 80 % EtOH. EtOH was removed and the RNA pellet was air dried for 5 minutes and then resuspended in 8 µl DEPC-treated water.

4.17 Generation of targeting construct and donor flies for the knock-out of miR-986

A targeting construct for homologous recombination was generated by cloning 4 kb upstream and 4 kb downstream sequences flanking the miR-986 gene into the targeting vector pW25 (Gong and Golic, 2004). Upstream flanking sequence was cloned into BsiWI and AscI restriction sites with primers 140 and 141 using the In-Fusion® HD Cloning Kit (Clontech). Downstream flanking sequence was cloned into SphI and NotI using primer 154 and 155 and the In-Fusion® HD Cloning Kit (Clontech). The correct sequence of the vector containing the mir-986 flanking sequences was verified by sequencing. The construct was injected by BestGene *Drosophila* Embryo Injection Services (www.thebestgene.com). The insertion of resulting donor flies was mapped to the 3rd chromosome.

4.18 Generation of *miR-986^{KO}* flies

In order to generate *miR-986^{KO}* flies, donor flies with insertion on the 3rd chromosome were crossed to flies expressing FLP recombinase and I-SceI endonuclease (*y^1*, *w**; *P{70FLP}11*, *P{70I-SceI}2B*, *sna^{Sco}/CyO*, S^2). The FLP recombinase mobilizes the DNA from the targeting

construct and the I-SceI endonuclease linerarizes the extrachromosomal circular DNA to enable effective homologous recombination with the endogenous DNA at the target locus. Activation of FLP recombinase and I-SceI endonuclease was induced by heatshock of first instar larvae at 38 °C for 1h. Putative homologous recombination events were identified by the fast screening method (Gong and Golic, 2003). Therefore, mosaic-eyed or white-eyed flies were crossed to flies expressing FLP recombinase (*w^{1118}; P{70FLP}10*) and first instar larvae were heatshocked at 38 °C for 1 h. Flies were screened for red eyes as marker for targeting events. PCR was used for the identification of *miR-986^{KO}* mutants using primer 185 and 186.
To generate *miR-986^{KO*}* flies lacking the mini-*white* marker gene, which is flanked by *lox*P-sites, *miR-986^{KO}* flies were crossed to flies providing expression of Cre recombinase (*$y^{1}w^{67c23}$P{Crey}1b; sna^{Sco}/CyO*). First instar larvae were heat-shocked at 38°C for 1 h to induce expression of Cre recombinase and the removal of the mini-*white* gene. Resulting mosaic-eyed F1 males were crossed to *w; +/CyO* virgins. Removal of mini-*white* gene in white-eyed F2 flies was verified by eye color.

4.19 Microarrays

For microarray analyses 50 thoraces of 10 days old female wild type and 100 thoraces of *dilp2-3,5* flies were mechanically separated or dissected. Per sample we used 50 wild type and 100 *dilp2-3,5* abdomen or digestive tracts, respectively. 200 brains were used per genotype and sample.Total RNA was isolated, labeled with the Genisphere FlashTag® Biotin HSR kit and hybridized to Affymetrix GeneChip® miRNA Arrays 1.0 or 2.0 according to the protocols of the manufacturer by Dr. Bruno Hüttel at the Max-Planck Institute for plant breeding in cologne. Affymetrix GeneChip 1.0 contained probes for 152 and GeneChip 2.0 contained probes for 186 *Drosophila* microRNAs. Three biological replicates were used per tissue and genotype.

4.20 RNA column fractionation

In order to isolate small RNA for sequencing, total RNA was fractionated using the LabChip® XT by Dr. Bruno Hüttel at the Mack-Planck Institute for plant breeding in cologne.

4.21 rRNA depletion using magnetic beads

In order to deplete the most abundant rRNA species in the samples, streptavidin coupled Dynabeads® were used. This technique is based on magnetic separation of biotinylated DNA oligonucleotides complementary to the target rRNA sequence of the input RNA. The rRNA-

complementary oligonucleotide was used at a final concentration of 2 pM/µl and had the sequence: 5'BIO-TGCTTGGACTACATATGGTTGAGGGTTGTAA-3' A6T. Total RNA or gel-isolated small RNA was mixed with DEPC-treated water in a non-stick microfuge tube to a total volume of 21 µl. 5 µl rRNA-complementary oligonucleotide and 3 µl 20 x SSC was added. The mixture was incubated for 2 minutes at 70 °C and then put on ice. 1 µl SUPERaseIn™ was added and the mixture was incubated for 15 minutes at 37 °C with shaking at 400 rpm in an Eppendorf thermomixer. The sample was chilled on ice for 5 minutes. In the meantime, 150 µl vortexed MyOne Streptavidin C1 dynabeads were prepared by washing 3 times in 150 µl 1 x MyOne C1 dynabead B&W buffer + 0.01 % Tween, 2 times in 150 µl solution A and 2 times in 150 µl solution B. The beads were resuspended in 30 µl 2 x MyOne C1 dynabead B&W buffer + 0.01 % Tween. The sample was briefly centrifuged and added to the beads. Target rRNA bound to the antisense oligonucleotides by incubation for 15 minutes at room temperature with gentle agitation at 400 rpm. To remove the beads the tube was placed on a magnetic stand and the supernatant was transferred into a new non-stick tube. The depleted RNA was precipitated by mixing with 468 µl DEPC-treated water, 70 µl 3M Sodium Acetate pH 5.5, 2 µl GlycoBlue™ and 600 µl isopropanol and placing it at -80 °C for 30 minutes. The tube was centrifuged at 4 °C at 20000 g for 30 minutes, the supernatant was discarded and the pellet was washed with cold 80 % EtOH. EtOH was removed and the RNA pellet was air dried for 5 minutes and then resuspended in 8 µl DEPC-treated water.

4.22 Illumina small RNA library preparation

Small RNA sequencing libraries were generated using the Small RNA v1.5 Kit from Illumina following the manufacturers protocol. Small RNA was isolated from 2 µg total RNA and used as input for the library. In brief, adapters for reverse transcription and amplification were ligated on both ends of the small RNA fragments. The adapter-ligated RNA was reverse transcribed and then amplified. The cDNA was further gel-purified to exclude adapter dimer sequences in the library.

4.23 Cluster generation and sequencing

Cluster generation and 100 bp single read next generation sequencing was done using the Illumina HiSeq2500 sequencer by Dr. Bruno Hüttel at the Mack-Planck Institute for plant breeding in cologne.

4.24 Data analysis

4.24.1 Statistics

Lifespan data were subjected to survival analysis by Log-rank test (Peto and Peto, 1972) using Excel software. Unless otherwise noted, following statistic tests were used: Fecundity was tested by Wilcoxon rank test. Single qRT-PCR data was analyzed using Student's t-test. In order to analyze differences between groups, analysis of variance (ANOVA) was used and groups with significant differences were identified using Tukey-Kramer post-hoc analysis. Statistical analysis of microarray data is described in chapter 4.24.4.6 and statistical analysis of sequencing data is described in chapter 4.24.5.

4.24.2 Calculation of melting temperature (Tm)

Melting temperature of miRNAs was calculated with the formula: Tm= 0.41 x (%GC-content)+69.3-(650/sequence length).

4.24.3 Calculation of tissue specificity score

The specificity score evaluates the tissue specificity of the expression of a specific miRNA and is calculated as described in Landgraf *et al*. (Landgraf *et al*., 2007):

$\text{Specificity score}_m = \log_2(\text{number of tissue types}) + \Sigma_t\, G_{m,t} \log_2(G_{m,t})$

$G_{m,t} = F_{m,t} / \Sigma_{t'} F_{m,t'}$. $F_{m,t}$ = normalized count; t= tissue type; m = miRNA; t' = other tissue types; m' = other miRNAs. Only microRNAs with reads >10 or chip expression >15 in wt and *dilp2-3,5* flies were used for analysis of tissue-specificity.

4.24.4 Computational miRNA target prediction

MiRNA targets were predicted using the miRanda algorithm (Enright *et al*., 2003) and rated using SVR score (Betel *et al*., 2010) of the online miRNA.org source (for details see chapter 2.3.2).

4.24.5 Data analysis of microarray data

4.24.5.1 Preprocessing

Microarray data preprocessing was conducted by Affymetrix® miRNA QC tool and included image analysis, background adjustment, normalization and summarization.

4.24.5.2 Image analysis

Probe sets consisting of perfect match probes and mismatch probes were used to estimate the microRNA signal intensity. The intensity of a signal detection call was determined by the Wilcoxon Rank-Sum test of the probe set signals compared to the signals from GC content matched anti-genomic probes. Probes with p-values > 0.06 were counted as „not detected“ above background. Fischer’s exact test is used for computing the probe set p-value.

4.24.5.3 Background adjustment

GC content matched background signals were determined by the same set of anti-genomic probes used for signal detection calls. The background was subtracted from each miRNA probe signal value.

4.24.5.4 Normalization

Measurements across microarrays can vary due to differences in reagent batches, sample preparation, hybridization, in physical differences of the arrays or differences in scanning. To allow inter-array comparisons of probe intensities, the Affymetrix® miRNA QC tool uses quantile normalization (Boldstad *et al*., 2003). This normalization method forces the data to have the same distribution of log(probe intensities).

4.24.5.5 Summarization

To obtain one value from a set of probes for each miRNA, the Affymetrix® miRNA QC tool uses median polish. This summarization method ignores outlier probe-level values (Irizarry *et al*., 2003).

Data preprocessing by the Affymetrix® miRNA QC tool gives rise to a miRNA expression matrix with expression values in rows and arrays in columns. These data were used for further analyses. Probe sets of microRNAs that were not called „present“ by detection call in 2 of 3 samples in one tissue group were assessed as „not detected“.

4.24.5.6 Statistics

Statistical significance of miRNA expression fold changes in *dilp2-3,5* flies by microarray were evaluated by Student's *t*-test. P-values of multiple comparisons were adjusted by the Benjamini Hochberg procedure (Benjamini and Hochberg, 1995).

4.24.6 Analysis of sequencing data

For the analysis, adapter sequences were computationally clipped from the raw sequencing data. MiRNAs in the sequencing datasets were identified using the algorithm miRDeep (Friedländer *et al*., 2008). This algorithm aligns reads to the genome and decides whether a plausible miRNA precursor is formed. It then scores the probability for a predicted precursor to be a real miRNA precursor.

MiRDeep aligns mature *Drosophila* miRNA sequences to the sequencing reads and allows for mismatches in the last three nucleotides of the mature sequences. At the end the algorithm counts the number of reads mapping to a miRNA. In order to compare different libraries, read counts were normalized to total read number.

To identify the source of the reads that did not map to *Drosophila* miRNAs the dataset was aligned to the genome of Wolbachia pipientis (NC_002978.6), the genome of Saccharomyces cerevisiae and to *Drosophila* 18s-2s-5s-28s rRNA by BLAST.

4.24.7 Computational identification of differentially expressed miRNAs

Differential expressed miRNAs were identified using the "R"-package DESeq, which provides methods to test for differential expression (Anders and Huber, 2010).

5 Supplements

5.1 Supplemental Figures

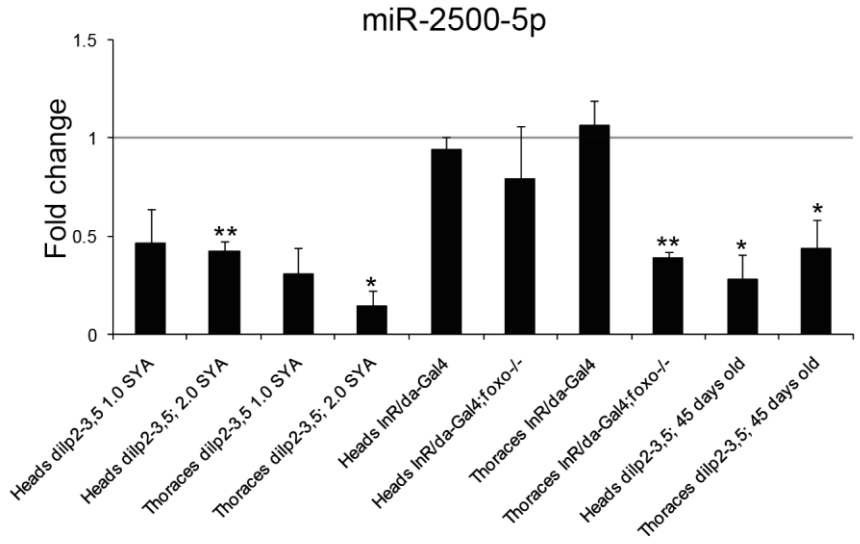

Figure S1: Differential expression of *miR-2500-5p* in tissues of different insulin mutants and at two SYA food concentrations. Significant downregulation was detected by qRT-PCR in different samples as indicated by asterisks. miRNA transcript level was normalized to wild type samples, which by default was set to 1.* p<0.05; ** p<0.01, Student'st-test.

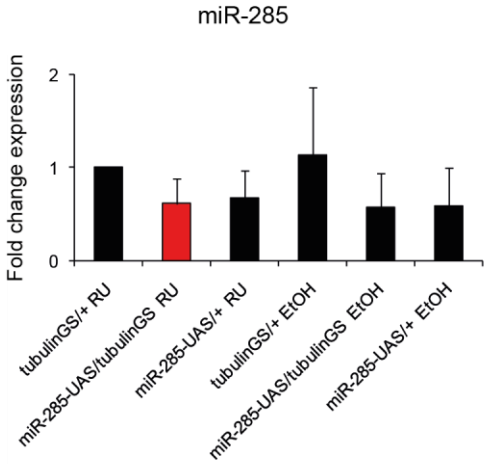

Figure S2: Overexpression of *miR-285* was not detected. qRT-PCR analysis reveals no upregulation of *miR-285*. miRNA transcript level was normalized to tubulinGS/+ with RU, which by default was set to 1.* p<0.05; ** p<0.01, Student'st-test

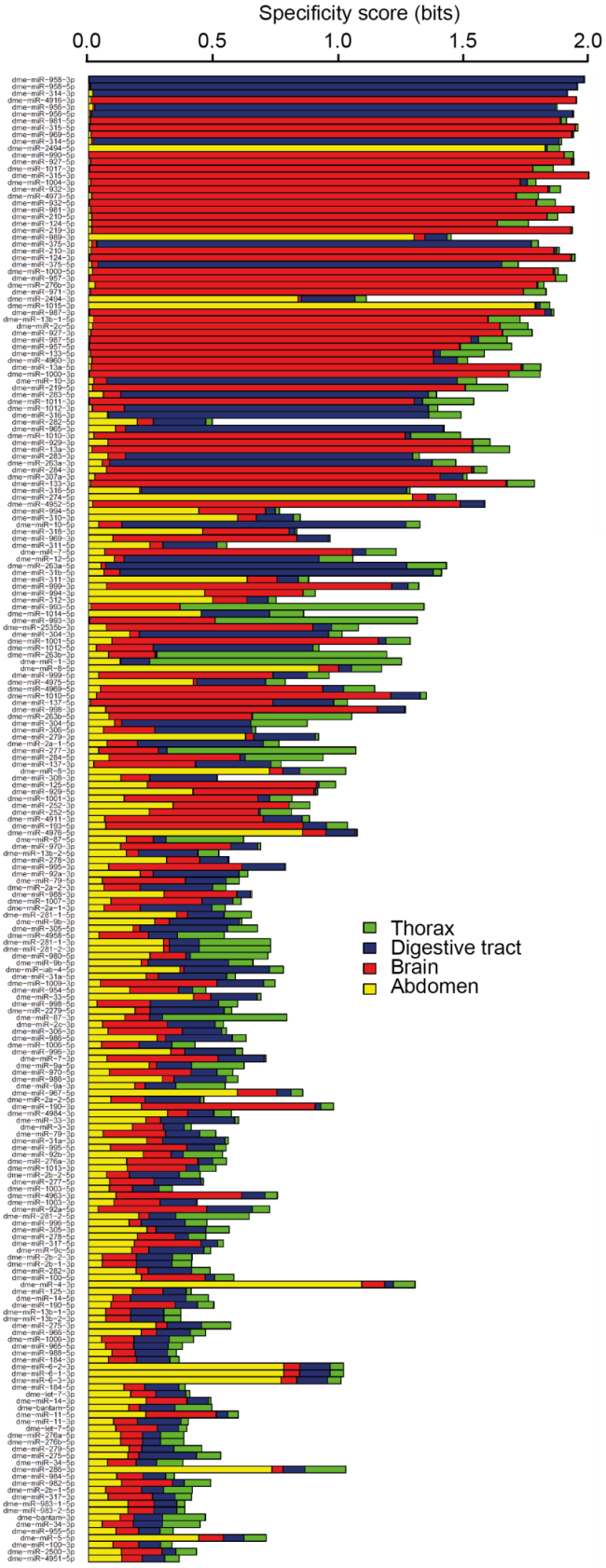

Figure S3: Tissue specificity of miRNA expression in *dilp2-3,5* flies as detected by next-generation sequencing. Tissue specificity of several miRNAs differs in *dilp2-3,5* flies. The total height of each bar represents the tissue specificity and the relative heights for each of the tissues are proportional to miRNA expression in a given tissue type relative to all tissue types. miRNAs with at least 10 reads are included in the analysis.

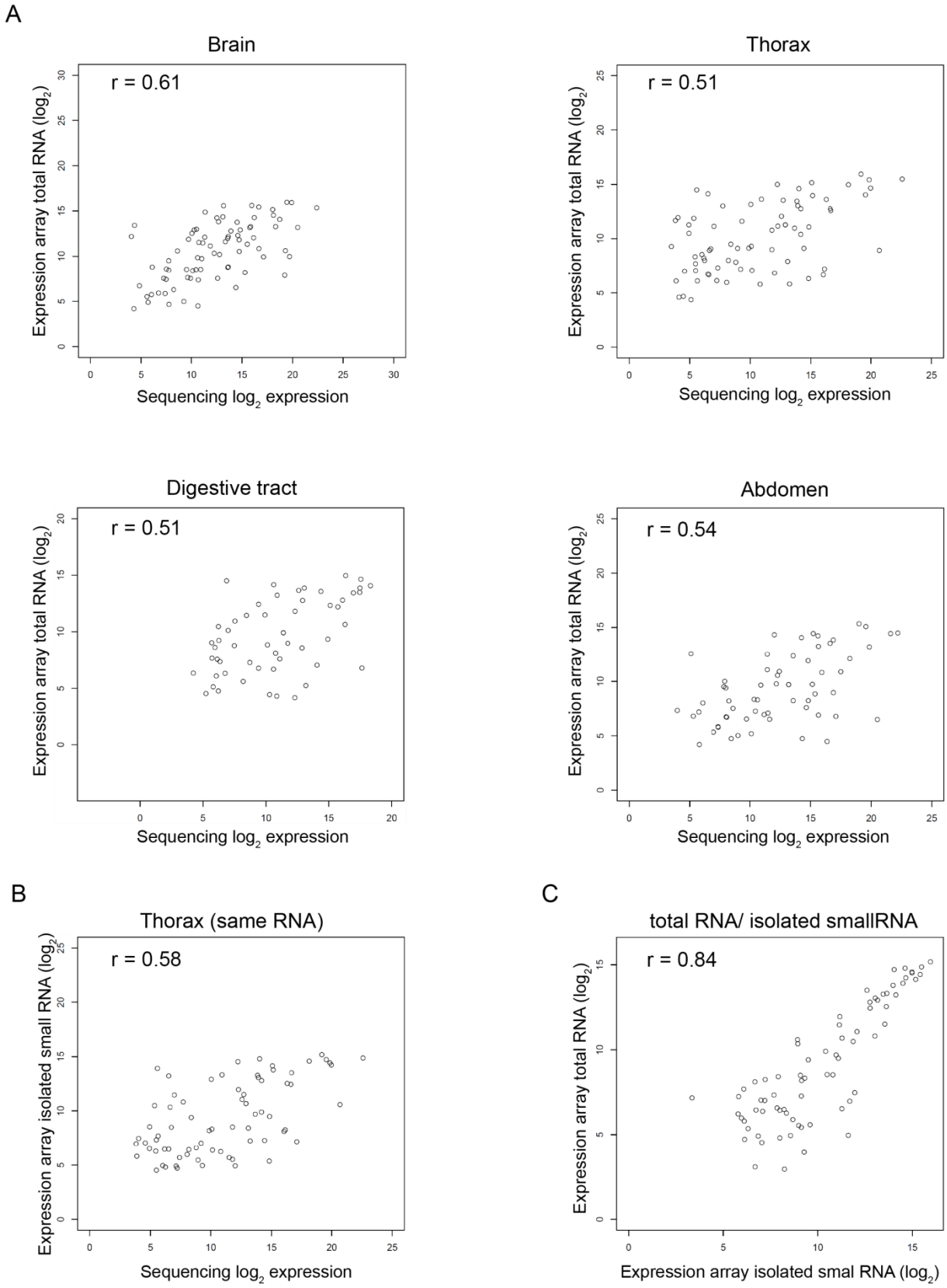

Figure S4: Comparison of *dilp2-3,5* absolute expression data as detected by microarrays and next generation sequencing. *dilp2-3,5* absolute expression data are similar to wild type data. (A) Comparison of expression data in brain, thorax, digestive tract and abdomen as detected by microarray hybridized with total RNA and sequencing of libraries generated from isolated small RNA. Pearson correlation coefficient of fold change data was computed. (B) Comparison of expression of

sequencing datasets and datasets from microarrays hybridized with the same isolated RNA as used for sequencing. Using the same RNA for both platforms does not increase correlation. (C) Comparison of datasets from microarrays hybridized with total RNA and isolated RNA show strong correlation.

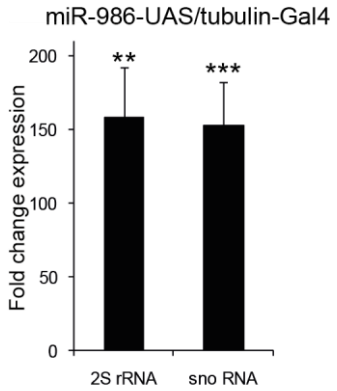

Figure S5: Comparison of performance of the internal miRNA controls 2S rRNA and sno RNA. The usage of sno RNA leads to a better significance of results due to more suitable Ct values for the raw data analysis via the ΔΔCt method. miRNA transcript level was normalized to tubulin-Gal4 samples, which by default was set to 1. ** p<0.01; *** p<0.001, Student's t-test

5.2 Supplemental Tables

microRNA	conservation level	sequencing reads (pooled tissues)
dme-mir-276a	4	1607779.82
dme-mir-1	5	1059892.77
dme-mir-8	5	898535.04
dme-bantam	5	662351.58
dme-mir-184	5	409008.16
dme-mir-10	5	401430.01
dme-mir-14	3	332219.85
dme-mir-34	5	322346.89
dme-mir-263a	5	285094.50
dme-mir-276b	4	222985.93
dme-mir-956	1	209390.08
dme-mir-277	3	175067.85
dme-let-7	5	145879.60
dme-mir-999	3	136730.78
dme-mir-7	5	106241.11
dme-mir-305	4	98811.07
dme-mir-283	5	90028.42
dme-mir-375	5	67902.49
dme-mir-9a	5	67606.33
dme-mir-11	3	63844.16
dme-mir-31a	5	42876.11
dme-mir-317	4	41535.06
dme-mir-957	3	39215.73
dme-mir-33	5	32028.52
dme-mir-281-2	5	30571.98
dme-mir-9b	5	28122.78

dme-mir-190	5	27088.38
dme-mir-275	4	26223.56
dme-mir-281-1	5	26089.99
dme-mir-958	2	25061.65
dme-mir-987	2	21260.57
dme-mir-9c	5	19220.19
dme-mir-100	5	17301.80
dme-mir-314	2	17051.61
dme-mir-986	2	16809.10
dme-mir-252	5	16420.49
dme-mir-278	5	16409.36
dme-mir-125	5	15634.15
dme-mir-284	2	12932.56
dme-mir-263b	5	12017.82
dme-mir-927	3	10399.92
dme-mir-315	5	9194.69
dme-mir-133	5	8663.25
dme-mir-13b-2	5	7615.46
dme-mir-13b-1	5	7530.33
dme-mir-12	5	7153.42
dme-mir-2b-2	5	6784.09
dme-mir-981	5	6722.11
dme-mir-1012	2	6701.53
dme-mir-279	5	5883.85
dme-mir-306	3	5359.71
dme-mir-932	3	4566.55
dme-mir-993	5	4378.74
dme-mir-988	3	4175.03
dme-mir-2b-1	5	4139.65
dme-mir-2a-2	5	4060.51
dme-mir-137	5	3861.05
dme-mir-274	2	3772.99
dme-mir-2a-1	5	3458.05
dme-mir-318	2	3231.93
dme-mir-316	3	2843.58
dme-mir-304	2	2502.21
dme-mir-970	3	2224.68
dme-mir-1010	2	2087.70
dme-mir-989	3	1999.94
dme-mir-996	3	1752.74
dme-mir-994	2	1709.17
dme-mir-965	4	1591.64
dme-mir-1000	3	1372.23
dme-mir-998	3	998.46
dme-mir-210	5	993.74
dme-mir-929	3	965.99
dme-mir-92a	5	864.41

dme-mir-6-3	2	760.97
dme-mir-6-1	2	750.12
dme-mir-6-2	2	749.79
dme-mir-31b	5	637.20
dme-mir-87	5	636.43
dme-mir-995	2	581.18
dme-mir-1015	1	571.72
dme-mir-124	5	559.56
dme-mir-1006	2	553.85
dme-mir-219	5	553.18
dme-mir-92b	5	517.46
dme-mir-2535b	1	487.41
dme-mir-2c	5	453.23
dme-mir-5	2	413.76
dme-mir-1017	1	387.60
dme-mir-1013	2	373.90
dme-mir-1001	2	367.14
dme-mir-286	3	354.41
dme-mir-307a	5	320.42
dme-mir-312	2	304.65
dme-mir-966	1	266.72
dme-mir-13a	5	256.12
dme-mir-iab-4	4	221.54
dme-mir-4951	1	214.89
dme-mir-2279	1	193.69
dme-mir-990	1	135.89
dme-mir-971	3	123.35
dme-mir-282	3	116.27
dme-mir-980	3	113.70
dme-mir-969	2	108.13
dme-mir-79	5	107.42
dme-mir-311	2	106.14
dme-mir-1003	2	98.82
dme-mir-4	2	65.00
dme-mir-1004	1	64.33
dme-mir-954	1	59.97
dme-mir-310	2	54.37
dme-mir-4984	1	51.48
dme-mir-2494	2	50.22
dme-mir-4969	1	48.00
dme-mir-4975	1	38.00
dme-mir-3	3	36.15
dme-mir-1007	1	35.79
dme-mir-308	3	35.39
dme-mir-4911	1	27.77
dme-mir-955	2	27.30
dme-mir-967	2	27.19

dme-mir-1009	1	26.22
dme-mir-1002	2	22.00
dme-mir-4976	1	20.12
dme-mir-1014	1	18.73
dme-mir-4960	1	17.90
dme-mir-984	1	16.80
dme-mir-193	5	16.33
dme-mir-983-1	2	14.69
dme-mir-983-2	2	14.69
dme-mir-1016	1	13.45
dme-mir-2500	1	13.10
dme-mir-982	2	12.00
dme-mir-4963	1	11.75
dme-mir-313	2	11.66
dme-mir-4952	1	10.78
dme-mir-285	5	9.25
dme-mir-4958	1	9.23
dme-mir-1011	2	8.99
dme-mir-4916	1	8.89
dme-mir-4973	1	6.85
dme-mir-4940	1	6.72
dme-mir-4956	1	5.85
dme-mir-964	2	5.58
dme-mir-2489	2	4.76
dme-mir-4962	1	4.48
dme-mir-3645	1	4.36
dme-mir-991	2	4.15
dme-mir-1005	2	4.02
dme-mir-960	2	3.47
dme-mir-4949	1	3.28
dme-mir-3642	1	3.12
dme-mir-4961	1	3.12
dme-mir-976	2	2.93
dme-mir-2282	1	2.90
dme-mir-962	2	2.58
dme-mir-2501	1	2.53
dme-mir-2283	1	2.44
dme-mir-4964	1	2.28
dme-mir-961	2	2.20
dme-mir-4955	1	2.18
dme-mir-4944	1	2.16
dme-mir-974	1	2.14
dme-mir-3641	1	2.10
dme-mir-973	1	1.98
dme-mir-4983	1	1.92
dme-mir-4953	1	1.84
dme-mir-4945	1	1.77

dme-mir-289	2	1.74
dme-mir-4957	1	1.64
dme-mir-959	2	1.63
dme-mir-4943	1	1.58
dme-mir-4972	1	1.57
dme-mir-2492	1	1.46
dme-mir-979	1	1.39
dme-mir-968	2	1.31
dme-mir-975	2	1.30
dme-mir-iab-8	3	1.27
dme-mir-963	2	1.20
dme-mir-4948	1	1.17
dme-mir-4985	1	1.16
dme-mir-4913	1	1.04
dme-mir-4987	1	0.98
dme-mir-4950	1	0.83
dme-mir-4982	1	0.82
dme-mir-4968	1	0.81
dme-mir-4966	1	0.79
dme-mir-4915	1	0.75
dme-mir-4977	1	0.74
dme-mir-4942	1	0.72
dme-mir-4910	1	0.71
dme-mir-309	3	0.67
dme-mir-4979	1	0.63
dme-mir-4965	1	0.55
dme-mir-4939	1	0.53
dme-mir-977	2	0.48
dme-mir-972	1	0.47
dme-mir-2498	1	0.46
dme-mir-978	2	0.43
dme-mir-4971	1	0.41
dme-mir-4978	1	0.35
dme-mir-4981	1	0.32
dme-mir-1008	1	0.31
dme-mir-4974	1	0.27
dme-mir-2496	1	0.23
dme-mir-2497	1	0.20
dme-mir-4912	1	0.20
dme-mir-4967	1	0.18
dme-mir-3644	1	0.16
dme-mir-303	2	0.15
dme-mir-307b	2	0.14
dme-mir-2499	1	0.13
dme-mir-2281	1	0.13
dme-mir-985	1	0.13
dme-mir-4980	1	0.12

dme-mir-2491	1	0.10
dme-mir-4941	1	0.10
dme-mir-4919	1	0.09
dme-mir-4917	1	0.07
dme-mir-2495	1	0.05
dme-mir-3643	1	0.05
dme-mir-4954	1	0.05
dme-mir-4947	1	0.04
dme-mir-997	1	0.03
dme-mir-2280	1	0.03
dme-mir-4970	1	0.02
dme-mir-2490	1	0.00
dme-mir-2493	1	0.00
dme-mir-280	2	0.00
dme-mir-287	2	0.00
dme-mir-288	2	0.00
dme-mir-4908	1	0.00
dme-mir-4909	1	0.00
dme-mir-4914	1	0.00
dme-mir-4918	1	0.00
dme-mir-4946	1	0.00
dme-mir-4959	1	0.00
dme-mir-4986	1	0.00
dme-mir-992	2	0.00

Supplemental table 1: Phylogenetic conservation and expression level of miRNAs as determined by sequencing reads. Conservation level code: 1, *Drosophila melanogaster* (species); 2, Drosophilidae (family); 3, Insecta (class), 4, Ecdysozoa (superphylum); 5, Bilateria.

miRNA	calculated melting temperature
dme-miR-1014-3p	48.11
dme-miR-2279-5p	49.07
dme-miR-1006-3p	49.95
dme-miR-283-5p	50.06
dme-miR-2279-3p	50.94
dme-miR-2280-5p	50.94
dme-miR-2489-3p	50.94
dme-miR-958-3p	50.94
dme-miR-983-5p	50.94
dme-miR-991-3p	50.94
dme-miR-1009-3p	51.73
dme-miR-2283-5p	51.73
dme-miR-304-5p	51.73
dme-miR-1008-3p	52.01
dme-miR-4-3p	52.01
dme-miR-977-3p	52.01
dme-miR-1003-3p	52.80
dme-miR-1007-3p	52.80
dme-miR-2280-3p	52.80
dme-miR-2282-3p	52.80
dme-miR-2497-3p	52.80

dme-miR-375-3p	52.80
dme-miR-79-3p	52.80
dme-miR-972-3p	52.80
dme-miR-976-3p	52.80
dme-miR-iab-8-3p	52.80
dme-miR-1013-3p	53.20
dme-bantam-3p	53.52
dme-miR-2501-3p	53.52
dme-miR-288-3p	53.52
dme-miR-982-5p	53.52
dme-let-7-5p	53.97
dme-miR-1005-3p	53.97
dme-miR-14-3p	53.97
dme-miR-2281-3p	53.97
dme-miR-287-3p	53.97
dme-miR-87-3p	53.97
dme-miR-969-5p	53.97
dme-miR-190-5p	54.18
dme-miR-2498-5p	54.18
dme-miR-987-5p	54.18
dme-miR-137-3p	54.66
dme-miR-13a-3p	54.66
dme-miR-1-3p	54.66
dme-miR-279-3p	54.66
dme-miR-308-3p	54.66
dme-miR-315-5p	54.66
dme-miR-6-3p	54.66
dme-miR-927-5p	54.66
dme-miR-961-5p	54.66
dme-miR-964-5p	54.66
dme-miR-971-3p	54.66
dme-miR-974-5p	54.66
dme-miR-999-3p	54.66
dme-miR-9c-5p	54.66
dme-miR-iab-4-5p	54.66
dme-miR-1012-3p	55.30
dme-miR-2492-3p	55.30
dme-miR-7-5p	55.30
dme-miR-8-3p	55.30
dme-miR-975-5p	55.30
dme-miR-984-5p	55.30
dme-miR-9a-5p	55.30
dme-miR-9b-5p	55.30
dme-miR-280-5p	55.86
dme-miR-963-5p	55.88
dme-miR-968-5p	55.88
dme-miR-1000-5p	55.92
dme-miR-1016-3p	55.92
dme-miR-314-3p	55.92
dme-miR-2497-5p	56.42
dme-miR-10-5p	56.53
dme-miR-13b-3p	56.53
dme-miR-276b-3p	56.53
dme-miR-306-5p	56.53
dme-miR-318-3p	56.53
dme-miR-959-3p	56.53

dme-miR-960-5p	56.53
dme-miR-965-3p	56.53
dme-miR-992-3p	56.53
dme-miR-994-5p	56.53
dme-miR-996-3p	56.53
dme-miR-10-3p	57.08
dme-miR-12-5p	57.08
dme-miR-219-5p	57.08
dme-miR-277-3p	57.08
dme-miR-281-3p	57.08
dme-miR-303-5p	57.08
dme-miR-5-5p	57.08
dme-miR-956-3p	57.08
dme-miR-iab-8-5p	57.08
dme-miR-307-3p	57.30
dme-miR-1001-5p	57.87
dme-miR-11-3p	57.87
dme-miR-2494-5p	57.87
dme-miR-33-5p	57.87
dme-miR-970-3p	57.87
dme-miR-979-3p	57.87
dme-miR-989-3p	57.87
dme-miR-995-3p	57.87
dme-miR-997-5p	57.87
dme-miR-998-3p	57.87
dme-miR-2500-5p	58.06
dme-miR-962-5p	58.06
dme-miR-100-5p	58.39
dme-miR-276a-3p	58.39
dme-miR-285-3p	58.39
dme-miR-309-3p	58.39
dme-miR-313-3p	58.39
dme-miR-932-5p	58.39
dme-miR-986-5p	58.39
dme-miR-1011-3p	58.87
dme-miR-2281-5p	58.87
dme-miR-2490-5p	58.87
dme-miR-2498-3p	58.87
dme-miR-305-5p	58.87
dme-miR-1002-5p	59.30
dme-miR-1010-3p	59.30
dme-miR-2494-3p	59.30
dme-miR-263a-3p	59.30
dme-miR-iab-4-3p	59.30
dme-miR-973-5p	59.70
dme-miR-263b-3p	59.82
dme-miR-929-3p	59.82
dme-miR-954-5p	59.82
dme-miR-967-5p	59.82
dme-miR-990-5p	59.82
dme-miR-289-5p	60.07
dme-miR-1004-3p	60.25
dme-miR-125-5p	60.25
dme-miR-193-3p	60.25
dme-miR-2495-5p	60.25
dme-miR-2500-3p	60.25

dme-miR-281-2-5p	60.25
dme-miR-307-as-5p	60.25
dme-miR-310-3p	60.25
dme-miR-311-3p	60.25
dme-miR-312-3p	60.25
dme-miR-316-5p	60.25
dme-miR-31b-5p	60.25
dme-miR-3-3p	60.25
dme-miR-957-3p	60.25
dme-miR-978-3p	60.25
dme-miR-980-3p	60.25
dme-miR-981-3p	60.25
dme-miR-985-3p	60.25
dme-miR-1017-3p	60.65
dme-miR-2a-3p	60.65
dme-miR-993-3p	60.65
dme-miR-274-5p	61.65
dme-miR-184-5p	61.78
dme-miR-210-3p	61.78
dme-miR-2493-5p	61.78
dme-miR-1015-3p	62.12
dme-miR-133-3p	62.12
dme-miR-184-3p	62.12
dme-miR-2491-5p	62.12
dme-miR-252-5p	62.12
dme-miR-278-3p	62.12
dme-miR-281-1-5p	62.12
dme-miR-307-as-3p	62.12
dme-miR-92a-3p	62.12
dme-miR-276-5p	62.43
dme-miR-286-3p	62.43
dme-miR-2b-3p	62.43
dme-miR-2c-3p	62.43
dme-miR-31a-5p	62.43
dme-miR-955-5p	62.43
dme-miR-2499-5p	62.72
dme-miR-2501-5p	62.72
dme-miR-317-3p	62.72
dme-miR-282-5p	63.66
dme-miR-966-5p	63.73
dme-miR-284-3p	63.85
dme-miR-92b-3p	63.98
dme-miR-988-3p	63.98
dme-miR-995-5p	63.98
dme-miR-124-3p	64.21
dme-miR-2493-3p	64.21
dme-miR-34-5p	64.43
dme-miR-2496-3p	65.85
dme-miR-275-3p	66.00
dme-miR-2495-3p	66.13
dme-miR-2496-5p	66.13
dme-miR-306-3p	67.71
dme-miR-2499-3p	67.84

Supplemental table 2: Calculated melting temperatures for miRNAs. For calculation see chapter 4.24.1

Internal primer name	Sequence	Description
JW109	ACTGGTGAGGAGGCCAT	Sequencing miR-986 construct upstream sequence
JW110	CCATATTGAAATGGAACCCCAG	Sequencing miR-986 construct upstream sequence
JW111	CGCAATGCCGCACAG	Sequencing miR-986 construct upstream sequence
JW112	TTATACTTACCAGACGATCATGAC	Sequencing miR-986 construct upstream sequence
JW113	GTCATGATGCAGAGACAATGTAA	Sequencing miR-986 construct upstream sequence
JW114	TTGCTGCCATAAAACAATATATACTGG	Sequencing miR-986 construct upstream sequence
JW115	AGCGACTTTACGACCGG	Sequencing miR-986 construct downstream sequence
JW116	GATCACCCCAGCATTCCAC	Sequencing miR-986 construct downstream sequence
JW117	GATACTACCACTTCTGGAGTGTC	Sequencing miR-986 construct downstream sequence
JW118	TCTGGATGAGCTCGTCTCTAA	Sequencing miR-986 construct downstream sequence
JW119	CTCAAATCCGATTTACTCGCTG	Sequencing miR-986 construct downstream sequence
JW120	TGTGACATGTTAATAACGCTAAGG	Sequencing miR-986 construct downstream sequence
JW121	ACTTTGCTCCTGAATATCCAGAA	Sequencing miR-986 construct downstream sequence
JW140	TCCCTAGGGGATCACGTACGGATGCAGCAGGCCTCGAC	miR-986 Infusion cloning forward primer of upstream 4 kb
JW141	CTAGTCTAGGGCGCGCCTCCTCTGCGTGGCTAACG	miR-986 Infusion cloning reverse primer of upstream 4 kb
JW154	TAGTCTAGGGTACCGCATGCAGCGACTTTACGACCGGA	miR-986 Infusion cloning forward primer of downstream 4 kb
JW155	AGGGTAATGTACCGCGGCCGCACGTTGCGCCTCCTTTATAAAC	miR-986 Infusion cloning reverse primer of downstream 4 kb
JW185	GCAAGTCATGCTGAAAGCAC	miR-986^{KO} genotyping primer
JW186	CAGTCACAACGCTATTCGAG	miR-986^{KO} genotyping primer
rRNA depletion oligo	5'BIOTIN-TGCTTGGACTACATATGGTTGAGGGTTGTAA-3' A6T	Primer for rRNA oligo depletion

Supplemental table 3: List of oligonucleotides.

Index of figures

References

Aboobaker AA, Tomancak P, Patel N, Rubin GM, Lai EC.(2005). Drosophila microRNAs exhibit diverse spatial expression patterns during embryonic development. *Proc Natl Acad Sci USA* **102(50)**, 18017-22.

Allen E, Xie Z, Gustafson AM, Sung GH, Spatafora JW, Carrington JC. (2004). Evolution of microRNA genes by inverted duplication of target gene sequences in Arabidopsis thaliana. *Nat Genet***36(12)**, 1282-90.

Anders S, Huber W. (2010). Differential expression analysis for sequence count data. *Genome Biol***11(10)**, 106.

Axtell MJ, Bartel DP.(2005). Antiquity of microRNAs and their targets in land plants. *Plant* Cell**17(6)**, 1658-73.

Bartel DP. (2004). MicroRNAs: genomics, biogenesis, mechanism, and function. *Cell***116(2)**, 281-97.

Baskerville S, Bartel DP. (2005). Microarray profiling of microRNAs reveals frequent coexpression with neighboring miRNAs and host genes. *RNA***11(3)**, 241-7.

Bauer JH, Poon PC, Glatt-Deeley H, Abrams JM, Helfand SL.(2005). Neuronal expression of p53 dominant-negative proteins in adult Drosophila melanogaster extends life span. *Curr Biol***15(22),** 2063-8.

Bejarano F, Bortolamiol-Becet D, Dai Q, Sun K, Saj A, Chou YT, Raleigh DR, Kim K, Ni JQ, Duan H, Yang JS, Fulga TA, Van Vactor D, Perrimon N, Lai EC.(2012). A genome-wide transgenic resource for conditional expression of Drosophila microRNAs. *Development***139(15)**, 2821-31.

Benjamini, Yoav; Hochberg, Yosef. (1995). Controlling the false discovery rate: a practical and powerful approach to multiple testing. *Journal of the Royal Statistical Society*, Series B**57(1)**, 289–300.

Berezikov E, Chung WJ, Willis J, Cuppen E, Lai EC.(2007). Mammalian mirtron genes. *Mol Cell**28***(2),328-36.

Berezikov E, Robine N, Samsonova A, Westholm JO, Naqvi A, Hung JH, Okamura K, Dai Q, Bortolamiol-Becet D, Martin R, Zhao Y, Zamore PD, Hannon GJ, Marra MA, Weng Z, Perrimon N, Lai EC.(2011). Deep annotation of Drosophila melanogaster microRNAs yields insights into their processing, modification, and emergence. *Genome Res***21(2)**, 203-15.

Bernstein E, Caudy AA, Hammond SM, Hannon GJ.(2001). Role for a bidentate ribonuclease in the initiation step of RNA interference. *Nature* **409(6818)**,363-6.

Betel D, Koppal A, Agius P, Sander C, Leslie C. (2010). Comprehensive modeling of microRNA targets predicts functional non-conserved and non-canonical sites. *Genome Biol***11(8)**, R90.

Betel D, Wilson M, Gabow A, Marks DS, Sander C.(2008). The microRNA.org resource: targets and expression. *Nucleic Acids Res***36**(Database issue), D149-53.

Boehm M, Slack F.(2005). A developmental timing microRNA and its target regulate life span in C. elegans. *Science***310(5756)**, 1954-7.

Borchert GM, Lanier W, Davidson BL.(2006). RNA polymerase III transcribes human microRNAs. *Nat Struct Mol Biol***13(12)**, 1097-101.

Brand AH, Perrimon N.(1993). Targeted gene expression as a means of altering cell fates and generating dominant phenotypes. *Development***118(2)**, 401-15.

Brennecke J, Hipfner DR, Stark A, Russell RB, Cohen SM.(2003). Bantam encodes a developmentally regulated microRNA that controls cell proliferation and regulates the proapoptotic gene hid in Drosophila. *Cell***113(1)**, 25-36.

Brett JO, Renault VM, Rafalski VA, Webb AE, Brunet A.(2011). The microRNA cluster miR-106b~25 regulates adult neural stem/progenitor cell proliferation and neuronal differentiation. *Aging***3(2)**, 108-24.

Britton JS, Lockwood WK, Li L, Cohen SM, Edgar BA.(2002). Drosophila's insulin/PI3-kinase pathway coordinates cellular metabolism with nutritional conditions. *Dev Cell***2(2)**, 239-49.

Broughton S, Partridge L.(2009). Insulin/IGF-like signalling, the central nervous system and aging. *Biochem J***418(1)**, 1-12.

Broughton SJ, Piper MD, Ikeya T, Bass TM, Jacobson J, Driege Y, Martinez P, Hafen E, Withers DJ, Leevers SJ, Partridge L.(2005). Longer lifespan, altered metabolism, and stress resistance in Drosophila from ablation of cells making insulin-like ligands. *Proc Natl Acad Sci USA***102(8)**, 3105-10.

Caygill EE, Johnston LA.(2008). Temporal regulation of metamorphic processes in Drosophila by the let-7 and miR-125 heterochronic microRNAs. *Curr Biol***18(13)**, 943-50.

Chen K, Rajewsky N.(2006). Deep conservation of microRNA-target relationships and 3'UTR motifs in vertebrates, flies, and nematodes. *Cold Spring Harb Symp Quant Biol***71**, 149-56.

Chen K, Rajewsky N.(2007). The evolution of gene regulation by transcription factors and microRNAs. *Nat Rev Genet***8(2)**, 93-103.

Chen Y, Gelfond JA, McManus LM, Shireman PK.(2009). Reproducibility of quantitative RT-PCR array in miRNA expression profiling and comparison with microarray analysis. *BMC Genomics***10**, 407.

Chin L, Artandi SE, Shen Q, Tam A, Lee SL, Gottlieb GJ, Greider CW, DePinho RA. (1999). p53 deficiency rescues the adverse effects of telomere loss and cooperates with telomere dysfunction to accelerate carcinogenesis. *Cell* 1999 **97(4)**, 527-38.

Chung H, Sztal T, Pasricha S, Sridhar M, Batterham P, Daborn PJ.(2009). Characterization of Drosophila melanogaster cytochrome P450 genes.*Proc Natl Acad Sci USA***106(14)**, 5731-6.

Clancy DJ, Gems D, Harshman LG, Oldham S, Stocker H, Hafen E, Leevers SJ, Partridge L.(2001). Extension of life-span by loss of CHICO, a Drosophila insulin receptor substrate protein. *Science***292(5514)**,104-6.

Clare MJ, Luckinbill LS.(1985). The effects of gene-environment interaction on the expression of longevity. *Heredity***55**, 19-26.

Clark ME, Anderson CL, Cande J, Karr TL.(2005). Widespread prevalence of wolbachia in laboratory stocks and the implications for Drosophila research. *Genetics***170(4)**, 1667-75.

Cock JM, Sterck L, Rouzé P, Scornet D, Allen AE, Amoutzias G, Anthouard V, Artiguenave F, Aury JM, Badger JH, Beszteri B, Billiau K, Bonnet E, Bothwell JH, Bowler C, Boyen C, Brownlee C, Carrano CJ, Charrier B, Cho GY, Coelho SM, Collén J, Corre E, Da Silva C, Delage L, Delaroque N, Dittami SM, Doulbeau S, Elias M, Farnham G, Gachon CM, Gschloessl B, Heesch S, Jabbari K, Jubin C, Kawai H, Kimura K, Kloareg B, Küpper FC, Lang D, Le Bail A, Leblanc C, Lerouge P, Lohr M, Lopez PJ, Martens C, Maumus F, Michel G, Miranda-Saavedra D, Morales J, Moreau H, Motomura T, Nagasato C, Napoli CA, Nelson DR, Nyvall-Collén P, Peters AF, Pommier C, Potin P, Poulain J, Quesneville H, Read B, Rensing SA, Ritter A, Rousvoal S, Samanta M, Samson G, Schroeder DC, Ségurens B, Strittmatter M, Tonon T, Tregear JW, Valentin K, von Dassow P, Yamagishi T, Van de Peer Y, Wincker P.(2010). The Ectocarpus genome and the independent evolution of multicellularity in brown algae. *Nature***465(7298)**, 617-21.

Corcoran DL, Pandit KV, Gordon B, Bhattacharjee A, Kaminski N, Benos PV.(2009). Features of mammalian microRNA promoters emerge from polymerase II chromatin immunoprecipitation data. *PLoS One***4(4)**, e5279.

Dávalos A, Goedeke L, Smibert P, Ramírez CM, Warrier NP, Andreo U, Cirera-Salinas D, Rayner K, Suresh U, Pastor-Pareja JC, Esplugues E, Fisher EA, Penalva LO, Moore KJ, Suárez Y, Lai EC, Fernández-Hernando C.(2011). miR-33a/b contribute to the regulation of fatty acid metabolism and insulin signaling. *Proc Natl Acad Sci USA***108(22)**, 9232-7.

de Lencastre A, Pincus Z, Zhou K, Kato M, Lee SS, Slack FJ.(2010). MicroRNAs both promote and antagonize longevity in C. elegans. *Curr Biol***20(24)**, 2159-68.

Dekanty A, Lavista-Llanos S, Irisarri M, Oldham S, Wappner P.(2005). The insulin-PI3K/TOR pathway induces a HIF-dependent transcriptional response in Drosophila by promoting nuclear localization of HIF-alpha/Sima. *J Cell Sci***118**, 5431-41.

Demontis F, Perrimon N.(2010). FOXO/4E-BP signaling in Drosophila muscles regulates organism-wide proteostasis during aging. *Cell***143(5)**, 813-25.

Denli AM, Tops BB, Plasterk RH, Ketting RF, Hannon GJ.(2004). Processing of primary microRNAs by the Microprocessor complex. *Nature***432(7014)**, 231-5.

Derry WB, Putzke AP, Rothman JH. (2001). Caenorhabditis elegans p53: role in apoptosis, meiosis, and stress resistance. *Science***294(5542)**, 591-5.

Elia, L., Contu, R., Quintavalle, M., Varrone, F., Chimenti, C., Russo MA, Cimino V, De Marinis L, Frustaci A, Catalucci D, Condorelli G. (2009). Reciprocal regulation of miRNA-1 and insulin-like growth factor-1 signal transduction cascade in cardiac and skeletal muscle in physiological and pathological conditions. *Circulation***120**, 2377–2385.

Enright AJ, John B, Gaul U, Tuschl T, Sander C, Marks DS.(2003). MicroRNA targets in Drosophila. *Genome Biol***5(1)**, R1.

Erkosar B, Storelli G, Defaye A, Leulier F.(2013). Host-intestinal microbiota mutualism: "learning on the fly". *Cell Host Microbe***13(1)**, 8-14.

Esslinger SM, Schwalb B, Helfer S, Michalik KM, Witte H, Maier KC, Martin D, Michalke B, Tresch A, Cramer P, Förstemann K.(2013). Drosophila miR-277 controls branched-chain amino acid catabolism and affects lifespan. *RNA Biol***10(6)**, 1042-56.

Fernandez-Ayala DJ, Sanz A, Vartiainen S, Kemppainen KK, Babusiak M, Mustalahti E, Costa R, Tuomela T, Zeviani M, Chung J, O'Dell KM, Rustin P, Jacobs HT.(2009). Expression of the Ciona intestinalis alternative oxidase (AOX) in Drosophila complemeants defects in mitochondrial oxidative phosphorylation. *Cell Metab***9(5)**, 449-60.

Flachsbart F, Caliebe A, Kleindorp R, Blanché H, von Eller-Eberstein H, Nikolaus S, Schreiber S, Nebel A. (2009). Association of FOXO3A variation with human longevity confirmed in German centenarians. *Proc Natl Acad Sci USA***106(8)**, 2700-5.

Friedländer MR, Chen W, Adamidi C, Maaskola J, Einspanier R, Knespel S, Rajewsky N.(2008). Discovering microRNAs from deep sequencing data using miRDeep. *Nat Biotechnol***26(4)**, 407-15.

Gáliková M, Klepsatel P, Senti G, Flatt T.(2011). Steroid hormone regulation of C. elegans and Drosophila aging and life history. *Exp Gerontol***46(2-3)**, 141-7.

Ge Y, Sun Y, Chen J. (2011). IGF-II is regulated by microRNA-125b in skeletal myogenesis. *J Cell Biol***192(1)**, 69-81.

Giannakou ME, Goss M, Jünger MA, Hafen E, Leevers SJ, Partridge L.(2004). Long-lived Drosophila with overexpressed dFOXO in adult fat body. *Science*. **305(5682)**, 361.

Gong WJ, Golic KG.(2003). Ends-out, or replacement, gene targeting in Drosophila. *Proc Natl Acad Sci USA***100(5)**, 2556-61.

Gregory RI, Chendrimada TP, Cooch N, Shiekhattar R.(2005). Human RISC couples microRNA biogenesis and posttranscriptional gene silencing. *Cell*. **123(4)**, 631-40.

Griffiths-Jones S.(2006). miRBase: the microRNA sequence database. *Methods Mol Biol***342**, 129-38.

Grimson A, Srivastava M, Fahey B, Woodcroft BJ, Chiang HR, King N, Degnan BM, Rokhsar DS, Bartel DP.(2008). Early origins and evolution of microRNAs and Piwi-interacting RNAs in animals. *Nature***455(7217)**, 1193-7.

Grönke S, Clarke DF, Broughton S, Andrews TD, Partridge L.(2010). Molecular evolution and functional characterization of Drosophila insulin-like peptides. *PLoS Genet***6(2)**, e1000857.

Grün D, Wang YL, Langenberger D, Gunsalus KC, Rajewsky N.(2005). microRNA target predictions across seven Drosophila species and comparison to mammalian targets. *PLoS Comput Biol***1(1)**, e13.

Hale CR, Zhao P, Olson S, Duff MO, Graveley BR, Wells L, Terns RM, Terns MP.(2009). RNA-guided RNA cleavage by a CRISPR RNA-Cas protein complex. *Cell***139(5)**, 945-56.

Hammond SM, Bernstein E, Beach D, Hannon GJ.(2000). An RNA-directed nuclease mediates post-transcriptional gene silencing in Drosophila cells. *Nature***404(6775)**, 293-6.

Han JF, Wang SL, He XY, Liu CY, Hong JY.(2006). Effect of genetic variation on human cytochrome p450 reductase-mediated paraquat cytotoxicity. *Toxicol Sci***91(1)**, 42-8.

Han L, Witmer PD, Casey E, Valle D, Sukumar S. (2007). DNA methylation regulates MicroRNA expression.*Cancer Biol Ther.* **6(8)**:1284-8.

Hansen M, Taubert S, Crawford D, Libina N, Lee SJ, Kenyon C.(2007). Lifespan extension by conditions that inhibit translation in Caenorhabditis elegans. *Aging Cell***6**, 95-110.

Heimberg AM, Sempere LF, Moy VN, Donoghue PC, Peterson KJ. (2008). MicroRNAs and the advent of vertebrate morphological complexity. *Proc Natl Acad Sci USA***105(8)**, 2946-50.

Holzenberger M, Dupont J, Ducos B, Leneuve P,Geloen A, Even PC, Cervera P, Le Bouc Y.(2003). IGF-1 receptor regulates life span and resistance to oxidative stress in mice. *Nature***421**, 182–187.

Hussain M, Frentiu FD, Moreira LA, O'Neill SL, Asgari S.(2011). Wolbachia uses host microRNAs to manipulate host gene expression and facilitate colonization of the dengue vector Aedes aegypti. *Proc Natl Acad Sci USA***108(22)**, 9250-5.

Hutvágner G, Zamore PD.(2002). A microRNA in a multiple-turnover RNAi enzyme complex. *Science***297(5589)**, 2056-60.

Hwangbo DS, Gershman B, Tu MP, Palmer M, Tatar M.(2004). Drosophila dFOXO controls lifespan and regulates insulin signalling in brain and fat body. *Nature***429(6991)**, 562-6.

Kaeberlein M, Powers RW 3rd, Steffen KK, Westman EA, Hu D, Dang N, Kerr EO, Kirkland KT, Fields S, Kennedy BK.(2005). Regulation of yeast replicative life span by TOR and Sch9 in response to nutrients. *Science***310**, 1193-1196.

Kapsimali M, Kloosterman WP, de Bruijn E, Rosa F, Plasterk RH, Wilson SW.(2007). MicroRNAs show a wide diversity of expression profiles in the developing and mature central nervous system. *Genome Biol***8(8)**, R173.

Karolina DS, Armugam A, Tavintharan S, Wong MT, Lim SC, Sum CF, Jeyaseelan K.(2011). MicroRNA 144 impairs insulin signaling by inhibiting the expression of insulin receptor substrate 1 in type 2 diabetes mellitus. *PLoS One***6(8)**, e22839.

Katayama S, Tomaru Y, Kasukawa T, Waki K, Nakanishi M, Nakamura M, Nishida H, Yap CC, Suzuki M, Kawai J, Suzuki H, Carninci P, Hayashizaki Y, Wells C, Frith M, Ravasi T, Pang KC, Hallinan J, Mattick J, Hume DA, Lipovich L, Batalov S, Engström PG, Mizuno Y, Faghihi MA, Sandelin A, Chalk AM, Mottagui-Tabar S, Liang Z, Lenhard B, Wahlestedt C; RIKEN Genome Exploration Research Group; Genome Science Group (Genome Network Project Core Group); FANTOM Consortium.(2005). Antisense transcription in the mammalian transcriptome. *Science*. **309(5740)**, 1564-6.

Kawahara Y, Megraw M, Kreider E, Iizasa H, Valente L, Hatzigeorgiou AG, Nishikura K.(2008). Frequency and fate of microRNA editing in human brain. *Nucleic Acids Res***36(16)**, 5270-80.

Kawahara Y, Zinshteyn B, Chendrimada TP, Shiekhattar R, Nishikura K.(2007). RNA editing of the microRNA-151 precursor blocks cleavage by the Dicer-TRBP complex. *EMBO Rep***8(8)**, 763-9.

Kenyon C, Chang J, Gensch E, Rudner A, Tabtiang R. (1993). A C. elegans mutant that lives twice as long as wild type. *Nature***366(6454)**, 461-4.

Kwon C, Han Z, Olson EN, Srivastava D.(2005). MicroRNA1 influences cardiac differentiation in Drosophila and regulates Notch signaling. *Proc Natl Acad Sci USA***102(52)**, 18986-91.

La Rocca G, Shi B, Badin M, De Angelis T, Sepp-Lorenzino L, Baserga R. (2009). Growth inhibition by miRNAs that target the insulin receptor substrate-1. *Cell Cycle***8**, 2255–2259.

Landgraf P, Rusu M, Sheridan R, Sewer A, Iovino N, Aravin A, Pfeffer S, Rice A, Kamphorst AO, Landthaler M, Lin C, Socci ND, Hermida L, Fulci V, Chiaretti S, Foà R, Schliwka J, Fuchs U, Novosel A, Müller RU, Schermer B, Bissels U, Inman J, Phan Q, Chien M, Weir DB, Choksi R, De Vita G, Frezzetti D, Trompeter HI, Hornung V, Teng G, Hartmann G, Palkovits M, Di Lauro R, Wernet P, Macino G, Rogler CE, Nagle JW, Ju J, Papavasiliou FN, Benzing T, Lichter P, Tam W, Brownstein MJ, Bosio A, Borkhardt A, Russo JJ, Sander C, Zavolan M, Tuschl T.(2007). A mammalian microRNA expression atlas based on small RNA library sequencing. *Cel***129(7)**, 1401-14.

Lau NC, Lim LP, Weinstein EG, Bartel DP.(2001). An abundant class of tiny RNAs with probable regulatory roles in Caenorhabditis elegans. *Science***294(5543)**, 858-62.

Lavigueur A, Maltby V, Mock D, Rossant J, Pawson T, Bernstein A.(1989). High incidence of lung, bone, and lymphoid tumors in transgenic mice overexpressing mutant alleles of the p53 oncogene. *Mol Cell Biol***9(9)**, 3982-91.

Leaman D, Chen PY, Fak J, Yalcin A, Pearce M, Unnerstall U, Marks DS, Sander C, Tuschl T, Gaul U.(2005). Antisense-mediated depletion reveals essential and specific functions of microRNAs in Drosophila development. *Cell***121(7)**, 1097-108.

Lee JH, Lee E, Park J, Kim E, Kim J, Chung J. (2003). In vivo p53 function is indispensable for DNA damage-induced apoptotic signaling in Drosophila. *FEBS Lett.* **550(1-3)**, 5-10.

Lee Y, Ahn C, Han J, Choi H, Kim J, Yim J, Lee J, Provost P, Rådmark O, Kim S, Kim VN.(2003). The nuclear RNase III Drosha initiates microRNA processing. *Nature*. **425(6956)**, 415-9.

Lee Y, Kim M, Han J, Yeom KH, Lee S, Baek SH, Kim VN.(2004). MicroRNA genes are transcribed by RNA polymerase II. *EMBO J***23(20)**, 4051-60.

Li X, Khanna A, Li N, Wang E.(2011). Circulatory miR34a as an RNAbased, noninvasive biomarker for brain aging. *Aging***3(10)**, 985-1002.

Li Y, Wang F, Lee JA, Gao FB.(2006). MicroRNA-9a ensures the precise specification of sensory organ precursors in Drosophila. *Genes Dev***20(20)**, 2793-805.

Liang H, Masoro EJ, Nelson JF, Strong R, McMahan CA, Richardson A.(2003). Genetic mouse models of extended lifespan. *Exp Gerontol***38(11-12)**, 1353-64.

Lim LP, Lau NC, Garrett-Engele P, Grimson A, Schelter JM, Castle J, Bartel DP, Linsley PS, Johnson JM.(2005). Microarray analysis shows that some microRNAs downregulate large numbers of target mRNAs. *Nature***433(7027)**, 769-73.

Lin K, Hsin H, Libina N, Kenyon C.(2001). Regulation of the Caenorhabditis elegans longevity protein DAF-16 by insulin/IGF-1 and germline signaling. *Nat Gene***28(2)**, 139-45.

Liu N, Landreh M, Cao K, Abe M, Hendriks GJ, Kennerdell JR, Zhu Y, Wang LS, Bonini NM.(2012). The microRNA miR-34 modulates ageing and neurodegeneration in Drosophila. *Nature***482(7386)**, 519-23.

Liu ZH, Yang G, Zhao T, Cao GJ, Xiong L, Xia W, Huang X, Wu LY, Wu K, Fan M, Shao NS, Zhu LL.(2011). Small ncRNA expression and regulation under hypoxia in neural progenitor cells. *Cell Mol Neurobiol***31(1)**, 1-5.

Malone JH, Oliver B.(2011). Microarrays, deep sequencing and the true measure of the transcriptome. *BMC Biol***9**, 34.

Martinez NJ, Ow MC, Reece-Hoyes JS, Barrasa MI, Ambros VR, Walhout AJ. (2008). Genome-scale spatiotemporal analysis of Caenorhabditis elegans microRNA promoter activity. *Genome Res***(12)**, 2005-15.
McElwee JJ, Schuster E, Blanc E, Piper MD, Thomas JH, Patel DS, Selman C, Withers DJ, Thornton JM, Partridge L, Gems D.(2007). Evolutionary conservation of regulated longevity assurance mechanisms. *Genome Biol***8(7)**, R132.

McKinsey EL, Parrish JK, Irwin AE, Niemeyer BF, Kern HB, Birks DK, Jedlicka P. (2011).A novel oncogenic mechanism in Ewing sarcoma involving IGF pathway targeting by EWS/Fli1-regulated microRNAs. *Oncogene***30(49)**, 4910-20.

Melkman-Zehavi T, Oren R, Kredo-Russo S, Shapira T, Mandelbaum AD, Rivkin N, Nir T, Lennox KA, Behlke MA, Dor Y, Hornstein E.(2011). miRNAs control insulin content in pancreatic β-cells via downregulation of transcriptional repressors. *EMBO J***30(5)**, 835-45.

Munker R, Calin GA.(2011). MicroRNA profiling in cancer. *Clin Sci***121(4)**, 141-58.

Nairz K, Rottig C, Rintelen F, Zdobnov E, Moser M, Hafen E. (2006). Overgrowth caused by misexpression of a microRNA with dispensable wild-type function. *Dev Biol***291(2)**, 314-24.

Nelson DW, Padgett RW.(2003). Insulin worms its way into the spotlight. *Genes Dev***17(7)**, 813-8.

Nozawa M, Miura S, Nei M.(2010). Origins and evolution of microRNA genes in Drosophila species. *Genome Biol Evol***2**, 180-9.

Okamura K, Hagen JW, Duan H, Tyler DM, Lai EC.(2007). The mirtron pathway generates microRNA-class regulatory RNAs in Drosophila. *Cell***130(1)**, 89-100.

Osterwalder T, Yoon KS, White BH, Keshishian H.(2001). A conditional tissue-specific transgene expression system using inducible GAL4. *Proc Natl Acad Sci USA***98(22)**, 12596-601.

Ouyang YB, Xu L, Lu Y, Sun X, Yue S, Xiong XX, Giffard RG.(2013). Astrocyte-enriched miR-29a targets PUMA and reduces neuronal vulnerability to forebrain ischemia. *Glia***61(11)**, 1784-94.

Pan KZ, Palter JE, Rogers AN, Olsen A, Chen D, Lithgow GJ, Kapahi P.(2007). Inhibition of mRNA translation extends lifespan in Caenorhabditis elegans. *Aging Cell***6**, 111-119.

Park MY, Wu G, Gonzalez-Sulser A, Vaucheret H, Poethig RS.(2005). Nuclear processing and export of microRNAs in Arabidopsis. *Proc Natl Acad Sci USA***102(10)**, 3691-6.

Partridge L, Gems D.(2002). Mechanisms of ageing: public or private? *Nat Rev Genet***3(3)**, 165-75.

Pasquinelli AE, Reinhart BJ, Slack F, Martindale MQ, Kuroda MI, Maller B, Hayward DC, Ball EE, Degnan B, Müller P, Spring J, Srinivasan A, Fishman M, Finnerty J, Corbo J, Levine M, Leahy P, Davidson E, Ruvkun G.(2000). Conservation of the sequence and temporal expression of let-7 heterochronic regulatory RNA. *Nature***408(6808)**, 86-9.

Pearl, R. (1928). The Rate of Living. Being an account of some experimental studies on the biology of life duration. London, University of London Press.

Peto R, Peto J. (1972). Asymptotically efficient rank invariant testprocedures. *J R Stat Soc A***135**, 185-207.

Pincus Z, Smith-Vikos T, Slack FJ. (2011). MicroRNA predictors of longevity in Caenorhabditis elegans. *PLoS Genet***7(9)**, e1002306.

Piriyapongsa J, Jordan IK. (2007). A family of human microRNA genes from miniature inverted-repeat transposable elements. *PLoS One***2(2)**, e203.

Poy MN, Eliasson L, Krutzfeldt J, Kuwajima S, Ma X, Macdonald PE, Pfeffer S, Tuschl T, Rajewsky N, Rorsman P, Stoffel M.(2004). A pancreatic islet-specific microRNA regulates insulin secretion. *Nature***432**, 226–230.

Poy MN, Hausser J, Trajkovski M, Braun M, Collins S, Rorsman P, Zavolan M, Stoffel M.(2009). miR-375 maintains normal pancreatic alpha- and beta-cell mass. *Proc Natl Acad Sci USA***106(14)**, 5813-8.

Rayner KJ, Suárez Y, Dávalos A, Parathath S, Fitzgerald ML, Tamehiro N, Fisher EA, Moore KJ, Fernández-Hernando C.(2010). MiR-33 contributes to the regulation of cholesterol homeostasis. *Science***328(5985)**, 1570-3.

Reinhart BJ, Weinstein EG, Rhoades MW, Bartel B, Bartel DP. (2002). MicroRNAs in plants. *Genes Dev***16(13)**, 1616-26.

Roman G, Endo K, Zong L, Davis RL. (2001).P[Switch], a system for spatial and temporal control of gene expression in Drosophila melanogaster. *Proc Natl Acad Sci USA***98(22)**, 12602-7.

Ronshaugen M, Biemar F, Piel J, Levine M, Lai EC.(2005). The Drosophila microRNA iab-4 causes a dominant homeotic transformation of halteres to wings. *Genes Dev***19(24)**, 2947-52.

R**uby JG, Jan C, Player C, Axtell MJ, Lee W, Nusbaum C, Ge H, Bartel DP.**(2006). Large-scale sequencing reveals 21U-RNAs and additional microRNAs and endogenous siRNAs in C. elegans. *Cell***127(6)**, 1193-207.

Ruby JG, Jan CH, Bartel DP.(2007). Intronic microRNA precursors that bypass Drosha processing. *Nature***448(7149)**, 83-6.

Ruby JG, Stark A, Johnston WK, Kellis M, Bartel DP, Lai EC.(2007). Evolution, biogenesis, expression, and target predictions of a substantially expanded set of Drosophila microRNAs. *Genome Res***17(12)**, 1850-64.

Rulifson EJ, Kim SK, Nusse R.(2002). Ablation of insulin-producing neurons in flies: growth and diabetic phenotypes. *Science***296(5570)**, 1118-20.

Saiki RK, Gelfand DH, Stoffel S, Scharf SJ, Higuchi R, Horn GT, Mullis KB, Erlich HA.(1988). Primer-directed enzymatic amplification of DNA with a thermostable DNA polymerase. *Science***239**, 487-91.

Selman C, Lingard S, Choudhury AI, Batterham RL, Claret M, Clements M, Ramadani F, Okkenhaug K, Schuster E, Blanc E, Piper MD, Al-Qassab H, Speakman JR, Carmignac D, Robinson IC, Thornton JM, Gems D, Partridge L, Withers DJ.(2008). Evidence for lifespan extension and delayed age-related biomarkers in insulin receptor substrate 1 null mice. *FASEB J***22(3)**, 807-18.

Sempere LF, Dubrovsky EB, Dubrovskaya VA, Berger EM, Ambros V.(2002). The expression of the let-7 small regulatory RNA is controlled by ecdysone during metamorphosis in Drosophila melanogaster. *Dev Biol***244(1)**, 170-9.

Sempere LF, Freemantle S, Pitha-Rowe I, Moss E, Dmitrovsky E, Ambros V. (2004). Expression profiling of mammalian microRNAs uncovers a subset of brain-expressed microRNAs with possible roles in murine and human neuronal differentiation. *Genome Biol***5(3)**, R13.

Sempere LF, Sokol NS, Dubrovsky EB, Berger EM, Ambros V.(2003). Temporal regulation of microRNA expression in Drosophila melanogaster mediated by hormonal signals and broad-Complex gene activity. *Dev Biol***259(1)**, 9-18.

Shan ZX, Lin QX, Fu YH, Deng CY, Zhou ZL, Zhu JN, Liu XY, Zhang YY, Li Y, Lin SG, Yu XY.(2009). Up-regulated expression of miR-1/miR-206 in a rat model of myocardial infarction. *Biochem Biophys ResCommun***381**, 597–601.

Shannon CE. (1948). A mathematical theory of communication. *Bell System Technical Journal***27**, 379-423, 623-656.

Shen Y, Wollam J, Magner D, Karalay O, Antebi A.(2012). A steroid receptor-microRNA switch regulates life span in response to signals from the gonad. *Science***338(6113)**, 1472-6.

Simon DJ, Madison JM, Conery AL, Thompson-Peer KL, Soskis M, Ruvkun GB, Kaplan JM, Kim JK. (2008). The microRNA miR-1 regulates a MEF-2-dependent retrograde signal at neuromuscular junctions. *Cell***133(5)**, 903-15.

Siomi MC, Sato K, Pezic D, Aravin AA. (2011). PIWI-interacting small RNAs: the vanguard of genome defence. *Nat Rev Mol Cell Biol***12(4)**, 246-58.

Slack C, Giannakou ME, Foley A, Goss M, Partridge L.(2011). dFOXO-independent effects of reduced insulin-like signaling in Drosophila. *Aging Cell***10(5)**, 735-48.

Slack C, Werz C, Wieser D, Alic N, Foley A, Stocker H, Withers DJ, Thornton JM, Hafen E, Partridge L.(2010). Regulation of lifespan, metabolism, and stress responses by the Drosophila SH2B protein, Lnk. *PLoS Genet***6(3)**, e1000881.

Sokol NS, Ambros V. (2005). Mesodermally expressed Drosophila microRNA-1 is regulated by Twist and is required in muscles during larval growth. *Genes Dev***19(19)**, 2343-54.

Sokol NS, Xu P, Jan YN, Ambros V. (2008). Drosophila let-7 microRNA is required for remodeling of the neuromusculature during metamorphosis. *Genes Dev***22(12)**, 1591-6.

Sun K, Westholm JO, Tsurudome K, Hagen JW, Lu Y, Kohwi M, Betel D, Gao FB, Haghighi AP, Doe CQ, Lai EC. (2012). Neurophysiological defects and neuronal gene deregulation in Drosophila mir-124 mutants. *PLoS Genet***8(2)**, e1002515.

Sun LL, Jiang BG, Li WT, Zou JJ, Shi YQ, Liu ZM. (2011). MicroRNA-15a positively regulates insulin synthesis by inhibiting uncoupling protein-2 expression. *Diabetes Res Clin Pract***91(1)**, 94-100.

Tatar M, Bartke A, Antebi A.(2003). The endocrine regulation of aging by insulin-like signals. *Science***299(5611)**, 1346-51.

Tatar M, Kopelman A, Epstein D, Tu MP, Yin CM, Garofalo RS.(2001). A mutant Drosophila insulin receptor homolog that extends life-span and impairs neuroendocrine function. *Science***292(5514)**, 107-10.

Teleman AA, Maitra S, Cohen SM.(2006). Drosophila lacking microRNA miR-278 are defective in energy homeostasis. *Genes Dev***20(4)**, 417-22.

Toivonen JM, Partridge L.(2009). Endocrine regulation of aging and reproduction in Drosophila. *Mol Cell Endocrinol***299(1)**, 39-50.

Tricoire H, Battisti V, Trannoy S, Lasbleiz C, Pret AM, Monnier V.(2009). The steroid hormone receptor EcR finely modulates Drosophila lifespan during adulthood in a sex-specific manner. *Mech Ageing Dev***130(8)**, 547-52.

Ugalde AP, Ramsay AJ, de la Rosa J, Varela I, Mariño G, Cadiñanos J, Lu J, Freije JM, López-Otín C. (2011). Aging and chronic DNA damage response activate a regulatory pathway involving miR-29 and p53. *EMBO J***30(11)**, 2219-32.

Varghese J, Cohen SM.(2007). microRNA miR-14 acts to modulate a positive autoregulatory loop controlling steroid hormone signaling in Drosophila. *Genes Dev***21(18)**,2277-82.

Varghese J, Lim SF, Cohen SM.(2010). Drosophila miR-14 regulates insulin production and metabolism through its target, sugarbabe. *Genes Dev***24(24)**, 2748-53.

Wang SP, He GL, Chen RR, Li F, Li GQ.(2012). The involvement of cytochrome P450 monooxygenases in methanol elimination in Drosophila melanogaster larvae. *Arch Insect Biochem Physiol***79(4-5)**, 264-75.

Wang XH, Qian RZ, Zhang W, Chen SF, Jin HM, Hu RM. (2009). MicroRNA-320 expression in myocardial microvascular endothelial cells and its relationship with insulin-like growth factor-1 in type 2 diabetic rats. *Clin Exp Pharmacol Physiol***36**, 181–188.

Weinkove D, Leevers SJ.(2000). The genetic control of organ growth: insights from Drosophila. *Curr Opin Genet Dev***10(1)**, 75-80.

Werz C, Köhler K, Hafen E, Stocker H. (2009). The Drosophila SH2B family adaptor Lnk acts in parallel to chico in the insulin signaling pathway. *PLoS Genet***5(8)**, e1000596.

Willcox BJ, Donlon TA, He Q, Chen R, Grove JS, Yano K, Masaki KH, Willcox DC, Rodriguez B, Curb JD.(2008). FOXO3A genotype is strongly associated with human longevity. *Proc Natl Acad Sci USA***105(37)**, 13987-92.

Woltering JM, Durston AJ.(2008). MiR-10 represses HoxB1a and HoxB3a in zebrafish. *PLoS One* **2;3(1)**:e1396.

Xu P, Vernooy SY, Guo M, Hay BA.(2003). The Drosophila microRNA Mir-14 suppresses cell death and is required for normal fat metabolism. *Curr Biol***13(9)**, 790-5.

Yamakuchi M, Lowenstein CJ.(2009). MiR-34, SIRT1 and p53: the feedback loop. *Cell Cycle***8(5)**, 712-5.

Yi R, Qin Y, Macara IG, Cullen BR.(2003). Exportin-5 mediates the nuclear export of pre microRNAs and short hairpin RNAs. *Genes Dev***17(24)**, 3011-6.

Zhang B, Wang Q, Pan X. (2007). MicroRNAs and their regulatory roles in animals and plants. *J Cell Physiol***210(2)**, 279-89.

Zhang L, Hou D, Chen X, Li D, Zhu L, Zhang Y, Li J, Bian Z, Liang X, Cai X, Yin Y, Wang C, Zhang T, Zhu D, Zhang D, Xu J, Chen Q, Ba Y, Liu J, Wang Q, Chen J, Wang J, Wang M, Zhang Q, Zhang J, Zen K, Zhang CY.(2012). Exogenous plant MIR168a specifically targets mammalian LDLRAP1: evidence of cross-kingdom regulation by microRNA. *Cell Res***22(1)**, 107-26.

Zhao X, He X, Han X, Yu Y, Ye F, Chen Y, Hoang T, Xu X, Mi QS, Xin M, Wang F, Appel B, Lu QR.(2010). MicroRNA-mediated control of oligodendrocyte differentiation. *Neuron***65(5)**, 612-26.

Zhao Y, Ransom JF, Li A, Vedantham V, von Drehle M, Muth AN, Tsuchihashi T, McManus MT, Schwartz RJ, Srivastava D. (2007). Dysregulation of cardiogenesis, cardiac conduction, and cell cycle in mice lacking miRNA-1-2. *Cell***129(2)**, 303-17.

Zhu H, Shyh-Chang N, Segrè AV, Shinoda G, Shah SP, Einhorn WS, Takeuchi A, Engreitz JM, Hagan JP, Kharas MG, Urbach A, Thornton JE, Triboulet R, Gregory RI; DIAGRAM Consortium; MAGIC Investigators, Altshuler D, Daley GQ.(2011). The Lin28/let-7 axis regulates glucose metabolism. *Cell***147(1)**, 81-94.

Zovoilis A, Agbemenyah HY, Agis-Balboa RC, Stilling RM, Edbauer D, Rao P, Farinelli L, Delalle I, Schmitt A, Falkai P, Bahari-Javan S, Burkhardt S, Sananbenesi F, Fischer A.(2011). microRNA-34c is a novel target to treat dementias. *EMBO J***30(20)**, 4299-308.

Erklärung

Ich versichere, dass ich die von mir vorgelegte Dissertation selbstständig angefertigt, die benutzten Quellen und Hilfsmittel vollständig angegeben und die Stellen der Arbeit - einschließlich Tabellen, Karten und Abbildungen -, die anderen Werken im Wortlaut oder dem Sinn nach entnommen sind, in jedem Einzelfall als Entlehnung kenntlich gemacht habe; dass diese Dissertation noch keiner anderen Fakultät oder Universität zur Prüfung vorgelegen hat; dass sie noch nicht veröffentlicht worden ist sowie, dass ich eine solche Veröffentlichung vor Abschluss des Promotionsverfahrens nicht vornehmen werde.
Die Bestimmungen dieser Promotionsordnung sind mir bekannt. Die von mir vorgelegte Dissertation ist von Prof. Dr. Linda Partridge betreut worden.
Teilpublikationen liegen nicht vor.

Jennifer Annette Werner

Lebenslauf

Jennifer Annette Werner •Martinstrasse 6a•50259 Pulheim

Tel. 02173 – 1689191 • Mobil 0176 – 314 333 56 • email: jwerner@age.mpg.de

Name:	Jennifer Annette Werner
Nationalität:	deutsch
Geburtstag:	November 9, 1983
Geburtsort:	Leverkusen

Ausbildung

08/1994 - 05/2003	Abitur (1.6), Landrat-Lucas-Gymnasium, Leverkusen
10/2003 - 03/2009	Studium der Biologie an der Universität zu Köln
03/2009	Abschluss Diplom Biologie (sehr gut) an der Universität zu Köln, Hauptfach Genetik
04/2014	Promotion im Fach Molekulargenetik an der Universität zu Köln. Titel der Dissertation: " Identification and characterization of differentially expressed microRNAs in adult tissues of the long-lived *Drosophila dilp2-3,5* mutant"

Forschung und Laborerfahrung

01 - 03/2006	Praktikum bei Bayer CropScience AG im Bereich Forschung und Entwicklung, Abteilung Ökotoxikologie
06 - 07/2006	Projektmodul am Forschungszentrum Jülich, Institut für zelluläre Biophysik, Abteilung Molekulare Neurobiologie und Zelluläre Signaltransduktion unter der Leitung von Prof. Dr. Baumann
02 - 03/2007	Praktikum am Medical College der Jagiellonian Universität, Krakau (Polen), Fakultät Health Care, Abteilung Health and Environment unter der Leitung von Prof. Dr. Janusz Hałuszka
05/2008 - 03/2009	Diplomarbeit: “Untersuchung zum Abbau von Regulatoren der Trichomentwicklung bei Arabidopsis thaliana durch die putative HECT-Ubiquitin Ligase KAKTUS”, Abteilung molekulare Zellbiologie und Entwicklungsgenetik unter der Leitung von Prof. Dr. Martin Hülskamp, Universität zu Köln
08/2009-04/2014	Doktorandin in der Abteilung Biologische Mechanismen des Alterns unter der Leitung von Prof. Dr. Linda Partridge, Max-Planck Institut für Biologie des Alterns, Köln